DPhil in Physiology, Anatomy and Genetics

Clara Howcroft Ferreira

Corpus Christi College

Molecular and neural mechanisms of olfactory decision making in *Drosophila melanogaster*



Supervisor: Prof. Gero Miesenböck

Trinity term 2014

Molecular and neural mechanisms of olfactory decision making in *Drosophila melanogaster*

Clara Howcroft Ferreira
Corpus Christi College
DPhil in Physiology, Anatomy and Genetics
Trinity term 2014

Abstract

Traditional studies of simple perceptual choice tasks in vertebrates identified behavioural characteristics of deliberate decision-making that guided the development of general mathematical models, and the search for neurophysiological correlates. Current experimental and modelling efforts aim to uncover biophysical and circuit level mechanisms of decision-making processes. However, genetic manipulability constraints and lack of high-throughput assays make further progress in vertebrate studies a steep endeavour. In this thesis I studied decision-making in *Drosophila melanogaster* in trained two-alternative forced-choice olfactory tasks with varying stimulus contrast, using a high-resolution single fly behavioural assay. Analysing accuracy and reaction time as a function of task difficulty (i.e., stimulus contrast) showed that flies display behavioural characteristics of evidence accumulation processes, a signature of vertebrate decision-making: reaction times increased and perceptual accuracy declined as stimulus contrast decreased. Mutants for the gene encoding the transcription factor FoxP took longer than wild-type flies to form decisions of similar or reduced accuracy, especially in difficult tasks. Using the putative *FoxP* promoter to ascertain FoxP expression identified subsets of mushroom body intrinsic Kenyon cells, αβ core and γ neurons, as potential sites of FoxP action. Disrupting FoxP expression or decreasing neuronal excitability specifically in αβ core neurons mimicked the phenotype observed in FoxP mutants. FoxP expression therefore affects the development or function of αβ core neurons in the progression of a decision process towards commitment. To identify molecular processes involved in evidence integration regulated by FoxP I further screened 2nd and 3rd chromosome deficiency lines in a sensitised *FoxP* mutant background, uncovering genomic regions of interest for further study. Finally, analysing naive performance in tasks of increasing difficulty showed that naive discriminations are faster and less accurate than trained ones, pointing to the existence of two decision-making systems. *FoxP* mutants appear to engage the slower, more accurate decision making system and the mushroom body seems to be involved in naive discriminations. The molecular and neuronal players involved in olfactory decision making in *Drosophila melanogaster* uncovered in this thesis will allow researching decision making systems to an unprecedented level of detail.

Acknowledgments

The Champalimaud Neuroscience Programme made this PhD possible: it provided for me financially and intellectually, allowing me to acquire a broad basis in Neuroscience and discover my interest for fruit fly research before moving to the University of Oxford. Besides colleagues, many of the people there have been my advisors and friends, and I wish to thank this collaborative research family for all their support.

I am very grateful to my supervisor Professor Gero Miesenböck for providing scientific and intellectual guidance, as well as the material fabric for my research. My colleague and friend Dr Shamik DasGupta, that initiated the decision-making project and with whom I collaborated, was pivotal for my PhD research.

I wish to thank my family, mother, father, brother and his partner, always supportive, interested and full of love. Oxford further provided me with my own family, Wolf and little David, who bring me overwhelming joy and for whom my gratitude and love cannot be put into words.

I further wish to express my appreciation for the Centre for Neural Circuits and Behaviour team and specifically the Miesenböck and Waddell groups. These lovely people not only made my working day happy and the research environment stimulating and fun, but some of them and their partners also became good friends.

Finally, my wonderful friends, in Oxford (Hania, Natasha, José, João, Caroline and Nuno) and elsewhere (Sis, Serginho, Azulinha, Sara, Manuel, Chiquitito, Esmeralda, Marco, Ainhoa and Marine), thank you for always being there throughout the years.

Index

Chapter I. Introduction 1
Decision making in perceptual choices 3
Behavioural signature 4
Models of decision-making 6
The neural basis of decision making 9
Studying decision-making in *Drosophila melanogaster* 13
Olfaction in *Drosophila melanogaster* 16
Olfactory sensory neurons 18
Local interneurons 22
Projection neurons 25
Lateral horn 28
Mushroom body 32
The DPhil project 42

Chapter II. Materials and methods 45
Fly Strains 45
FoxP promoter strain 46
Behavioural experiments 47
Data analysis 50
Statistics 52
Data modelling 52
Structural imaging 54

Chapter III. The role of *FoxP* in trained olfactory decision making 55
Behavioural characterization of the *FoxP* phenotype 64
Drift-diffusion model 69
***FoxP* allelles 71**

Chapter IV. A neural substrate for trained olfactory decision making ... 74
***FoxP* expression pattern 74**
Manipulating *FoxP* expression in the mushroom body 78
Manipulating *FoxP* expressing neurons 82

Chapter V. Identifying new molecular players in decision making..... 87
A simplified protocol for initial screening 88
Results of the screen 89
Specific deficiencies uncovered for further analysis 91
Chapter VI. Naive olfactory discrimination 93
Behavioural characteristics 93
The role of *FoxP* 95
The role of the mushroom body 97
Chapter VII. Discussion..... 103
Trained decision making behaviour..... 103
Molecular players in trained decision making 108
Mutating *FoxP* impairs decision making 108
Targets of FoxP action 112
Trained olfactory decision-making circuitry 118
Naive olfactory discrimination..... 126
Summary of future work..... 129
Conclusions..... 130
Bibliography..... 131
Appendix 166

Chapter I. Introduction

Decision-making processes in the brain allow individuals to form judgments in a variety of situations, ranging from simple sensory detection, such as asserting whether the longed for morning toast is sadly burning, to choosing between multiple alternatives with differing values, temporal contingencies and outcomes, like deciding what to do after a PhD. Decisions are not however only pervasive and important processes in individual lives, but also in society. This realisation has led computer scientists, psychologists, economists and political scientists (see for example Neumann and Morgenstern, 1947; Savage, 1954; Howard, 1966) to extensively analyse which factors are used and how they are combined to form a decision, the basis of how these judgments are made. Descriptive and normative theories arising from these studies are used widely to grasp and optimise decision-makers' strategies in many fields, from private businesses to public health and personal life. Decision making is not however restricted to humans, and non-human animals also face many difficult choice problems (reviewed in Adams et al., 2012; Yapici et al., 2014), imposed by their habitat and/or social system, where judgments must be made concerning for example foraging, mating and predation threat.

During the past decade, systems neuroscience approaches to study decision-making have gained momentum, striving to move beyond mere ethological characterisation towards a holistic understanding of how the brain performs

decision-making processes. For this purpose perceptual tasks used to investigate decision making in humans have been adapted to also study these processes in, mainly, non-human vertebrates (for reviews see for example Gold and Shadlen, 2007, Wang, 2012 and Carandini and Churchland, 2013). These studies combine behavioural, electrophysiological and modelling approaches, and aim to understand the circuit mechanisms and biophysical details underlying decision-making processes in the brain.

In my DPhil project I used the fruit fly *Drosophila melanogaster* to uncover the molecular and neuronal basis of olfactory decision-making systems in the fly brain. Fruit flies produce a variety of complex behaviours from a limited number of neurons, meaning that the challenge of understanding the circuits, neuronal computations and cellular mechanisms responsible for producing these behaviours is less daunting than in vertebrates. In addition, the wealth of molecular-genetic tools to identify and manipulate circuits, and to probe molecular mechanisms within these circuits in the *Drosophila* brain is unmatched in other organisms.

The Introduction of this thesis therefore covers the current knowledge of perceptual decision-making in vertebrates and approaches to studying decision-making in *Drosophila melanogaster*. This is then followed by a description of olfaction in the fruit fly, specifically focusing on the anatomy of the olfactory system and the processing each component performs, along with a description of the canonical view on the emergence of naive and trained odour-evoked behaviours. The Introduction culminates with a description of the aims of my research project.

Decision making in perceptual choices

Tasks for studying decision-making in controlled laboratory settings have ranged from simple stimulus detection (see for example Donders, 1969 (original work 1868)) to choices between multiple alternatives (reviewed in Churchland and Ditterich, 2012) or more complex tasks such as, for example, those involving other organisms and changing task contingencies (reviewed for example in Lee et al., 2012). Whether simple or complex, decisions encompass a deliberation process that leads to a commitment to a proposition.

Perceptual decisions, particularly in the context of two-alternative forced-choice (Fechner, 1966 (original work 1860)) sensorimotor discrimination tasks, have fruitfully yielded many insights to decision-making processes. Two-alternative forced-choice tasks have been extensively used to characterise human perceptual decisions since the 19th century, and extended to investigate decision-making in non-human primates and rodents at the end of the 20th and beginning of 21st century, respectively. These tasks constitute simplified, albeit representative, decision-making tasks that allow maximal experimental control: subjects discriminate between two alternatives that differ in a specific stimulus property (such as intensity, for example) and report a choice, generally through the production of a motor output. The wealth of behavioural data generated, the models developed to capture performance, the physiological data obtained, and the potential to search for the underlying

circuit and biophysical mechanisms makes these tasks perfect for studying decision-making.

Behavioural signature

Two-alternative forced-choice tasks to probe human decision making have involved discriminations between, for example, somatosensory (Mountcastle et al., 1967, 1990), visual (Vickers, 1970; Morgan and Ward, 1980), olfactory (Wise and Cain, 2000; Bowman et al., 2012) and auditory (Brunton et al., 2013; Gifford et al., 2014) stimuli. Non-human primate studies have focused mostly on somatosensory (Mountcastle et al., 1967, 1990) and visual (Newsome and Paré, 1988) discrimination tasks, while decision-making studies in rodents have involved mostly olfactory (Uchida and Mainen, 2003; Rinberg et al., 2006), but also visual (Busse et al., 2011) and auditory (Yang et al., 2008b; Sanders and Kepecs, 2012) discriminations.

These perceptual discrimination studies permit measurements of decision accuracy and the time required to elicit a decision, designated reaction time (Fechner, 1966 (original work 1860); Donders, 1969 (original work 1868); Luce, 1986). Two-alternative forced-choice tasks can be made easier or more difficult by altering stimulus strength or contrast. The measurements of accuracy and reaction time as a function of task difficulty, known as psychometric and chronometric functions, respectively, display similar

signature characteristics in human, non-human primates and rodents, as well as across sensory stimuli.

Psychometric functions, central elements of psychophysics studies, reflect the empirical probability of a decision maker's choice with task difficulty and allow determining response threshold. In humans, non-human primates and rodents alike these functions display the decline in discrimination ability with the increase in difficulty of the task (see for example Vickers and Packer, 1982; Britten et al., 1992; Uchida and Mainen, 2003).

Chronometric functions in the same vertebrates show that reaction times increase with task difficulty (see for example Vickers and Packer, 1982; Roitman and Shadlen, 2002; Rinberg et al., 2006). Reaction time distributions further ubiquitously display a tail of extended reaction times (see for example Vickers, 1970; Luce, 1986; Roitman and Shadlen, 2002).

Crucially, psychometric and chronometric functions are coupled and perceptual discriminations display speed-accuracy trade-offs: tasks can be performed quickly at expense of accuracy and, conversely, more accurate choices can be made by taking longer to decide (reviewed in Wickelgren, 1977 and Heitz, 2014). Speed-accuracy trade-offs can be imposed by direct experimental control of stimulus exposure time (Rinberg et al., 2006), or also by instruction in humans (reviewed in Wickelgren, 1977 and Heitz, 2014; see for example Vickers and Packer, 1982) and non-human primates (Heitz and Schall, 2012).

Based on these behavioural characteristics, mathematical models of decision-making have been proposed in order to capture potential mechanisms by

which the brain could implement these processes and therefore provide a framework for investigations of neuronal function and circuit architecture.

Models of decision-making

The performance of two-alternative forced-choice sensorimotor tasks involves, in general terms, a complex sequence of neural processes which accomplish the following main steps: encoding sensory stimuli and extracting relevant features; maintaining a representation of these features in the build up to the commitment to a choice, incorporating any other indicators of previous experience; and finally, conveying the result of this process to the motor apparatus to produce an output, implementing a choice between alternative courses of action.

The decision-making process itself can be thought of as a form of statistical inference and its elements described in terms of probability theory (reviewed in Gold and Shadlen, 2007). A decision variable is construed based on any available previous relevant knowledge, on the evidence that one of the hypotheses that underlie the alternative choices is true and on the value of the potential outcomes of the decision process. The evidence arises from noisy sensory stimuli and their sequential variable/noisy representation in the central nervous system (reviewed in Faisal et al., 2008), and is accrued over time. The decision variable is interpreted by a conceptual entity, the decision rule, which imposes a criterion value that when reached leads to a

commitment to a particular choice. This commitment is followed by a specific course of action thereby reflecting an intention to either avoid or pursue a particular outcome, based on the goals of the decision maker.

In order to capture the relationship between psychometric and chronometric performance in two-alternative forced-choice tasks, sequential analysis framework was applied to model decision-making behavioural data (Wald, 1947; Stone, 1960; Luce, 1986). Sequential analysis models assume that the noisy sensory evidence must be accumulated over time by repeated sampling and comparison to a criterion. In order to produce a choice, they involve not only the decision concerning the nature of the evidence, i.e., deciding to which alternative it belongs, but also a decision regarding when to stop the integration process and commit to a choice, that is, imposing a stopping rule. This stopping rule is implemented by integrating new evidence into the decision variable until a bound is reached; the time taken to reach this bound is the reaction time. Performance in these tasks therefore reflects not only the quality of the sensory evidence, but also the quantity of information required for a response, which, through changes in the values of the decision criteria, can be controlled to achieve a specific goal.

Several sequential sampling models have been developed, differing in aspects such as how the evidence is sampled (discretely in equally or randomly spaced time intervals, or continuously), how it is accrued (fixed or varying-sized portions) and on the nature of the stopping rule (absolute – the amount of evidence must reach a particular criterion value for one of the responses –, or relative – the evidence for one of the alternatives must exceed the other by a specific amount) (reviewed in Ratcliff and Smith, 2004).

Several one- and two-dimensional models (i.e., models in which there is either a single integrator that accumulates net evidence or in which evidence supporting each alternative is accumulated independently) have been used to model two-alternative forced-choice task performance and help bridge the gap between the observed behaviour and potential underlying processes (reviewed in Bogacz et al., 2006). One-dimensional models include random walk models (Stone, 1960; Laming, 1968; Link, 1975; Link and Heath, 1975) and their continuous analogues, in which evidence is accumulated continuously with a virtual trajectory equivalent to a particle in Brownian motion with a particular drift rate. Two of these models, drift diffusion (Wiener) models (Ratcliff, 1978; Ratcliff and Smith, 2004; Smith and Ratcliff, 2004; Bogacz et al., 2006) and Ornstein–Uhlenbeck models (Busemeyer and Townsend, 1993) differ only in drift rate, with the former being constant whereas the drift in the latter decreases with the increase in accumulated evidence. Two-dimensional models include, for example: race models that involve independent integrators accumulating evidence for each alternative and encompass variations in how time and evidence are discretised – the recruitment model (LaBerge, 1962), the accumulator model (Vickers, 1970), and the Poisson counter model (Pike, 1966); mutual inhibition models with leaky integrators that inhibit each other (Usher and McClelland, 2001); and feed-forward inhibition models with perfect non-leaky integrators that receive inhibition from crossed inputs (Shadlen and Newsome, 2001; Ditterich et al., 2003; Mazurek et al., 2003).

Drift diffusion models are favourites among these models: they are based on relatively simple parameters, many other models can be reduced to them

(Bogacz et al., 2006) and they have been extensively used to model human and non-human primate behavioural data, as well as neurophysiological data (further described below) in a comprehensive way (Ratcliff and Smith, 2004; Smith and Ratcliff, 2004; Palmer et al., 2005; Gold and Shadlen, 2007). As more information is gathered regarding circuit level elements underlying decision-making, current approaches aim to surpass these more abstract normative-type models by developing biologically-based mechanistic models (reviewed in Wang, 2012).

The neural basis of decision making

The formalisation of decision-making models of two-alternative forced-choice data predicts neuronal behaviour during the decision process: sensory neurons, responsible for providing evidence, respond variably and discreetly to stimuli; neurons involved in calculating the decision variable accumulate information from pools of neurons in time and therefore display features of a evidence integration; neurons responsible for signalling choice should display discrete activity. Since choice involves a particular course of action, it is possible that the regions responsible for selecting or planning behaviours play critical roles in forming decisions that lead to those behaviours (reviewed in Gold and Shadlen, 2007 and Andersen and Cui, 2009).

These predictions allow investigations of the circuit elements in decision-making and, conversely, electrophysiological studies act as tests of the

proposed models of evidence integration. Studying perceptual decision-making in humans is obviously restricted to the identification of low spatial resolution brain regions (reviewed in Heekeren et al., 2008; Bogacz et al., 2010) and further entails the inability to probe neuronal function. Non-human vertebrates are more amenable for in-depth mechanistic studies. Indeed several neuronal populations involved in decision-making tasks have been identified in primates (reviewed in Gold and Shadlen, 2007; Andersen and Cui, 2009) and rodents (reviewed in Carandini and Churchland, 2013), from the neurons responsible for representing sensory evidence to the neurons involved in action selection.

A particular two-alternative forced-choice assay, the random dot motion discrimination task (Morgan and Ward, 1980; Newsome and Paré, 1988), has allowed the identification of neural correlates of evidence integration. In non-human primates, this task involves a binary decision regarding the direction of the net movement of a display of random dots and reporting the choice by means of a saccade to a target in the chosen direction; the movement coherence of the dots can be titrated thereby controlling task difficulty. Consistent with the behavioural signature in these types of tasks, monkeys improve the accuracy of decision when given more time to view the stimulus (Britten et al., 1992; Gold and Shadlen, 2003), and, in a reaction-time version of the task, where the subjects control the viewing time and report a choice when ready, easier tasks involve faster and more accurate decisions than more difficult ones (Roitman and Shadlen, 2002).

Based on behavioural experiments with parallel lesion (Newsome and Paré, 1988; Pasternak and Merigan, 1994), recording (Britten et al., 1992, 1996;

Britten and Shadlen, 1993) and microstimulation (Salzman et al., 1992; Ditterich et al., 2003) studies, neurons in the middle temporal area (MT/V5) were found to encode the evidence used to form the decision: they are responsible for conveying information regarding the direction of visual motion; the strength and variability of their responses correlates with accuracy; microstimulating direction-selective MT neurons increases the accuracy and decreases the reaction time for decisions relating to their preferred direction, mimicking the effect of stronger evidence (conversely for decisions in the opposite direction).

Evidence accrual, the build up to the choice in the decision process itself, occurs downstream of MT, potentially in the lateral intraparietal area (LIP), anatomically positioned midway through the sensory-motor processing chain, with inputs from MT and the medial superior temporal cortex (tuned for large-field motion patterns that comprise optic flow) and outputs to the frontal eye field (FEF) and superior colliculus (SC) (involved in the selection and preparation of eye movements together with LIP itself) (reviewed in Gold and Shadlen, 2007). The activity of LIP neurons, that combine sensory and motor receptive fields, correlates with the behavioural performance and the accrual process (Shadlen and Newsome, 1996, 2001; Roitman and Shadlen, 2002): their firing increases or decreases as evidence accumulates in favour or against the choice associated with the target in their receptive field; the difficulty of the task modulates the activity changes , i.e., more coherence in the direction of movement of the dots leads to faster and more intense changes in spike rate; just before the saccade LIP neurons display a stereotyped level of activity, independent of motion strength, thought to

represent the termination of the decision process, when the criterion level of activity is reached. Furthermore, microstimulating LIP neurons has a small effect on both choice and reaction time, indicative of an additive change to the decision variable, not a rate change of evidence accrual but rather, depending on the receptive field, a shift of the decision variable making it closer to or further from the threshold for terminating the decision (Hanks et al., 2006). LIP neurons therefore display the expected characteristics of a neural integrator, stochastically ramping to threshold, and could therefore be responsible for evidence integration. The information from the LIP is thought to lead to the activation of higher-level motor areas such as the SC, which are supposed to select a motor action (McPeek and Keller, 2004; Lo and Wang, 2006).

Despite these invaluable findings, the biophysical properties that allow the integral of evidence accumulation to be computed remain elusive. Furthermore several circuit level questions also linger: it is still unknown if LIP itself computes the decision variable or merely reflects its computation undertaken elsewhere; the role of FEF and SC neurons also achieving a threshold level of activity just before the saccade in the reaction time task (Hanes and Schall, 1996; Ratcliff et al., 2003) is unknown; finally, how the choice criterion is set, what happens when it is met and whether the same neural circuit accumulates the functions of representing the decision variable and translating it to a choice (or whether additional areas are required) are all still open questions.

Based on the data from these and other decision making tasks a series of computational models of network activity have been developed in the past decade (Wang, 2002, 2008; Goldman et al., 2005; Machens et al., 2005;

Deco and Rolls, 2006; Wong and Wang, 2006; Lo and Wang, 2006; Deco et al., 2007; Beck et al., 2008; Furman and Wang, 2008; Liu and Wang, 2008; Zylberberg et al., 2010), some of which attempt to bridge biophysical and circuit level properties underlying integration and choice threshold in decision-making. The complexity of the vertebrate brain combined with the complications of molecular interventions in primates and the effort in generating and analysing genetic variants in rodents hinders research in these organisms. In these animal models, it is therefore hard to probe the biophysical properties and disentangle the full circuitry and neuronal computations involved in integrating sensory evidence, comparing the accumulated signal to a response criterion, and discharging the behaviour when the criterion is met. Fruit flies, in comparison, allow easy genetic tractability and manipulation, which promises to open up these currently inscrutable research avenues.

Studying decision-making in *Drosophila melanogaster*

The appeal of studying decision-making in *Drosophila melanogaster* has not gone unnoticed. Some studies in the fruit fly have investigated choices between two-alternative courses of actions such as: the choice to court or engage in aggressive behaviours in males (Certel et al., 2007, 2010); the male choice to court or not based on previous courtship experiences and the female choice to mate or not based on internal state (reviewed in Dickson, 2008); and the choice to approach or avoid differently sized visual stimuli

(Maimon et al., 2008). Other studies have shown that fruit flies can choose between visual cues (Tang and Guo, 2001), egg-laying sites (Yang et al., 2008a) and feeding substrates (Tanimura et al., 1982; reviewed in Itskov and Ribeiro, 2013). However, how the fruit fly makes a decision in two-alternative forced-choice tasks with two sensory stimuli of the same nature differing in a specific property is still under-characterised.

Studying olfactory decision-making presents itself as the perfect paradigm to understand the underlying biophysical and circuit mechanisms. Firstly, the detailed knowledge of the olfactory circuitry and the computations it performs (described in the next section) makes identifying decision-making circuit elements an approachable endeavour.

Secondly, the naive and trained behaviour of fruit flies in response to a wide variety of odorants has been extensively studied. Although many of these behavioural studies were performed in traditional population T-maze (Quinn et al., 1974; Tully and Quinn, 1985) or trap (Woodard et al., 1989; Park et al., 2002; Larsson et al., 2004; Ruebenbauer et al., 2008) assays, where only the proportion of flies committing to a particular choice is assessed, more recent approaches have attempted to analyse individual olfactory behaviour dynamics in-depth. Single fly behaviour has been studied using for example the 4-way olfactometer (Vet et al., 1983; Faucher et al., 2006; Semmelhack and Wang, 2009), rectangular or circular arenas (Wolf et al., 2002; Keller and Vosshall, 2007), wind tunnels (Budick and Dickinson, 2006; Becher et al., 2010) and the tethered-fly setup (Frye et al., 2003; Frye, 2004; Duistermars et al., 2009; Bhandawat et al., 2010). While the currently used 4-way olfactometer allows analysing the amount of time a fly spends in a particular

area and the exact position of the fly throughout testing, contemporary arenas further allow examining rapid odour induced responses. These endpoints pale however compared to those analysed in the wind tunnel and tethered-fly paradigms, in which the subtleties of olfactory responses can be further assessed in terms of, for example, response latency and sensitivity. These two paradigms, however, only allow studying one fly at a time, while other even more recent assays permit simultaneous multiple individual analysis (Claridge-Chang et al., 2009; Steck et al., 2012). These setups, in which several organisms are tracked individually, allow studying not only odorant preferences and olfactory sensitivities, but also response latencies (Steck et al., 2012) and other parameters that could be deemed important to characterise olfactory decision-making.

Thirdly, there are indications that adult (Budick and Dickinson, 2006; Steck et al., 2012; reviewed in Gaudry et al., 2012) and larval (Gomez-Marin et al., 2011) *Drosophila melanogaster* engage in active sampling, tracking an odour gradient by choosing where to move based on information obtained through head casts that allow the olfactory sensory organs to acquire and integrate olfactory information. Furthermore, fruit flies also respond to different odorants with different behavioural dynamics (Keller and Vosshall, 2007; Steck et al., 2012). However, while these detection studies show that reaction times differ according to the olfactory stimulus presented, reaction times in olfactory discrimination choice tasks between two odours or two concentrations of the same odour are yet to be studied.

Given all these reasons, in my research project, I used a two-choice single fly multiplex setup (Claridge-Chang et al., 2009) to study accuracy and the

temporal dynamics of olfactory discrimination in order to uncover molecular and neuronal mechanisms of decision-making.

Olfaction in *Drosophila melanogaster*

Drosophila melanogaster relies heavily on olfaction to find food (Zhu et al., 2003a; Semmelhack and Wang, 2009; Stökl et al., 2010) and places to oviposit (Stensmyr et al., 2012; Azanchi et al., 2013; Dweck et al., 2013), for mating (Kurtovic et al., 2007; van der Goes van Naters and Carlson, 2007; Datta et al., 2008; Ruta et al., 2010; Kohl et al., 2013) and avoiding dangers (Suh et al., 2004, 2007; Stensmyr et al., 2012; Lin et al., 2013).

The fruit fly displays innate olfactory behaviours, stereotyped hardwired responses, exhibiting attraction, aversion and indifference to different odorants (Keller and Vosshall, 2007; Knaden et al., 2012). The behavioural responses to some of these odorants vary with many factors (reviewed in Su and Wang, 2014) including concentration (Devaud et al., 2001; Heimbeck et al., 2001; Faucher et al., 2006; Keller and Vosshall, 2007; Semmelhack and Wang, 2009), context (Faucher et al., 2006, 2013; Keller and Vosshall, 2007; Turner and Ray, 2009; Bräcker et al., 2013; reviewed in Su and Wang, 2014) and internal state (Ruebenbauer et al., 2008; Azanchi et al., 2013; Beshel and Zhong, 2013; Bräcker et al., 2013; reviewed in Su and Wang, 2014). Fruit flies are also able to form odorant-related associations, leading to trained avoidance or approach olfactory behaviours (reviewed in Dubnau et al., 2003;

Heisenberg, 2003; Keene and Waddell, 2007), also dependent on the fly's state (Krashes et al., 2009; Plaçais and Preat, 2013).

Naive and trained olfactory behaviours are thought to differ in processing complexity and recruit different neuronal circuitries at higher levels. Naive responses are presumed to engage a relatively straightforward circuitry that leads to fast behavioural discharge. Trained responses are supposed to engage a more elaborate circuit that involves forming associations, storing and recalling information to produce a trained behaviour.

In this section I review the anatomy and computations of the olfactory system, from the initial odorant detecting neurons to higher centres (Figure I-1), and relate these findings to the naive and trained dichotomy.

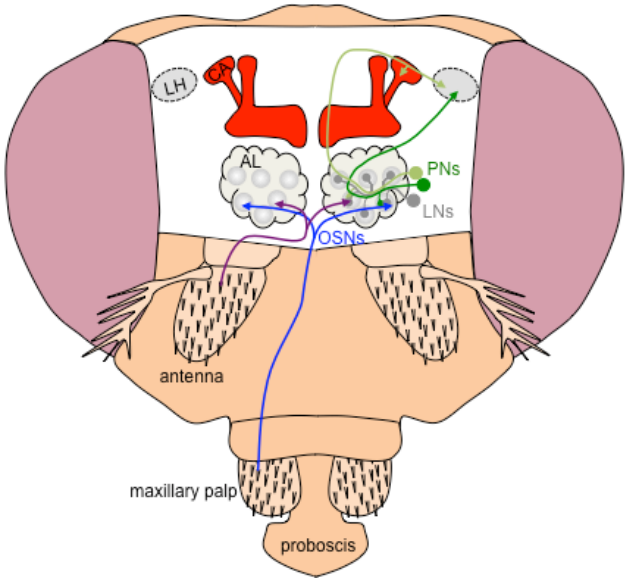


Figure I-1: Schematic representation of *Drosophila melanogaster*'s olfactory system. Olfactory sensing neurons (OSNs) in sensilla on the third antennal segments and the maxillary palps project their axons into glomeruli in the antennal lobe (AL). At the level of the glomeruli olfactory information is processed by local neurons (LNs) and relayed to the calyx (CA) of the mushroom body (MB) and the lateral horn (LH) by projection neurons (PNs). Adapted with permission from Perisse et al., 2013a.

Olfactory sensory neurons

The fly's olfactory sensory neurons (OSNs) are found in two bilaterally symmetrical olfactory organs, the third segment of the antenna and the maxillary palps. In these organs, the dendrites of typically two OSNs are contained in sensory hairs, finger-like protrusions designated sensilla (Stocker, 1994; Shanbhag et al., 1999). The sensilla, which consist of a cuticular wall and pores through which odours enter, are classified into three major morphological types: basiconic, coeloconic and trichoid sensilla (Stocker, 1994; Shanbhag et al., 1999, 2000). Each antenna houses approximately 1,200 OSNs in all sensilla types and each maxillary palp approximately 120 OSNs only in basiconic sensilla (Venkatesh and Singh, 1984; Singh and Nayak, 1985; Stocker, 1994; Shanbhag et al., 1999).

OSNs express different types of receptor proteins, designated odorant receptors (ORs), gustatory receptors (GRs) and ionotropic receptors (IRs) (Clyne et al., 1999; Gao and Chess, 1999; Vosshall et al., 1999; Benton et al., 2009), that differ in structure: ORs and GRs are seven trans-membrane proteins, non-homologous to vertebrate G-protein coupled receptors; IRs are composed of three trans-membrane proteins and co-receptors with varying homology to ionotropic glutamate receptors (Clyne et al., 1999; Gao and Chess, 1999; Vosshall et al., 1999; Benton et al., 2006, 2009; Wistrand et al., 2006; Lundin et al., 2007; Croset et al., 2010).

The OR gene family comprises 62 ORs transcribed from 60 genes (Clyne et al., 1999; Gao and Chess, 1999; Vosshall et al., 1999, 2000; Robertson et al.,

2003), of which 45 are expressed in the adult olfactory organs (Couto et al., 2005). The GR gene family includes 68 GRs encoded by 60 genes (Clyne et al., 2000; Dunipace et al., 2001; Scott et al., 2001; Robertson et al., 2003), two of which are expressed in the adult olfactory organs and have known olfactory functions (Dunipace et al., 2001; Scott et al., 2001; Suh et al., 2004; Faucher et al., 2006; Jones et al., 2006; Kwon et al., 2007).

Most OSNs expressing ORs co-express a single OR and the obligate dimerization partner ORCO (previously know as Or83b), an essential subunit of OR-containing odorant-gated cation channels (Larsson et al., 2004; Neuhaus et al., 2005; Benton et al., 2006; Sato et al., 2008; Wicher et al., 2008). All OSNs innervating basiconic and trichoid sensilla, with the exception of carbon-dioxide-sensitive OSNs expressing Gr21a and Gr63a, require ORCO for OR trafficking and function (Suh et al., 2004; Benton et al., 2006; Faucher et al., 2006; Jones et al., 2006; Kwon et al., 2007). Except for OR35a/ORCO expressing neurons, OSNs housed in coeloconic sensilla do not express members of the OR or GR gene family (Couto et al., 2005; Yao et al., 2005).

The IR gene family, more recently described, consists of 66 IR genes, 16 of which are expressed in the antenna: ten are selectively expressed in subsets of coeloconic sensilla OSNs, either uniquely or co-expressed with one or two other IRs (Benton et al., 2009; Croset et al., 2010); two, expressed in many coeloconic OSNs, are thought to function as co-receptors (Benton et al., 2009; Abuin et al., 2011); four are expressed in neurons in two other antennal structures, the arista and sacculus (reviewed in Rytz et al., 2013).

Each OSN's single axon projects to the first bilateral brain region of the fly olfactory system, the antennal lobe (AL), either through the antennal (antennal OSNs) or labial nerve (maxillary palp OSNs) (Stocker et al., 1990). The AL is organized into 56 discrete spherical neuropils called glomeruli (Stocker et al., 1983, 1990; Laissue et al., 1999; Couto et al., 2005; Endo et al., 2007; Tanaka et al., 2012a). Most OSNs expressing the same receptor project bilaterally to the same single glomerulus (Gao et al., 2000; Vosshall et al., 2000; Couto et al., 2005; Fishilevich and Vosshall, 2005; Benton et al., 2009; Ai et al., 2010; Silbering et al., 2011).

The response properties of odorant receptors have been extensively surveyed using a large set of chemically diverse stimuli, in either their native context (de Bruyne et al., 1999, 2001; Yao et al., 2005; Silbering et al., 2011) or in an expression system that captures their native properties (Dobritsa et al., 2003; Hallem et al., 2004; Hallem and Carlson, 2006). These studies have allowed the categorisation of most adult OSNs into approximately 50 types (de Bruyne et al., 1999, 2001; Elmore et al., 2003; Hallem et al., 2004; Yao et al., 2005; van der Goes van Naters and Carlson, 2007; Silbering et al., 2011), whose responses mostly reflect the properties of their receptors; swapping receptors between neurons swaps their odour responses (Hallem and Carlson, 2004; Benton et al., 2009).

OSNs exhibit a wide array of response properties: most OSN types respond to multiple odours and most individual odours activate multiple OSN types (de Bruyne et al., 1999, 2001; Yao et al., 2005; Hallem and Carlson, 2006; Silbering et al., 2011); there is a continuous spectrum of receptor tuning curves from broadly tuned, responding to many odours (odour generalists), to

narrowly tuned, responding to one or very few odours (odour specialists) (Hallem et al., 2004; Hallem and Carlson, 2006; Silbering et al., 2011). OSNs exhibit a spontaneous firing rate in the absence of odorants and can be activated (modulated with concentration) or inhibited by different odorants (de Bruyne et al., 1999, 2001; Yao et al., 2005; Hallem and Carlson, 2006; Schuckel et al., 2009; Silbering et al., 2011). Their temporal patterns of odorant-evoked activity are also varied and dependent on the quantity, quality and duration of the stimulus (Schuckel et al., 2008, 2009; Kim et al., 2011; Nagel and Wilson, 2011; Getahun et al., 2012).

The organisation of the OSNs in the AL leads to the representation of their combinatorial activation patterns at the level of the glomeruli, suggesting a mechanism of odour coding that uses spatial patterns of glomerular activation to represent an odorant. Functional imaging studies have indeed shown highly odour-specific and stereotyped patterns of glomerular activation (Ng et al., 2002; Wang et al., 2003a); however the mechanism by which these patterns are actually used to drive behavioural responses is still unknown.

A minority of OSNs are exceptionally highly selective for pheromones, non-pheromonal social cues or important environmental odours; these odorants illicit robust activity patterns of selective glomeruli and stereotyped behavioural responses (Clyne et al., 1997; Suh et al., 2004; Xu et al., 2005; Ha and Smith, 2006; Kurtovic et al., 2007; van der Goes van Naters and Carlson, 2007; Semmelhack and Wang, 2009; Min et al., 2013), consistent with a labelled line model of odour coding.

At the level of the glomeruli, OSNs carrying olfactory information to the AL

form excitatory cholinergic synapses with second-order olfactory projection neurons (PNs) (Yasuyama and Salvaterra, 1999; Kazama and Wilson, 2008) responsible for conveying olfactory information to higher order brain centres (Stocker et al., 1990). The AL further contains arborisations of a third major type of neurons designated local interneurons (LNs) (Stocker et al., 1990).

Local interneurons

LNs are predominantly muliglomerular intrinsic neurons of the AL that lack axons (Stocker et al., 1990). There are approximately 200 LNs with diverse morphological patterns, half of which project ipsilaterally and the other half bilaterally (Chou et al., 2010). LNs with known neurotransmitter profiles and modes of action can be broadly categorised into two main groups: excitatory cholinergic local neurons (eLNs) that also form electrical synapses through gap junctions (Olsen et al., 2007; Shang et al., 2007; Huang et al., 2010; Yaksi and Wilson, 2010) and inhibitory local neurons (iLNs), which can be further subdivided in gamma-aminobutyric acid (GABAergic) iLNs (Ng et al., 2002; Wilson and Laurent, 2005) and glutamate (GLUergic) iLNs (Liu and Wilson, 2013).

The majority of LNs are GABAergic iLNs that innervate most or all glomeruli, although some innervate fewer than half of all glomeruli (Stocker et al., 1990; Das et al., 2008; Lai et al., 2008; Okada et al., 2009; Chou et al., 2010; Seki et al., 2010). Roughly one-third of LNs are GLUergic iLNs, some of which

innervate many glomeruli, while others have more selective innervation patterns, or densely innervate the region just posterior to the glomeruli (Chou et al., 2010; Das et al., 2011; Liu and Wilson, 2013). eLNs constitute a minority that innervates most (if not all) glomeruli and synapse with most (if not all) PNs (Shang et al., 2007; Chou et al., 2010; Yaksi and Wilson, 2010).

Most GABAergic iLNs are broadly tuned to odorants (Wilson and Laurent, 2005; Silbering et al., 2008; Chou et al., 2010) and are predominately responsible for presynaptic lateral inhibition at OSN terminals (Olsen and Wilson, 2008; Root et al., 2008), though they also hyperpolarise PNs (Wilson and Laurent, 2005; Yaksi and Wilson, 2010) and other LNs (Wilson and Laurent, 2005; Huang et al., 2010; Yaksi and Wilson, 2010). The connection between the heterogeneous morphology of GABAergic iLNs and the mode of action of GABAergic inhibition in the AL is still an on-going research topic, and indicators of both global (Silbering and Galizia, 2007; Silbering et al., 2008; Olsen et al., 2010) and selective (Ng et al., 2002; Root et al., 2007; Olsen et al., 2010) action have been reported. The main proposed role of GABAergic iLNs is gain control: they are thought to have minimal action when the stimulus evokes weak responses in OSNs, and to inhibit OSNs when the stimulus evokes strong input, preventing the saturation of the dynamic range of many PNs simultaneously (Root et al., 2007; Olsen and Wilson, 2008). The mechanism of gain control is therefore proposed to allow PNs to encode changes in concentration over a broader range of concentrations. More recently, a specific class of GABAergic iLNs has been proposed to be modestly involved in coordinating synchronous oscillations among PNs (Tanaka et al., 2009).

GLUergic iLNs have been less extensively studied. Though they are similar to GABAergic iLNs in odour tuning (broad) and inhibitory action on PNs, other LNs and OSNs, in terms of distribution, the vesicular glutamate and GABA transporters are primarily concentrated in non-overlapping spaces (Liu and Wilson, 2013). GLUergic iLNs are thought to have a dual role, that allows more robust gain control and rapid transitions between network states: direct inhibition and indirect disinhibition through the inhibition of the spontaneously active GABAergic iLNs that tonically inhibit PNs (Liu and Wilson, 2013).

Cholinergic eLNs respond broadly to odours with little glomerular specificity in their synaptic output, and show similar responses to different stimuli and concentrations (Shang et al., 2007; Yaksi and Wilson, 2010). They receive monosynaptic cholinergic input from OSNs and PNs, and form mainly electrical and mainly chemical synapses with PNs and iLNs, respectively (Huang et al., 2010; Yaksi and Wilson, 2010). Although the functional consequences of the network of eLNs are still poorly understood, they are proposed to have an excitatory role on PNs (Shang et al., 2007; Yaksi and Wilson, 2010) that improves odour detection by amplifying weak signals, and an indirect inhibitory role on PNs through the increase in excitatory drive onto iLNs when stimuli are strong (Olsen and Wilson, 2008; Olsen et al., 2010; Yaksi and Wilson, 2010).

The olfactory information conveyed by OSNs to the AL glomeruli, processed by LNs is then further relayed by PNs.

Projection neurons

Approximately 150 PNs (Jefferis et al., 2001), whose dendrites arborise in the AL, project primarily to secondary olfactory sites, the lateral horn (LH) and the mushroom body (MB), via the antennal lobe tracts (ALTs) (Stocker et al., 1990; Tanaka et al., 2012a). They can be categorised into four groups based on the trajectories from the AL: approximately 74 predominantly unilateral, uniglomerular, arborising neurons projecting through the medial antennal lobe tract (mALT) terminate both in the MB and LH (Stocker et al., 1990; Marin et al., 2002; Wong et al., 2002; Tanaka et al., 2004, 2012a, 2012b; Jefferis et al., 2007; Lai et al., 2008; Shinomiya et al., 2011); circa 36 unilateral neurons with predominantly multiglomerular arborisation patterns connect the AL with the LH directly and send projections through the mediolateral antennal tract (mlALT) (Stocker et al., 1990; Marin et al., 2002; Wong et al., 2002; Tanaka et al., 2012a); around 13 predominantly bilateral multiglomerular neurons project to the LH, MB and other brain areas via the lateral antennal tract (lALT) (Stocker et al., 1990; Tanaka et al., 2008, 2012a; Okada et al., 2009); approximately 11 exclusively unilateral multiglomerular neurons project through the transverse antennal tract (tALT) to the LH, MB and other brain areas (Sachse et al., 2007; Tanaka et al., 2008, 2012a).

PNs can also be categorised based on their neurotransmitters: most mALT and lALT neurons are cholinergic and excitatory (ePNs), while the majority of mlALT neurons are GABAergic and inhibitory (iPNs) (Jefferis et al., 2001; Yasuyama et al., 2003; Okada et al., 2009; Tanaka et al., 2012a). While iPNs

release neurotransmitters only at axonal terminals, ePNs further release them from their dendrites (Ng et al., 2002; Wilson et al., 2004). iPNs are additionally thought to receive inputs from both OSNs and mALT ePNs in the AL, and form gap junctions with other AL neurons (Wang et al., 2014).

OSNs and PNs innervating a particular glomerulus can be viewed as a discrete processing channel: OSNs with the same receptor project to the same glomerulus, releasing excitatory acetylcholine onto the dendrites of, on average, three predominantly uniglomerular PNs. Indeed, early functional imaging studies in the AL showed that the dendritic responses of PNs coarsely resembled those of their presynaptic OSNs (Ng et al., 2002; Wang et al., 2003a) and might arise from linear relay of OSN inputs, supporting a labelled-line theory of odour coding. Furthermore, comparative electrophysiological studies of OSNs and their cognate PNs (mainly uniglomerular mALT ePNs) also showed that OSN-PN synapses are extremely robust, with multiple release sites that scale with glomerular size, and that PNs postsynaptic to the same glomerulus display correlated spontaneous spikes and odour responses, implying that OSN-PN connections are convergent (though connections between PNs in the same glomerulus are also thought to play a role) (Kazama and Wilson, 2009). Moreover, PNs postsynaptic to highly selective OSNs for pheromones, non-pheromonal social cues or important environmental odours display specific properties and/or patterns of connectivity (Jefferis et al., 2007; Schlief and Wilson, 2007; Datta et al., 2008; Ruta et al., 2010; Lin et al., 2013; Min et al., 2013) that suggest specialisation for processing this type of odorants.

However OSN-PN activity has also been shown to be non-linear (Bhandawat

et al., 2007) and PNs exhibit less variable spiking responses, more complex firing patterns and varied, broader, tuning curves than their cognate OSNs (Wilson et al., 2004; Bhandawat et al., 2007; Schlief and Wilson, 2007). Some of the particularities of PN behaviour are thought to be the product of the dual inhibitory and excitatory action of LNs: in the absence of input from presynaptic OSNs, PN activity is reduced but not eliminated (Olsen et al., 2007; Root et al., 2007; Shang et al., 2007); PNs can be inhibited by stimuli that excite their cognate OSNs (Olsen and Wilson, 2008); activating a single OSN type causes excitation of non-cognate PNs (Olsen et al., 2007); PN responses are typically disinhibited by silencing input to other glomeruli (Olsen and Wilson, 2008; Asahina et al., 2009); adding new odours to a mixture, recruiting activity in additional glomeruli, typically produces a sublinear summation or suppression of odour responses in PNs (Silbering and Galizia, 2007; Olsen et al., 2010).

Multiglomerular iPNs projecting through the mlALT to the LH have been less extensively studied. Recent functional imaging studies (Liang et al., 2013; Parnas et al., 2013; Wang et al., 2014) with a few odorants showed that odour-evoked changes in iPNs correlate with stimulus strength (number of OSNs and number of glomeruli activated), vary with concentration and display overlapping but broader responses than mALT PNs. iPNs are thought to exert inhibition on excitatory signals carried by ePNs (Liang et al., 2013; Parnas et al., 2013; Wang et al., 2014).

Taken together the data here presented suggest that while some OSN-PN channels might be tightly coupled, in accordance with a labelled line model of odour coding, other channels are processed differently, encoding odorant

information by spatiotemporal activation patterns in the PN ensemble. This olfactory information is then conveyed to the LH and the MB, where third-order neurons combine signals arising from single or multiple glomeruli to extract information about olfactory features of the environment.

Lateral horn

The LH is a bilateral region in the lateral protocerebrum containing axonal arborisations of PNs (Stocker et al., 1990, 1997; reviewed in Stocker, 1994), presumed to be involved in naive olfactory behaviours. Innate olfactory behaviour is impaired by disrupting two-thirds of the PNs that project to both the MB and LH or LH alone (Heimbeck et al., 2001), but unaltered by chemically or genetically disrupting the MB (Heisenberg et al., 1985; de Belle and Heisenberg, 1994), or its output (Dubnau et al., 2001; McGuire et al., 2001; Parnas et al., 2013). This conveniently simplistic view might not constitute the complete picture, as at least one study claims that MB output is required for innate odour attraction, though not for avoidance (Wang et al., 2003).

LH anatomy has not been extensively characterised, and general anatomical features have been mainly assigned on the basis of the projection patterns of PNs (Marin et al., 2002; Wong et al., 2002; Tanaka et al., 2004, 2012a; Jefferis et al., 2007), which seem to terminate in stereotypic areas: the terminals of mALT and mlALT PNs collectively cover the entire LH and

overlap; tALT and lALT PNs have restricted terminal areas (Tanaka et al., 2009). PNs whose dendrites innervate glomeruli that contain OSNs responsive to food odours and pheromones have been proposed to project to segregated areas in the LH (Jefferis et al., 2007), though coupling between food detection and courtship circuitries is plausible, as a set of PNs that convey information about food odours also project to the area in the LH thought to receive primarily pheromone information (Grosjean et al., 2011).

Some environmental or socially salient odorants are processed through dedicated channels via the LH. The circuitry responsible for the behavioural responses to the male pheromone cis-vaccenyl acetate (cVA), for example, that elicits aggregation (Bartelt et al., 1985) and stereotyped behaviours in both sexes (Ejima et al., 2007; Kurtovic et al., 2007; Billeter et al., 2009; Wang and Anderson, 2010), has been traced from a particular set of OSNs, glomeruli and PNs through to sexually dimorphic third order LHNs with sex-specific responses, and fourth order descending neurons to the ventral chord (Kurtovic et al., 2007; van der Goes van Naters and Carlson, 2007; Datta et al., 2008; Ruta et al., 2010; Kohl et al., 2013). Nevertheless the responses to cVA are also thought to involve a learnt component which is mediated by the MB (Keleman et al., 2007, 2012).

CO_2 produced by stressed flies elicits avoidance behaviour mediated by one OSN, one glomerulus, and two PN types projecting to the LH, in an MB independent manner (Suh et al., 2004, 2007; Lin et al., 2013). However, CO_2 is also present in the environment and in rotting fruit, and the fly's behavioural responses to it are also concentration and context dependent (Faucher et al., 2006, 2013; Turner and Ray, 2009), and involve PNs projecting to the MB in a

context and state dependent manner (Bräcker et al., 2013).

The detection system for geosmyn, a compound produced by harmful microbes, and ammonia and amines, that emanate from decaying organic matter, are also examples of dedicated channels that elicit robust avoidance (Stensmyr et al., 2012) and attraction behaviours (Min et al., 2013), respectively. These olfactory stimuli activate single sets of OSNs that feed into dedicated glomerular channels and PNs (Stensmyr et al., 2012; Min et al., 2013). These PNs project to MB and LH, and while olfactory processing of ammonia and amines is MB independent (Min et al., 2013), how geosmyn inputs are further processed is still unknown.

In contrast to these examples of labelled-line processing of specific olfactory signals, processing of general odours that activate several glomeruli and elicit varied behavioural responses (Semmelhack and Wang, 2009; Knaden et al., 2012) has only recently started to be addressed. The distance between ePN activity patterns has been found to correlate with the fly's spontaneous binary odour discrimination capability, which can be altered by silencing subsets of ePNs and is MB-independent (Parnas et al., 2013). Inhibitory multiglomerular GABAergic iPNs projecting through the mlALT, whose odour responses increase with the number of active glomeruli, are thought to presynaptically regulate uniglomerular mALT ePNs (Parnas et al., 2013). Silencing these iPNs does not alter innate odour detection, but affects discrimination between two odours represented by closely related activity patterns of ePNs (Parnas et al., 2013). On the other hand, the iPNs are also thought to exert parallel inhibition to simultaneously arriving excitatory ePNs signals on third order ventrolateral protocerebrum neurons, suppressing their response to food

odours, but not to cVA (Liang et al., 2013), suggesting a gating role for iPNs to create specific odour processing in the LH.

Third-order LH neurons (LHNs), presumed to number several hundreds, are organised in large clusters of somata (Fişek and Wilson, 2014). They constitute morphologically varied groups whose putative connectivity with PNs is debated: on the one hand some LHNs seem to map to restricted areas, suggesting that they could link segregated groups of PNs with other brain areas (Tanaka et al., 2004); on the other hand, some LHNs branch extensively in the LH, suggesting that they could integrate information carried by PNs from different glomeruli (Jefferis et al., 2007).

A recent study has identified two types of LHNs: type I with somata in a dorsomedial cluster, innervating the superior medial protocerebrum, and type II with somata in a ventrolateral cluster, innervating the superior lateral protocerebrum (Fişek and Wilson, 2014). Type I LHNs receive inputs from three glomeruli co-activated by many fruity-smelling organic acetates, and form monosynaptic connections with their presynaptic PNs, with differential synaptic weighs, that seem to be relatively linearly summated (Fişek and Wilson, 2014). Compared to their presynaptic PNs, these LHNs are more broadly tuned, which could be a way to link a large region of odorant space with a particular behavioural programme (Fişek and Wilson, 2014), and display a broader dynamic concentration encoding range which could have a role in the behavioural concentration generalisation observed in *Drosophila* (Kreher et al., 2008; Asahina et al., 2009; Fişek and Wilson, 2014).

Type II LHNs, monosynaptically connected to only one glomerulus, show

strong, odour-selective gating of feed-forward excitation from a small number of glomeruli, mainly via local GABAergic neurons with narrow odour tuning (Fişek and Wilson, 2014). This combination of excitation with tuned inhibition (Luo et al., 2010; Fişek and Wilson, 2014) is proposed to be a way to generate selectivity, which could be responsible for discharging a behavioural program to a specific odour, thus accounting for the fly's ability to perform fine discriminations among odour stimuli.

A clear picture of the anatomy of the LH, including its subdivisions based on the projection patterns of PNs or third order local and projection LHNs they synapse with, remains mostly elusive. Further functional connectivity studies will allow a deeper understanding of its organisation and connections with other centres in the brain. Similarly, further studies that systematically characterise the responses of LHNs are required to understand how olfactory information is processed in this largely understudied area.

Mushroom body

The MB, a bilaterally prominent landmark in the insect brain, has received more attention than the LH, particularly due to its role in olfactory learning and memory. It is critical for the association of aversive (Quinn et al., 1974; Tully and Quinn, 1985) and appetitive (Tempel et al., 1983) unconditioned stimuli (US) with odours and the consequent conditioned avoidance or approach response to the conditioned stimulus (CS), as disrupting its structure

(Heisenberg et al., 1985; de Belle and Heisenberg, 1994), or output (Dubnau et al., 2001; McGuire et al., 2001), impairs olfactory learning and memory.

The MB can be subdivided into three main parts (Figure I-2): the calyx, the peduncle and the lobes. It is comprised of around 2,000-2,500 MB intrinsic neurons, Kenyon cells (KCs), per hemisphere (Hinke, 1961; Technau, 1984; Balling et al., 1987; Tanaka et al., 2008; Aso et al., 2009), whose cell bodies form a cluster in the dorsal posterior brain. KCs extend dendrites anteriorly in the calyx, and their neurites converge projecting downwards through the brain as a bundle designated peduncle. The peduncle projects anteriorly where the KC axons form in total five lobes: the vertical α and α' lobes, and the horizontal β, β', and γ lobes (Ito et al., 1997; Crittenden et al., 1998).

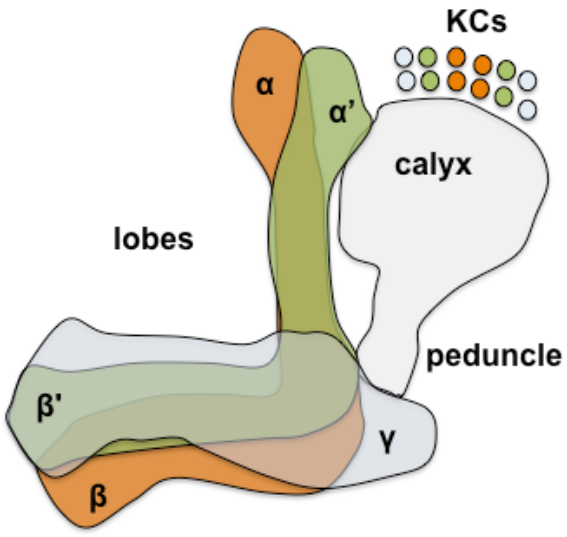


Figure I-2: Schematic representation of the mushroom body (MB). The MB is subdivided into three main parts: calyx, penducle and lobes. There are two vertical lobes (α and α') and three horizontal lobes (β, β', and γ). The somata of the Kenyon cells (KCs) cluster in the posterior brain (coloured spheres), extend their dendrites in the calyx and project their neurites through the peduncle to the lobes. They are subdivided into three major neuronal groups designated αβ, α'β' and γ.

KCs can be subdivided into three major neuronal groups according to morphology, developmental timing and gene expression patterns (Yang et al., 1995; Ito et al., 1997, 1998; Crittenden et al., 1998; Lee et al., 1999; Noveen et al., 2000; Zhu et al., 2003b): approximately 1,000 αβ neurons, 400 α'β' and 700 γ neurons (reviewed in Perisse et al., 2013). Bifurcated γ neurons are formed in the mid-larval stage and during metamorphosis undergo significant pruning and transformation, resulting in a single horizontal γ lobe in the adult (Lee et al., 1999; Zhu et al., 2003b). α'β' neurons are formed in the late third instar larval stage and bifurcate at the anterior peduncle to the vertical α' and horizontal β' lobes (Lee et al., 1999). αβ neurons, formed during metamorphosis, project vertically to form the α lobe and horizontally to the β lobe (Lee et al., 1999). αβ and α'β' lobes can be further subdivided into three strata each, and the γ lobe into two regions: αβ are divided into concentric core (αβc), surface (αβs) and posterior (αβp) strata (Strausfeld et al., 2003; Zhu et al., 2003b; Tanaka et al., 2004, 2008; Lin et al., 2007); α'β' are divided into planar anterior (α'β'a), medial (α'β'm) and posterior (α'β'p) strata (Strausfeld et al., 2003; Tanaka et al., 2008); γ is divided into main (γm) and dorsal (γd) regions (Aso et al., 2009).

The calyx comprises the main and accessory calyx, into which KCs differentially extended their dendrites: γ neuron dendrites occupy predominantly the centre, while αβc, αβs and α'β' mostly the periphery of the main calyx; αβp seem to be the only KCs arborising in the accessory calyx (Strausfeld et al., 2003; Zhu et al., 2003b; Jefferis et al., 2004; Lin et al., 2007; Tanaka et al., 2008). At the main calyx, input from 150 PNs (reviewed in Strausfeld et al., 1998; Fahrbach, 2006), arrives via an estimated 1,115 large

~5 µm cholinergic presynaptic boutons (Stocker et al., 1990; Yasuyama, 2002; Jefferis et al., 2007; Turner et al., 2008), that occupy the centres of complexes called microglomeruli, enwrapped by claw-like dendritic structures of several KCs (Yasuyama, 2002; Strausfeld et al., 2003; Leiss et al., 2009; Butcher et al., 2012). It is currently unresolved whether PNs form a broad zonal stereotypy in the calyx (Tanaka et al., 2004, 2008, 2012a; Jefferis et al., 2007; Lin et al., 2007; Gruntman and Turner, 2013) or not (Marin et al., 2002; Wong et al., 2002; Honegger et al., 2011; Caron et al., 2013).

KCs have a very low spontaneous firing rate (Turner et al., 2008), generally responding highly selectively to odour identity and sometimes also concentration (Wang et al., 2004; Murthy et al., 2008). Functional imaging and electrophysiological studies showed that KC responses are sparse over a broad range of mono- and muti-molecular odorants, as well as complex natural odours and concentrations (Wang et al., 2004; Turner et al., 2008; Honegger et al., 2011). The sparseness and selectivity of KC responses are thought to be essential for their role in learning and memory: reduced correlations between representations diminish the problem of synaptic interference permitting effective detection, discrimination, storage, and recall of olfactory information.

KCs are thought of as degenerate integrators: they require, on average, inputs to five of their typical seven claws to spike (Leiss et al., 2009; Caron et al., 2013; Gruntman and Turner, 2013), thereby responding specifically to combinations of coactive glomerular channels, which, through different combinations of PN input patterns, explains specific responses to multiple odours. KC subsets exhibit small physiological differences in odorant

responses (Yu et al., 2006; Turner et al., 2008; Wang et al., 2008; Honegger et al., 2011): α'β' KCs, which have the largest baseline and response firing rates, are more broadly tuned than αβ KCs and these more than γ KCs. αβ subsets respond differently to odorants: αβs and αβc KCs are activated while αβp KCs are inhibited by odorants (Perisse et al., 2013b).

Besides the main PN-KC synapses at the main calyx, several other less studied synapses are proposed to exist: a local GABAergic network presynaptic to KCs and PNs at microglomeruli (Yasuyama, 2002; Tanaka et al., 2008; Leiss et al., 2009; Liu and Davis, 2009; Butcher et al., 2012); input from octopaminergic (OA) (Sinakevitch and Strausfeld, 2006; Busch et al., 2009), dopaminergic (DA) (Mao and Davis, 2009) and possibly serotonergic neurons (Roy et al., 2007; Tanaka et al., 2008); potential presynaptic input from αβ and γ, but not in α'β', outside the microglomeruli, onto MB extrinsic neurons, dendrites of other KCs or PN axons (Christiansen et al., 2011).

At the level of the lobes, KCs are both pre- and postsynaptic to MB extrinsic neurons that provide afferent input and/or efferent output and define at least 15 zones in the MB (Ito et al., 1998; Tanaka et al., 2008). Input neurons include DA neurons and a couple of large paired neurons: the serotonergic dorsal paired medial neurons (DPM), that appear to arborise in all lobes and peduncle (Waddell et al., 2000; Tanaka et al., 2008; Lee et al., 2011; Pitman et al., 2011), and the GABAergic anterior paired lateral neurons (APL), that arborise in all areas of the MB, except potentially the distal α lobe (Tanaka et al., 2008; Liu and Davis, 2009; Pitman et al., 2011). All these neurons respond to odours (Yu et al., 2005; Liu and Davis, 2009; Mao and Davis, 2009), and together with KCs further respond to reinforcement stimuli (Yu et

al., 2005, 2006; Liu and Davis, 2009; Mao and Davis, 2009; Liu et al., 2012). APL neurons limit KC odour-evoked activity contributing to the sparseness of their responses (Lei et al., 2013; Lin et al., 2014). DPM neurons are not only post- but also presynaptic to KCs (Yu et al., 2005; Pitman et al., 2011), and gap junction coupled to APL neurons (Wu et al., 2011).

Learning and memory studies have focused on studying cellular and circuit elements of different memory stages, formed through different training protocols. Memories can be divided into those that can last up to hours and do not require protein synthesis, designated short-term memory (STM), middle-term memory (MTM) and anaesthesia-resistant memory (ARM) (Quinn and Dudai, 1976; Folkers et al., 1993; Isabel et al., 2004), and those that require protein synthesis and can last for days, which encompass the so called long-term memory (LTM) stage (Tully et al., 1994; Krashes and Waddell, 2008). Memories are thought to pass through a labile phase before being processed into a more stable phase, which involves morphological changes at synapses in longer-term memories. According to the standard model, the association between CS and US, conveyed by DA neurons, occurs at the MB and output from this structure then leads to the expression of the trained behaviours (reviewed in Perisse et al., 2013a).

In terms of cellular memory processes, many genes have been identified (reviewed in Dubnau et al., 2003; Heisenberg, 2003; Keene and Waddell, 2007), and the cyclic adenosine monophosphate (cAMP) signalling pathway pinpointed as crucial for memory formation. In this cascade, *rutabaga* (RUT), that encodes a type I calcium (Ca^{2+})/calmodulin-stimulated adenylyl cyclase (Livingstone et al., 1984; Levin et al., 1992), is thought to register the

coincidence between the CS and US in specific KCs (Zars et al., 2000; McGuire et al., 2001; Mao et al., 2004), through Ca^{2+} influx following PN-driven depolarization and reinforcement signalling conveyed by DA binding to G-protein-coupled dDA1 receptors (Connolly et al., 1996; Han et al., 1996; Kim et al., 2003, 2007; Qin et al., 2012). The duration of the cAMP response is thought to dictate the stability of memory, and a prolonged increase in its concentration results in LTM through the activation of cAMP-response-element-binding protein (CREB) (Yin et al., 1994; Yin and Wallach, 1995; Perazzona et al., 2004).

In terms of the learning and memory circuitry, different subsets of KCs and MB extrinsic neurons are thought to be recruited at different stages. Reinforcement signals from aversive electric shocks and appetitive sugars are conveyed by different DA neurons. Two classes of protocerebral posterior lateral 1 (PPL1) DA neurons (PPL1-MP1 and PPL1-MV1), that innervate MB vertical lobes and peduncle, and two classes of protocerebral anterior medial (PAM) cluster DA neurons (PAM-M2 and PAM-M3), which innervate horizontal lobes, can convey negative reinforcement (Claridge-Chang et al., 2009; Aso et al., 2010, 2012). It is suggested that the aversive reinforcement is distributed across the major MB subdivisions and DA neurons act in a combinatorial way, as they reinforce memories of differing strength and persistence (Aso et al., 2010, 2012) and induce compartmentalised elevations of cAMP in the MB (Boto et al., 2014). Appetitive sweet taste STM and nutritious LTM reinforcement signals are conveyed by DA PAM neurons that project to the medial lobes (Burke et al., 2012; Liu et al., 2012). OA neurons (Schwaerzel et al., 2003) provide the transient reinforcing properties of the

sweet taste to DA PAM neurons via the β-adrenergic-like receptor OCTβ2R, but play no role in LTM (Burke et al., 2012).

Output from α'β' is required during and after training to maintain stable memories (Krashes et al., 2007). DPM neurons, also required after training (Keene et al., 2004, 2006; Yu et al., 2005; Krashes and Waddell, 2008), with spatially restricted activity according to the reinforcer used (Burke et al., 2012; Cervantes-Sandoval and Davis, 2012; Liu et al., 2012), are involved in the consolidation process, potentially together with the DA neurons their innervation in the MB overlaps with (Berry et al., 2012; Plaçais et al., 2012). APL neurons are also required at this stage (Wu et al., 2011; Plaçais et al., 2012) and a recurrent DPM-α'β'-APL loop is therefore proposed to stabilise labile memory traces (Pitman et al., 2011).

Aversive STM, that lasts from a few minutes to an hour after training, relies on γ neurons, which display relatively specific Ca^{2+} response plasticity induced by DA, dependent on DA receptors and RUT (Zars et al., 2000; McGuire et al., 2003; Blum et al., 2009; Qin et al., 2012; Boto et al., 2014), though their output is not strongly required for retrieval (McGuire et al., 2001; Akalal et al., 2006). Presynaptic inhibition of γ neurons is further required during discriminative learning, suggesting a comparator role for these neurons (Zhang and Roman, 2013). In appetitive memory, RUT expression is required in αβ or γ neurons and blocking γ neurons impairs immediate and two hour memory (Trannoy et al., 2011); short neuropeptide F (sNPF) expression, strongest in αβ and γ lobes, is required for two hour memory (Knapek et al., 2013).

MTM is typically assessed three hours after training, but its status as a unique phase is unclear. Output from αβ but not α'β' neurons is required at this point (McGuire et al., 2001; Schwaerzel et al., 2002; Isabel et al., 2004; Krashes et al., 2007). As for LTM, aversive and appetitive retrieval requires output from αβ, but not γ, neurons (Isabel et al., 2004; Trannoy et al., 2011), in which a memory trace is observed from 9-24 hours (Yu et al., 2006; Akalal et al., 2010). Output from different αβ subsets, apparently coinciding with the stratified innervation of aversive and rewarding DA neurons, seems to be differentially required for LTM retrieval: αβs neurons for aversive and appetitive memory and αβc neurons specifically for appetitive memory (Perisse et al., 2013b). Although γ output is not required for LTM retrieval, an aversive trace has been reported in these neurons 18-48 h after training (Akalal et al., 2010).

Overall, it seems that distinct populations of MB neurons contribute to different memory phases and that aversive and appetitive memories display singular characteristics. These memories are thought to be represented as modifications in synaptic weights between KCs and MB output neurons, which in turn direct behaviour. Although several putative output neurons have been identified (Tanaka et al., 2008), only two types of cholinergic neurons, MB-V2 and MB-V3, that project to the superior intermediate protocerebrum and LH in the case of MB-V2 (Tanaka et al., 2008; Séjourné et al., 2011; Pai et al., 2013; Perisse et al., 2013b), have been shown to convey output from the MB. MB-V2 neurons, which can be divided into V2α (innervate the α lobe where the αβs neurons reside) and V2α' (innervate the α' lobe tip) (Tanaka et al., 2008; Séjourné et al., 2011; Perisse et al., 2013b), are required for aversive

STM and LTM retrieval and dispensable for appetitive STM retrieval, consistent with their innervation patterns (restricted to αβs neurons and apparently not pooling αβc neurons) (Séjourné et al., 2011; Perisse et al., 2013b). MB-V3 neurons, which innervate the tip of the α lobe (Tanaka et al., 2008; Pai et al., 2013), seem to be involved in appetitive and aversive fasting LTM retrieval (Pai et al., 2013; Plaçais et al., 2013).

Though a lot is now known about the anatomy of the MB and its involvement in learning and memory, many open questions remain. Apart from the identification of sNPF in γ and αβ neurons, except αβc (Johard and Enell, 2008; Knapek et al., 2013), and despite several attempts, no other neurotransmitters have been identified in KCs. The ALs also appear to have a role immediately after training (Yu et al., 2004) and PNs seem to be sufficient sites for RUT-dependent plasticity for appetitive memory formation (Thum et al., 2007), displaying synaptic protein synthesis that changes Ca^{2+}/calmodulin-dependent kinase II (CaMKII) levels, thought to be required for LTM formation (Ashraf et al., 2006). The connection between these findings and MB data has not been addressed.

How the output from MB drives behaviour, that is, how the MB connects with motor output regions is also still unknown. The locomotor control centre in *Drosophila melanogaster* is thought to be the central complex (CC) (reviewed in Strauss, 2002), and despite a couple of studies showing mutual requirements – a role for MB in initial motor activity (Serway et al., 2009) and a part for the ellipsoid body component of the CC in LTM (Wu et al., 2007) –, no functional connection between these two centres has been found. Furthermore, although putative connections and overlapping areas between

projection patterns of LH and the MB output neurons have been suggested (Tanaka et al., 2008), how these two higher olfactory brain centres are connected either directly or indirectly in order to gate naive and trained behavioural outputs remains elusive.

The DPhil project

In order to study the characteristics of perceptual decision making in *Drosophila melanogaster* I used a single fly olfactory behaviour setup (Claridge-Chang et al., 2009) to analyse accuracy and reaction time in two-alternative forced-choice discrimination tasks of varying difficulty. These tasks allowed the search for mutants with impaired decision-making and the characterisation of a defect in evidence integration, presented in Chapter III, when the gene encoding for the transcription factor *FoxP* is mutated.

Taking advantage of a dual expression system, GAL4-UAS (Brand and Perrimon, 1993), I developed a fly strain that allowed uncovering the circuitry underlying trained olfactory decision-making, based on the identification of the putative expression pattern of *FoxP*. Tampering with a subset of mushroom body neurons in which FoxP expression was identified, αβ core Kenyon cells, by diminishing their excitability and interfering with FoxP expression, mimicked the *FoxP* mutant phenotype. FoxP is though to affect developmental or functional processes required for appropriate evidence integration within these neurons. The identification of this neuronal substrate,

presented in Chapter IV, will permit further circuit level, physiological and mechanistic studies of the decision-making process.

The multiplex nature of the setup used allowed screening flies with a substantial number of deleted genomic regions, with the ultimate goal of identifying genes potentially regulated by *FoxP* and therefore involved in decision-making. This screen, presented in Chapter V, will eventually lead to uncovering the molecular processes underlying evidence integration.

Using the same setup employed to study trained decision-making, naive olfactory discrimination behaviour was also analysed and is presented in Chapter VI. Comparing naive and trained olfactory behaviour seems to point to the existence of two distinct decision-making systems with differing accuracies and/or choice consistencies as well as reaction times. It will be interesting to research how these two systems differ in the fruit fly brain.

Finally, in Chapter VII, I summarise the main findings of this research project and describe the research avenues it opens up, which will continue to provide valuable insight into the decision-making process, using a tractable system in which current models can be tested.

In summary the main aims of my DPhil were to:

- Use a trained olfactory intensity discrimination task to characterise a mutant strain with an altered decision-making process, in which evidence integration is impaired – Chapter III;
- Develop tools to identify the gene's expression pattern and uncover neuronal elements of trained decision-making circuitry – Chapter IV;

- Identify other molecular players in trained decision making to determine the biophysical mechanisms of the integration process – Chapter V;
- Characterise naive olfactory discrimination and study the differences between the underlying circuitry required for this behaviour as compared to trained olfactory discrimination behaviour – Chapter VI.

Chapter II. Materials and methods

Fly Strains

Flies were raised on cornmeal agar at 25 °C under a 12-h light/12-h dark cycle. The wild-type strain used was Canton-S (CS). The mutant *FoxP* strains *FoxP*$^{5\text{-SZ-}3955}$ (*w*^{1118}*; P{RS5}FoxP*$^{5\text{-SZ-}3955}$) (Ryder et al., 2004) and *FoxP*^{GS22100} (*y*^{1} *w*^{67c23}*; P{GSV7}GS22100/TM3 Sb*^{1} *Ser*^{1}) (*Drosophila* Gene Search Project) were obtained from the *Drosophila* Genetic Resource centre, Kyoto; the mutant strain *FoxP*^{f03746} (*PBac{WH}FoxP*^{f03746}) (Thibault et al., 2004) was obtained from the Exelixis Collection. The *UAS-FoxP*^{RNAi} line (*w*^{1118}; *P{GD4320}v15732*) was obtained from the Vienna *Drosophila* RNAi Center. *UAS-Kir2.1* (Baines et al., 2001) and *UAS-mcd8::GFP* (*y*^{1} *w***; Pin*^{Yt}*/CyO; P{UAS-mCD8::GFP.L}LL6*) flies (Lee et al., 1999) were obtained from the Bloomington stock centre; the 2 x *tubulin-GAL80*^{ts} line was a gift from Mani Ramaswami (Trinity College Dublin). Driver lines *NP6024-GAL4* (*y** *w** *P{GawB}NP6024/FM7c*) (Hayashi et al., 2002) and *NP1131-GAL4* (*y** *w***; P{GawB}NP1131/CyO, P{UAS-lacZ.UW14}UW14*) (Hayashi et al., 2002) were obtained from the *Drosophila* Genetic Resource centre, Kyoto; *OK107-GAL4* (*w***; P{wGawB}ey*^{OK107}*/In(4)ci*^{D}*, ci*^{D} *pan*^{ciD} *sv*$^{spa\text{-}pol}$) (Connolly et al., 1996) from the Bloomington stock centre. *mb247-LexA::VP16* (Pitman et al., 2011), *mb247-LexA::VP16:LexAop-rCD2::RFP* and *UAS-shi*^{ts} flies (Pfeiffer et al.,

2012) were obtained from Scott Waddell's laboratory (CNCB, Oxford). Andrew Lin (Miesenböck group, CNCB, Oxford) provided *LexAop-Gal80* flies (Thistle et al., 2012). Deficiency lines (Cook et al., 2012) for the 2nd and 3rd chromosomes were obtained from the Bloomington Deficiency Kit.

FoxP promoter strain

I generated a *FoxP-GAL4* line by amplifying a 1,373 bp putative promoter site immediately upstream of the predicted *FoxP* coding DNA sequence from a BAC (RPCI-98 BAC library, Hoskins et al., 2000). The amplification was done using the KAPA HiFi DNA polymerase protocol (KAPABIOSYSTEMS). The primer sequences used were F: CACCCGCCCGTTATTAAATATAATATTG and R: GTTTTTAAAACTGAAATTTATAATCATTAC. The PCR protocol involved an initial 5 min denaturation at 95 °C, followed by 30 cycles of denaturation for 20 s at 98 °C, 15 s annealing at 58 °C and 1 min 30 s extension at 72 °C, ending with a final 5 min extension at 72 °C, after which the samples were maintained at 4 °C until further use. The amplified product was cleaned using the Zymo Research DNA clean and concentrator protocol. The clean PCR product was then ligated in a TOPO cloning reaction (Invitrogen) to the pENTR TOPO cloning vector. One Shot TOP10 *Escherichia coli* were then transformed, through heat shock and incubation on ice for 30 min, and grown overnight. Plasmids were purified from individually recovered colonies using the QIAGEN QIAprep spin miniprep kit, and

sequenced by Source Biosciences. Finally, Gateway LR cloning (Invitrogen) was used to excise the *FoxP* promoter fragment from the pENTR-*FoxP* vector and integrate it in the pBPGUw vector which contains the *Drosophila* minimal core promoter (DSCP) (Pfeiffer et al., 2008). This was achieved by incubating both vectors in the enzyme mix for 60 min and then terminating the reaction with proteinase k at 37 °C for 10 min. Library Efficiency DH5α *E. coli* were transformed with the resulting pBPGUw-*FoxP* vector. The vector was recovered from individual colonies and sequenced. The Maxi kit protocol (QIAGEN) was used to obtain the appropriate quantity of the vector, which was then integrated into the genomic *attP-40B* site via ΦC31 recombination (Groth et al., 2004; Bischof et al., 2007) by Rainbow Transgenics. The resulting flies were crossed to w^{1118} flies.

Behavioural experiments

The olfactory choices of 20 flies were simultaneously analysed in a custom-built, fully automated apparatus (Claridge-Chang et al., 2009; Figure II-1 A). Individual flies were lodged in chambers made of clear polycarbonate (length 50 mm, width 5 mm, height 1.3 mm) to allow side-view movement tracking along the long chamber axis. Each chamber had odour/air inlet ports at the left and right extremes of the long chamber axis (Figure II-1 B). At the centre, laterally located outflow vents allowed the converging odour streams from each side of the chamber to exit (Figure II-1 B). The floors and ceilings of the chambers consisted of printed circuit boards (PCBs). The PCBs were

connected to a 70 V source via solid-state relays (Fairchild HSR312L). The odour/air inlets also served as electrical leads (Figure II-1 B).

Six mass flow controllers (CMOSens PerformanceLine, Sensirion) supplied with filtered, compressed air, regulated air and odour flow. Two 5,000 ml capacity MFCs controlled left and right arm carrier airflows and four 500 ml capacity MFCs regulated odour flows in the left and right chamber arms. The odour streams were drawn through vials containing pure 4-methylcyclohexanol (MCH; SIGMA) or MCH diluted in 100 ml liquid mineral oil. The left and right air-odour streams (5 l/min each) were split between 20 chambers, yielding a flow rate of 0.25 l/min per half-chamber. The stack of 20 chambers was backlit by 940 nm LEDs (TSAL6100, Vishay), and imaged simultaneously by a Stingray F080B CCD camera (Allied Vision Technologies) equipped with an 18 mm lens (Edmund Scientific) (Figure II-1 A). The apparatus was operated in a temperature-controlled incubator (Sanyo MIR-154). A LabVIEW 9 (National Instruments) written virtual instrument extracted the flies' position in the chambers from video images (Figure II-1 C), and also controlled the delivery of odours and electric shock.

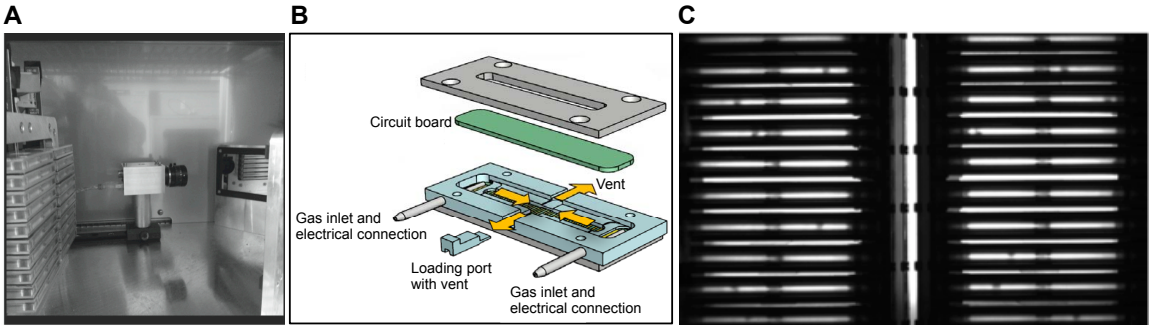


Figure II-1: The custom-built, fully automated apparatus for analysing olfactory choice (Claridge-Chang et al., 2009). (A) A stack of 20 chambers, arranged in two side-by-side stacks by slotting their metal air and odour inlet tubes into gas distribution manifolds, backlit by LEDs, was imaged side-on by a CCD camera; the gas tubes also served as electrical

leads. **(B)** Schematic representation of the behavioural chamber: flies were loaded through a lateral, centrally located port and viewed side-on through transparent polycarbonate walls; air and odour mixtures entered the chamber through inlets at the ends and exited through vents at the centre; electric shocks were delivered via floor and ceiling circuit boards (adapted from Claridge-Chang et al., 2009). **(C)** Image of 20 flies in individual chambers as viewed by the CCD camera.

Only male flies were analysed. Males of the appropriate genotype were analysed 5 days post-eclosion after being separated from the fly population 1 day before behavioural experiments.

Trained olfactory behavioural data presented in Chapters III and IV were obtained during a 2 min presentation of different relative concentrations of MCH on either side of the chamber. In the case of the masking odour and mixture experiments, 3-octanol (OCT; SIGMA) was also used. For electric shock reinforcement, the relays were activated once for 1 s during each of 12 consecutive 20 s odour presentations, which were interweaved with 20 s air presentations. Testing took place 50 s after reinforcement training. Flies were trained and tested at 25 °C and also at 30 °C in the case of experiments with *UAS-Kir2.1*. In all behavioural experiments presented in Chapter IV driver line females were crossed with effector strain males, and the controls were obtained by crossing the same sex parental line with CS flies.

Behavioural data relating to the deficiency screen, presented in Chapter V, were acquired using a simplified discrimination task, in which a concentration of 10^{-4} volumes of MCH per volume of air was reinforced with electric shock and tested against air. The deficiencies were analysed in a sensitised background, by crossing female *FoxP*$^{5\text{-SZ-}3955}$ mutants with males from each Bloomington Deficiency kit line for the 2nd and 3rd chromosomes. *FoxP*$^{5\text{-SZ-}3955}$

heterozygous males (obtained by crossing mutant females to CS) were used as controls.

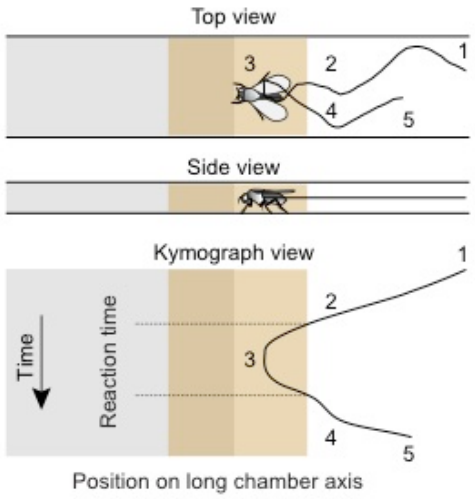
Naive olfactory discrimination data presented in Chapter VI were obtained during a 2 min odour presentation of different relative concentrations of MCH on either side of the chamber, or simply of air and MCH. Experiments with *UAS-shi*^{ts} were performed at 30 °C.

Data analysis

Experimental data were batch-processed offline in MATLAB 2012a (The MathWorks). Position measurements were smoothed by computing 0.5 s moving averages and filtered to discard flies making <2 end-to-centre runs per 2 min measurement period. Accuracy scores were determined as the percentage of entries into the side of the chamber with the lower odour concentration, either as the result of a reversal or a traversal [(number of decisions in favour of lower MCH concentration/total number of decisions) X 100%]. For naive behaviour, the fraction of choices in favour of the lower MCH concentration or air was calculated in the same way.

A central 7 mm wide zone was defined as the decision zone for reaction time measurements. The time between entry into and exit from the decision zone was quantified as the reaction time (Figure II-2). Each movement into the decision zone consisted of three phases: high velocity entry; slowdown, pausing, and/or short excursions at the interface; acceleration and exit. To

control for intra- and inter-individual variation in walking speed, reaction times were normalized to the fly's velocity upon entry into the decision zone. The baseline velocity was estimated as the average speed from the point of entry to the first pause, which was defined as a reduction in walking speed to 10% of the entry velocity.



FigureII-2: Schematic representation of a fly's movement trajectory during a reversal at the odour interface. The black like represents the trajectory of the fly: a movement sequence as seen from the top, when imaged from the side, results in position data on the long chamber axis over time, as represented in the kymograph view. The orange colour represents the 7 mm wide decision zone; the grey shading on the left represents the higher MCH concentration, previously reinforced or not (in the case of naive data), which must be distinguished from either a lower MCH concentration on the right, or air (in the case of the deficiency screen or detection data). Since it is the centroid of the fly's silhouette that is monitored, rather than the position of the antennae, the trajectory stops short of the odour interface.

Transit times were measured in a 7 mm wide zone located off centre, halfway within the 'correct' arm of the chamber, i.e., the side in which the lower odour concentration is presented.

Statistics

Data were analysed in Prism 6 (GraphPad) and MATLAB 2012a (The MathWorks). Kruskal-Wallis ANOVA, followed by planned pairwise post hoc analyses using Dunn's test, was used to compare mean decision accuracies or the fraction of choices in favour of the lower MCH concentration (in the case of naive behaviour) or air (in the case of deficiency screen data and naive odour detection data). Reaction and transit time distributions were evaluated with the Kolmogorov-Smirnov test, using the Bonferroni correction to adjust the level of statistical significance in cases involving multiple comparisons.

Data modelling

Behavioural data were fit to a simple drift-diffusion model (Palmer et al., 2005). This type of model decomposes reaction times into decision and residual times (Figure II-3). While the residual time encompasses sensory and motor latencies, procrastination, and time required to indicate a choice, the decision time constitutes the integration period *per se*. The duration of the decision time depends on the mean rate at which evidence accrues (the drift rate) and the level of the decision criterion (the bound height) (Figure II-3).

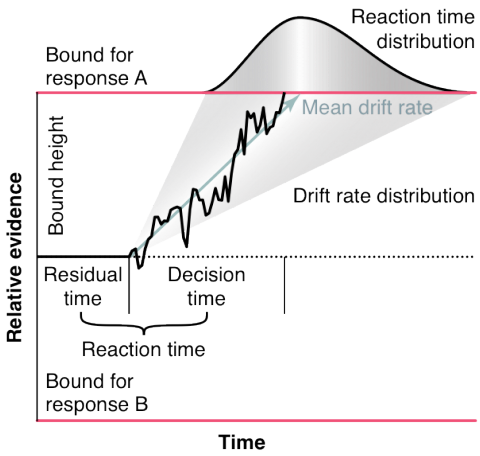


Figure II-3: Schematic representation of the drift-diffusion model of evidence accumulation. The evidence accumulation sequence depicted (black jagged line) reaches the bound for response A with a mean drift rate. The reaction time measured in the behavioural experiments encompasses both the residual time and the decision time itself. The symmetrical drift rate distribution results in a right skewed reaction time distribution.

The drift-diffusion model consists of coupled analytical expressions for chronometric and psychometric functions:

$$T(x) = \frac{A}{kx}\tanh Akx + t_{residual} \qquad (1)$$

$$F(x) = F_{max}\frac{1}{1+e^{-2Akx}} \qquad (2)$$

$T(x)$ and $F(x)$ are the reaction time and accuracy, respectively, and are functions of stimulus contrast, x, quantified as |log (odour concentration ratio)|. A is the height of the symmetrical bounds for the two alternative responses and k is the drift rate, both being normalized by the diffusion coefficient (Palmer et al., 2005). F_{max} is the empirically determined fraction of accurate choices in the easiest discrimination task (concentration ratio 0.1), typically 0.94–0.97; $t_{residual}$ is the residual time. The free model parameters A, k, and $t_{residual}$ were determined by fitting Eq. (1) to reaction time data,

using the trust-region algorithm for nonlinear least-squares regression implemented in MATLAB 2012a. The resulting parameter values were inserted into Eq. (2) to predict decision accuracies. The residual time was estimated as 1.452 s.

Structural imaging

To visualize native fluorescence, 1-day-old adult fly brains were dissected in ice-cold 4% paraformaldehyde solution in phosphate buffered saline (PBS) [1.86 mM NaH_2PO_4, 8.41 mM Na_2HPO_4, 175 mM NaCl] and fixed for an additional 60 min at room temperature. Samples were then washed 3 x 10 min with PBS containing 0.1% Triton-X100 (PBS-T), and 2 x 10 min in PBS before mounting in Vectashield (Vector Labs).

For immunostaining against Bruchpilot, a pan-neuronally expressed protein localised to active zones (Wagh et al., 2006), samples were blocked in 5% goat serum in PBS-T for an hour. They were subsequently incubated at 4 °C for 2 days in PBS-T containing mouse nc82 antibody (1:100) (hybridoma bank). After washing 5 x 20 min in PBS-T, secondary anti-mouse antibody conjugated to Alexa 546 (Life Technologies Corporation) (1:500) was applied for 1 day at 4 °C.

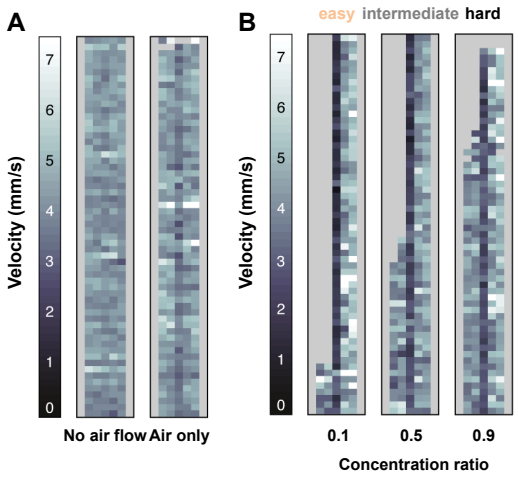
Imaging was performed on a Leica TCS SP5 X confocal microscope. Images were processed in AMIRA 5.3 (Mercury Systems).

Chapter III. The role of *FoxP* in trained olfactory decision making

A fully automated olfactory behaviour setup that tracks the positions of 20 flies in individual chambers (Claridge-Chang et al., 2009) was used to develop a two-alternative forced-choice intensity discrimination assay to study olfactory decision making (DasGupta et al., 2014), as described in the Materials and Methods section. Flies were trained, using electric shock reinforcement, to avoid a specific concentration of the odorant 4-methylcyclohexanol (MCH) and then had to distinguish the reinforced concentration from a lower concentration of the same odour. The difficulty of the task was titrated by changing the ratio of the odour intensities to be discriminated: easier tasks involved dissimilar odour concentrations (lower concentration ratios), whereas increasing the similarity of the odour intensities (higher concentration ratios) constituted more difficult discrimination tasks.

When no odour or air was flowing through the chambers, the flies paced the entire length of the chambers with uniform velocity (Figure III-1 A). When air or odour-air mixtures were perfused into the chambers, a central 7 mm wide decision zone was defined where the streams converged and the flies displayed a velocity drop (Figure II-2; Figure III-1 A–B). This velocity drop at the central decision zone was modest when airflow alone was introduced (Figure III-1 A), and pronounced when air-odour mixtures were perfused on both sides of the chamber (Figure III-1 B).

With odours present, the flies slowed upon entry into the decision zone, paused and/or made short excursions at the interface, accelerated and exited after committing to a choice (Figure II-2; Figure III-1). The time between entry and exit of the decision zone was quantified as the reaction time. The reaction time, but not the transit time in other 7 mm wide zones in the chamber, varied with the difficulty of the task presented (Figure III-1 C). Furthermore, the error rate in the choice between the reinforced and non-reinforced odour intensity also increased with task difficulty (Figure III-1 C). These difficulty-dependent changes are clearly evident in example movement trajectories (Figure III-1 D): in easy discrimination tasks (concentration ratio 0.1) the flies made quick incursions into the decision zone and rapidly exited to the non-reinforced odour side; in intermediate discrimination tasks (concentration ratio 0.5) the flies lingered longer at the interface and made some incorrect choices to the reinforced odour side; in difficult discrimination tasks the time spent at the interface was further increased, and choices in favour of the reinforced odour became as frequent as correct choices.



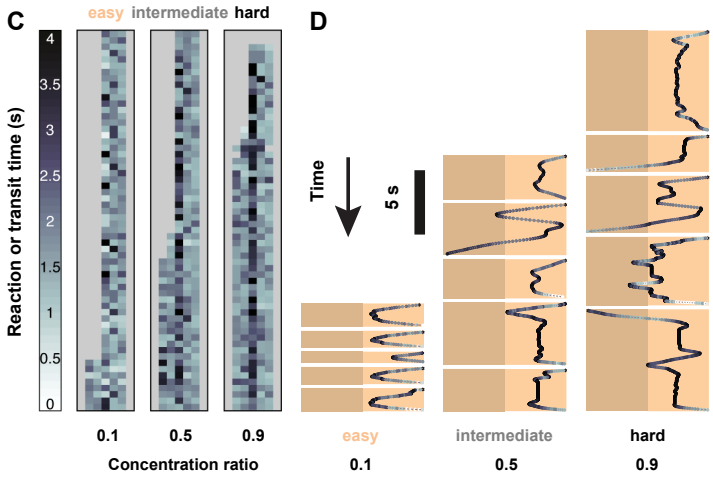


Figure III-1: Behaviour of wild-type flies in the individual chambers. (A–C) Colour-coded matrices of the average walking velocities **(A, B)** and reaction or transit times **(C)** of 60 randomly selected individuals (rows) during a 2 min experiment. The behavioural chambers are divided into seven equally sized zones, including the central decision zone. Only data from the five innermost zones are shown (columns) because behaviour in the 2 outermost zones is influenced by the wall. Blank entries are due to individuals making <2 decisions per measurement period or <2 entries into a particular zone. **(A)** Note the uniform velocity in the absence of airflow and a slight drop in velocity in the central decision zone in the presence of airflow, possibly due to turbulence from the converging airstreams. **(B, C)** The aversively reinforced concentration of MCH is present on the left and must be distinguished from a lower MCH concentration on the right; the concentration ratios of comparison to the reinforced odour are indicated at the bottom. Individuals are sorted by the number of zones they entered. In the central decision zone, note the uniform velocity drop (represented by dark colour) **(B)** and the difficulty-dependent increase in reaction time (represented by dark colour) and error rate (entries into the left half of the chamber) **(C)**. **(D)** Example kymographs of wild-type flies discriminating different MCH intensities.

Flies performed intensity discrimination tasks for nine odour concentration ratios at a reinforced MCH intensity of ~12 parts per billion (ppb), corresponding to 10^{-4} volumes of saturated vapour per volume of air (Figure III-2). Their accuracies, the percentage of decisions in favour of the non-reinforced odour, were nearly 100% in easy tasks involving the discrimination between large concentration differences (concentration ratios 0.1–0.2) (Figure III-2 A). Accuracies dropped, however, from intermediate discrimination tasks (from concentration ratio 0.5) compared to the performance in easy discrimination tasks (concentration ratio 0.1) (Figure III-2 A; Appendix Table

1), and the flies performed randomly when the odour concentrations differed by only 10% (concentration ratio 0.9) (Figure III-2 A). Reaction times also changed with the difficulty of the discrimination task (Figure III-1 C; Figure III-2 B–D), and from concentration ratio 0.2 were significantly increased compared to the easiest discrimination task (concentration ratio 0.1) (Figure III-2 B; Appendix Table 1). Reaction times were significantly increased (concentration ratio 0.2–0.4) even when flies maintained very high accuracies, comparable to that in the easiest discrimination task (concentration ratio 0.1) (Figure III-2 A–B; Appendix Table 1). Reaction times continued to increase from intermediate tasks (concentration ratio 0.5) to difficult tasks (concentration ratio 0.9), where they showed a ~55% increase compared to easy discrimination tasks (Figure III-2 B; Appendix Table 1). This task difficulty dependent increase in reaction times was further evident analysing the frequency and cumulative frequency distributions of reaction times in easy, intermediate and difficult tasks (concentration ratios 0.1, 0.5 and 0.9 respectively) (Figure III-2 C–D). In contrast, transit times, i.e. the times spent in a 7 mm wide zone located off-centre in the non-reinforced odour side of the chamber, were unaltered with task difficulty (Figure III-2 B–D; Appendix Table 2).

The data presented here are consistent with models of evidence accumulation to a decision threshold (Ratcliff and Smith, 2004; Palmer et al., 2005; Bogacz et al., 2006; reviewed in Gold and Shadlen, 2007): flies compensate for weaker evidence (lower stimulus contrast) by gathering information for longer periods of time. Indeed, since overall odour concentrations were highest in the low-contrast tasks that took the longest to complete and only relative stimulus contrast, not absolute stimulus intensity, affected reaction times (Figure III-2

B–D; Appendix Table 1), these data favour integration over probability summation (Watson, 1979): if the probability of odour detection were rate-limiting, reaction time would be expected to correlate inversely with stimulus intensity (Watson, 1979; Luce, 1986).

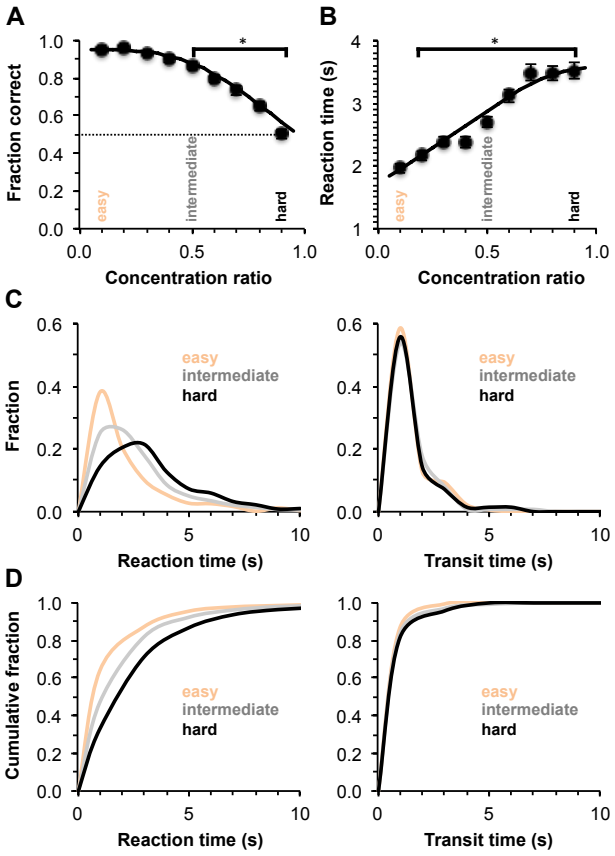


Figure III-2: Decision accuracies and reaction times of wild-type flies in a trained olfactory discrimination assay. (A–D) Wild-type flies were trained to perform intensity discrimination tasks at 10^{-4} MCH concentration. **(A)** Accuracies (mean±SEM; *N*=142–173 flies per data point) as a function of the difficulty of the task. Accuracies of 0.5 correspond to performance at chance level (dotted line). Asterisks indicate significant differences from concentration ratio 0.1 (Kruskal-Wallis ANOVA followed by Dunn's test; *P*<0.0111, Appendix Table 1). The black line depicts the psychometric function predicted by a drift diffusion model (Palmer et al., 2005). **(B)** Reaction times (mean±SEM; *N*=592–828 decisions per data point) as a function of the difficulty of the task. Asterisks indicate significant differences from concentration ratio 0.1 (Kolmogorov-Smirnov test; *P*<0.0005, Appendix Table 1). The black line depicts the chronometric function predicted by a drift diffusion model (Palmer et al., 2005). **(C–D)** Frequency **(C)** and cumulative frequency **(D)** distributions of reaction (right) and transit (left) times at odour concentration ratios corresponding to easy (0.1), intermediate (0.5) and hard (0.9) difficulty levels. Reaction time distributions differ between difficulty levels (Kolmogorov-Smirnov test; *P*<0.0001, Appendix Table 2) but transit time distributions do not (Kolmogorov-Smirnov test; Appendix Table 2).

A simple drift-diffusion model of evidence integration (Palmer et al., 2005), described in Materials and Methods, was used to quantitatively analyse the relationship between the psychometric and chronometric data (Figure II-3; Figure III-2 A–B). This type of model, used commonly to describe sensory-motor decisions in humans and non-human primates (Luce, 1986; Ratcliff and Smith, 2004; Palmer et al., 2005; Bogacz et al., 2006; reviewed in Gold and Shadlen, 2007), decomposes reaction times into residual and decision times. The decision time, which constitutes the integration period *per se*, depends on the mean rate at which evidence accumulates (drift rate) and the level of the response criterion (bound height). The residual time encompasses sensory and motor latencies, procrastination, and the time necessary to indicate a choice. The three free model parameters (residual time, drift rate and bound height) are estimated from reaction time measurements, and used to generate a prediction of the corresponding decision accuracies. The modelled chronometric and psychometric functions provided satisfying simultaneous fits to the performance data (Figure III-2 A–B).

Consistent with information accumulation to threshold, the reaction time distributions exhibited a characteristic positive skew (that is, a tail of extended reaction times), while transit times did not (Figure III-2 C). This type of distribution is explained by the drift-diffusion model, in which equal differences in drift rate give raise to unequal differences in reaction time at the intersection with the response bound (Figure II-3). Furthermore, for more difficult tasks, reaction time distributions are shifted to the right and display broader distributions, also consistent with the drift-diffusion model, and explained by changes in mean drift rate (Figure III-2 C). This modelling

exercise further confirmed that *Drosophila melanogaster*'s behaviour in this olfactory discrimination assay is consistent with evidence accumulation to threshold.

To assess whether the relationship between task difficulty and reaction time was specific to the intensity discrimination assay or generalised to other types of tasks, two further assays were designed and analysed: a masking odour task and a mixture discrimination task (Figure III-3). The masking odour task consisted in shock-reinforcing MCH and then testing flies for MCH detection in a ubiquitous background of 3-octanol (OCT) (Figure III-3 A). The difficulty of the task was adjusted by varying the level of masking odour while keeping the concentration of cue constant. Compared to the control task, in which only MCH and air were presented during the test, adding a masking odour decreased the flies' ability to accurately avoid MCH in both masking cue : odour ratios tested (1.25 and 1.75) (Figure III-3 B; Appendix Table 3). Reaction times significantly increased compared to the control task, for both ratios tested (Figure III-3 C; Appendix Table 3). Adding OCT during testing at the highest level of background odour concentration tested (masking odour : cue ratio of 1.75) increased reaction times by ~50%, but flies still maintained an accuracy of ~80% of that of the control situation (Figure III-3 B–C).

The binary mixture discrimination task (Uchida and Mainen, 2003; Abraham et al., 2004; Rinberg et al., 2006) consisted of shock reinforcing a mixture with a particular relative concentration of MCH and OCT and testing this mixture against a mixture with reversed relative concentrations of each odour (Figure III-3 D). Accuracies decreased for closer proportions of MCH and OCT, compared to a 80:20 MCH:OCT control ratio, significantly for a 55:45 ratio

(Figure III-3 E; Appendix Table 4). Reaction times increased in both 70:30 and 55:45 odour ratios (Figure III-3 E; Appendix Table 4), and were ~64% higher for the latter ratio, compared to an 80:20 mixture ratio.

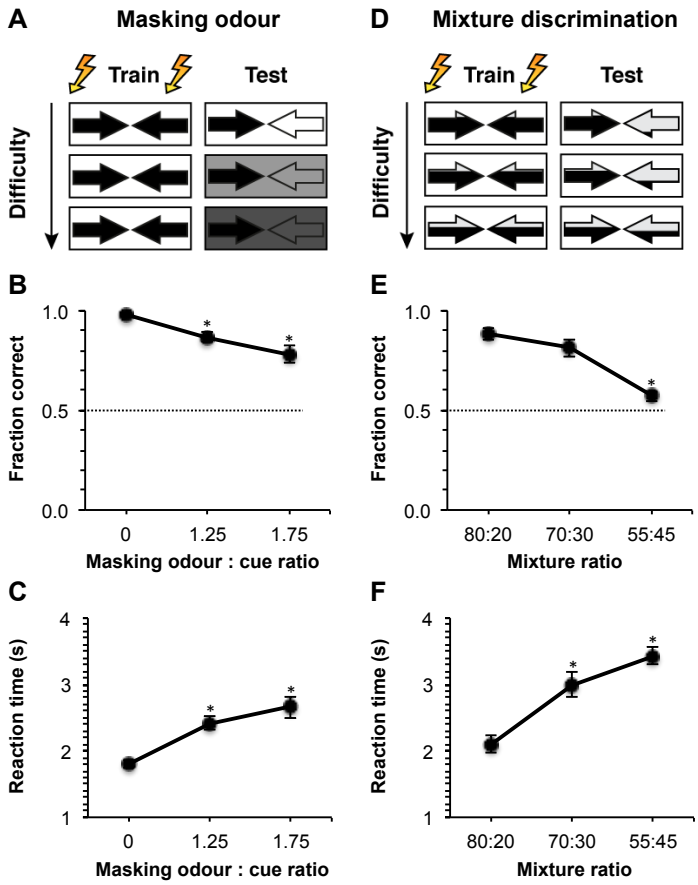


Figure III-3: Masking odour and mixture discrimination tasks. (A–C) Wild-type flies performed a masking odour discrimination task in which ~12 ppb MCH was discriminated in a background of OCT. **(A)** Schematic representation of experimental conditions during electric shock training and testing. Arrows symbolize the converging odour streams; black represents the odour MCH and the intensities of grey shading indicate OCT intensities. **(B)** Accuracies (mean±SEM; *N*=47–86 flies per data point) as a function of the difficulty of the task. Accuracies of 0.5 correspond to performance at chance level (dotted line). Asterisks indicate significant difference from masking odour : cue ratio of 0 (Kruskal-Wallis ANOVA followed by Dunn's test; *P*<0.0001, Appendix Table 3). **(C)** Reaction times (mean±SEM; *N*=169–341 decisions per data point) as a function of the difficulty of the task. Asterisks indicate significant differences from masking odour : cue ratio of 0 (Kolmogorov-Smirnov test; *P*<0.0001, Appendix Table 3). **(D–F)** Wild-type flies performed a MCH and OCT mixture discrimination task. **(D)** Schematic representation of experimental conditions during electric shock training and testing. Arrows symbolize the converging odour streams; black (MCH) and grey (OCT) fill represent the odour mixture composition. **(E)** Accuracies (mean±SEM; *N*=35–165 flies per data point) as a function of the difficulty of the task. Accuracies of 0.5 correspond to performance at chance level (dotted line). The asterisk indicates significant difference from mixture ratio 80:20 (Kruskal-Wallis ANOVA followed by Dunn's test; *P*<0.0001, Appendix Table 4). **(F)** Reaction times (mean±SEM; *N*=126–619 decisions per data point) as a function of the difficulty of the task. Asterisks indicate significant differences from mixture ratio 80:20 (Kolmogorov-Smirnov test; *P*<0.0001, Appendix Table 4).

The behavioural data acquired in three different types of trained olfactory assays showed that *Drosophila melanogaster* exhibits a decision making process consistent with evidence integration to threshold to discharge a behavioural output of choice. Furthermore, using the olfactory discrimination data, this process was found to be in agreement with a drift diffusion model, similarly to vertebrate decision-making processes (Luce, 1986; Ratcliff and Smith, 2004; Palmer et al., 2005; reviewed in Gold and Shadlen, 2007).

The circuit mechanisms responsible for the build-up of a decision and discharging the behaviour once the decision is made have so far remained elusive. An advantage of studying decision making in the fruit fly in a high throughput manner is the ability to use forward genetics to uncover cellular and molecular mechanisms.

A preliminary analysis of 41 fly strains carrying mutations in neuronally expressed candidate genes (DasGupta, unpublished results) uncovered a potential decision making phenotype in a strain homozygous for a P-element insertion in the locus encoding the transcription factor FoxP. *FoxP* genes are a subfamily of forkhead box (*Fox*) genes, with four members in vertebrates (reviewed in Takahashi and Takahashi, 2009). In *Drosophila*, the single *FoxP* gene consists of six constitutively and two alternatively spliced exons that give rise to two predicted transcripts (RD and RC) and corresponding 422 aa and 520 aa protein isoforms (FoxP-A and FoxP-B) (Santos et al., 2011) (Figure III-4). Both isoforms are expressed in the central nervous system from embryonic stage eight, and share an N-terminal zinc finger domain but possess different C-terminal forkhead domains (Santos et al., 2011) (Figure III-4).

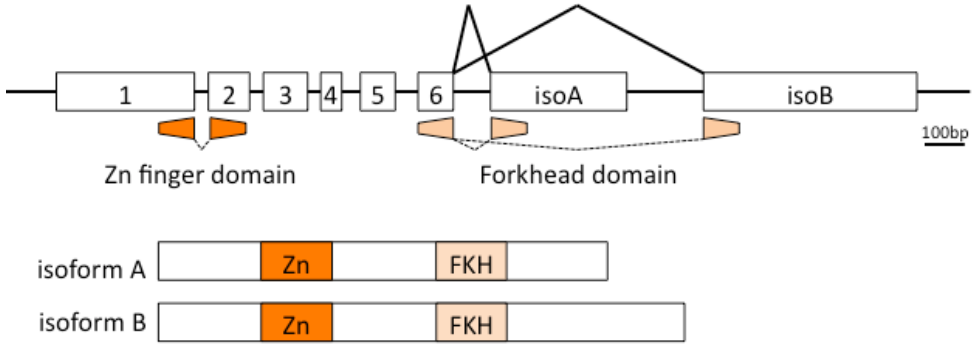


Figure III-4: Organisation of the *Drosophila FoxP* gene and isoforms. The *FoxP* gene contains six constitutively active and two alternatively spliced exons. The alternatively spliced exons give rise to two isoforms (A and B) that share a zinc finger domain (Zn) and possess different forkhead domains (FKH). Adapted from Santos et al., 2011.

Behavioural characterization of the *FoxP* phenotype

The *FoxP* mutant most extensively studied in this thesis, *FoxP*$^{5\text{-SZ-}3955}$, carries a P-element insertion in the *FoxP* locus, which is located on the right arm of the 3rd chromosome and spans 4,659 bp (Figure III-5). The insertion affects the alternatively spliced 8th exon that gives rise to the isoform FoxP-B.

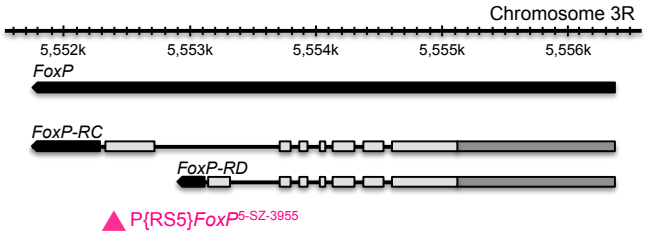


Figure III-5: The *FoxP* locus. The *FoxP* locus is located on the right arm of the 3rd chromosome and spans from 5,551,742 to 5,556,401 bp. The *FoxP*$^{5\text{-SZ-}3955}$ mutant strain results from a P-element insertion in the 8th exon, alternatively spliced to give rise to the transcript FoxP-RC and isoform FoxP-B.

I analysed the behaviour of wild-type (wt) and *FoxP*$^{5\text{-SZ-}3955}$ mutant flies in trained MCH discrimination tasks of varying difficulty, adjusted by changing

two parameters: the ratio of the odour concentrations to be discriminated, and the absolute odour intensities (Figure III-6). Four odour concentration ratios were tested at absolute odour concentrations of 10^{-1} and 10^{-4} volumes of saturated vapour per volume of air. Both wild-type and *FoxP*$^{5\text{-SZ-}3955}$ mutants showed a decrease in accuracy (Figure III-6 A and G; Appendix Table 5) in difficult tasks (concentration ratios 0.7–0.9), compared to that in easy tasks (concentration ratio 0.1), at both absolute MCH concentrations. Similarly, both fly strains took longer to decide (Figure III-6 B–D and H–J; Appendix Table 5) in difficult tasks (concentration ratios 0.7–0.9) than in easy discriminations (concentration ratio 0.1), for both absolute MCH concentrations tested. Furthermore, the distributions of reaction times of wild-type and *FoxP*$^{5\text{-SZ-}3955}$ in easy and difficult tasks at 10^{-1} and 10^{-4} absolute MCH concentration (Figure III-6 C and I) exhibited positive skew—a characteristic of information accumulation to threshold (Luce, 1986; Roitman and Shadlen, 2002; Ratcliff and Smith, 2004; reviewed in Gold and Shadlen, 2007).

FoxP$^{5\text{-SZ-}3955}$ mutants distinguished the shock-reinforced MCH concentration with the same accuracy as wild-type flies (Figure III-6 A and G; Appendix Table 6). However, the mutants exhibited longer reaction times than wild-type flies at both absolute MCH concentrations tested (Figure III-6 B–D and H–J; Appendix Table 6). The mutants displayed a subtle defect in easy discriminations (concentration ratios 0.1–0.4) and a strong defect in difficult tasks (concentration ratios 0.7–0.9) (Figure III-6 B–D and H–J; Appendix Table 6). Mutant reaction times approximately doubled in the 0.9 concentration ratio discrimination task compared to 0.1: while wild type flies took 2.576±0.094 s and 2.761±0.106 s (mean±SEM), *FoxP*$^{5\text{-SZ-}3955}$ mutants

took 4.302±0.217 s and 4.976±0.326 s (mean±SEM) to decide at 10^{-1} and 10^{-4} MCH, respectively (Figure III-6 B and H; Appendix Table 6). An analysis of the frequency and cumulative frequency distributions of reaction time further demonstrates this difference: the distributions differed subtly in easy discriminations (concentration ratio 0.1) but in a pronounced fashion in difficult tasks (concentration ratio 0.9) (Figure III-6 C–D and I–J; Appendix Table 6).

This two-alternative forced-choice intensity discrimination assay further allowed assessing potentially confounding problems that could influence reaction times: locomotor and olfactory acuity defects. Analysing the frequency and cumulative frequency distributions of transit times, which provide indices of walking speed, showed that *FoxP*$^{5\text{-SZ-}3955}$ mutants and wild-type flies display similar transit times and therefore do not differ in locomotor capabilities (Figure III-6 E–F and K–L; Appendix Table 7). These distributions corroborate the specificity of the reaction time defect in *FoxP*$^{5\text{-SZ-}3955}$: the performance of mutants differs from that of wild-type flies only at the central decision zone, where the choice between the two odour concentrations is made.

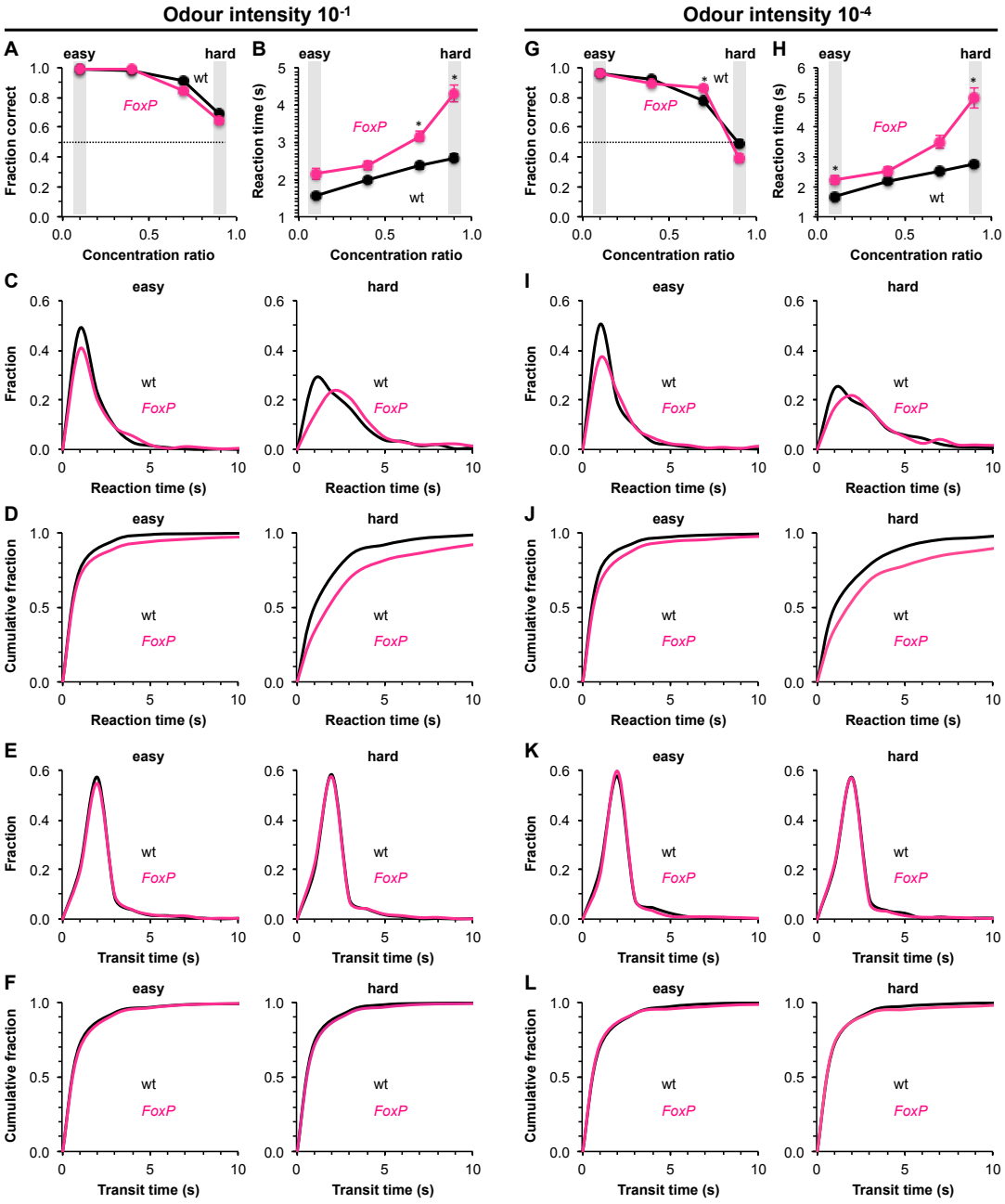


Figure III-6: Decision accuracies and reaction times of wild-type and *FoxP*$^{5\text{-SZ-3955}}$ mutants. (A–L) Wild-type (wt, black) and *FoxP*$^{5\text{-SZ-3955}}$ mutant (*FoxP*, red) flies were trained to perform intensity discrimination tasks at high (10^{-1}, **A–F**) and low (10^{-4}, **G–L**) concentrations of MCH. **(A, G)** Accuracies (mean±SEM; *N*=129–182 flies per data point) as a function of the difficulty of the task. Accuracies of 0.5 correspond to performance at chance level (dotted line). The asterisk indicates a significant difference between *FoxP*$^{5\text{-SZ-3955}}$ mutant and wild-type flies (Kruskal-Wallis ANOVA followed by Dunn's test; *P*<0.0463, Appendix Table 6). **(B, H)** Reaction times (mean±SEM; *N*=422–802 decisions per data point) as a function of the difficulty of the task. Asterisks indicate significant differences between *FoxP*$^{5\text{-SZ-3955}}$ mutant and wild-type flies (Kolmogorov-Smirnov test; *P*<0.0014, Appendix Table 6). **(C–D, I–J)** Frequency **(C, I)** and cumulative frequency **(D, J)** distributions of reaction times of wild-type and *FoxP*$^{5\text{-SZ-3955}}$ mutant flies at easy (left, 0.1 concentration ratio) and hard (right, 0.9 concentration ratio) difficulty levels. **(E–F, K–L)** Frequency **(E, K)** and cumulative frequency **(F, L)** distributions of transit times of wild-type and *FoxP*$^{5\text{-SZ-3955}}$ mutant flies at easy (left, 0.1 concentration ratio) and hard (right, 0.9 concentration ratio) difficulty levels. Reaction time

distributions differ between genotypes (Kolmogorov-Smirnov test; $P<0.0014$, Appendix Table 6) but transit time distribution do not (Kolmogorov-Smirnov test; Appendix Table 7).

Olfactory acuity defects could be ruled out by analysing accuracy scores, which are dependent not only on learning capabilities, but also on the ability to discriminate the different odour concentrations. *FoxP*$^{5\text{-SZ-}3955}$ mutant flies discriminate odours at least to the same level of wild-type flies and therefore display similar odour detecting abilities (Figure III-6 A and G; Appendix Table 6). Furthermore, a comparison between the performance accuracies displayed in the two odour intensities analysed, 10^{-1} and 10^{-4}, showed that neither genotype's scores changed with absolute odour concentration (Appendix Table 8). A 1,000-fold dilution therefore had no effect on the performance of *FoxP*$^{5\text{-SZ-}3955}$ or wild-type controls, showing that both detected odours with the same sensitivity.

Since learning, olfactory acuity and locomotion were similar between *FoxP*$^{5\text{-SZ-}3955}$ mutants and wild-type flies, the mutants differed from wild-type primarily in stimulus contrast dependant reaction time. *FoxP*$^{5\text{-SZ-}3955}$ mutants therefore appear impaired in the accumulation and/or retention of information in the lead-up to a difficult choice, and require more time before committing to a choice of similar accuracy as that made by wild-type flies.

Drift-diffusion model

Since the behavioural data of wild-type flies were well described by a simple drift-diffusion model (Palmer et al., 2005), applying the same model to the performance of the *FoxP*$^{5\text{-}SZ\text{-}3955}$ mutant should allow some insight into the nature of the changes in the decision making process in these flies. The behaviour of wild-type and mutant flies in 10^{-1} MCH discrimination tasks was therefore fit to a drift-diffusion model (Palmer et al., 2005), as outlined in Materials and Methods (Figure II-3 and Figure III-7). The residual time was determined as 1.452 s from wild-type reaction time data in 10^{-4} MCH discrimination tasks (Figure III-2). Wild-type and *FoxP*$^{5\text{-}SZ\text{-}3955}$ reaction time data in the 10^{-1} MCH discrimination tasks were used to estimate drift rates and bound heights (Figure III-7 B). The estimated model parameters (residual time, drift rate and bound height) were then used to predict decision accuracies (Figure III-7 A) for each fly strain. This modelling exercise provided satisfying simultaneous fits of the chronometric and psychometric functions for wild-type and *FoxP*$^{5\text{-}SZ\text{-}3955}$ data (Figure III-7 A–B) and allowed the identification of two parameter changes that account for the mutant's phenotype (Figure III-7 C–D): a 38% drop in drift rate and a 35% increase in the height of the decision bound.

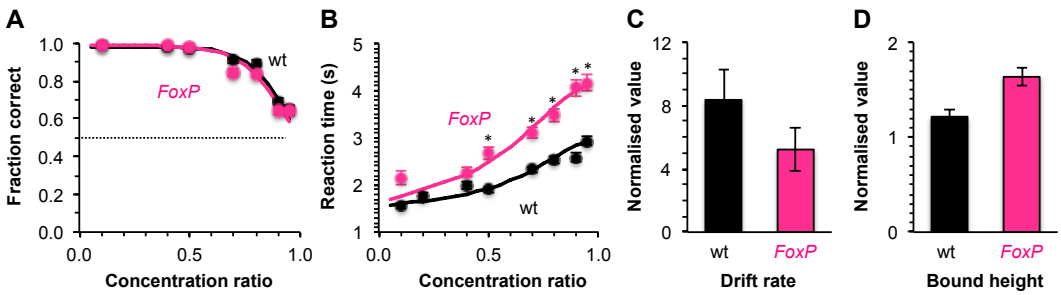


Figure III-7: Drift-diffusion models of decision accuracies and reaction times in wild-type and *FoxP*$^{5\text{-SZ-3955}}$ mutant flies. Wild-type (wt, black) and *FoxP*$^{5\text{-SZ-3955}}$ mutant (*FoxP*, red) flies were trained to perform intensity discrimination tasks at high (10^{-1}) concentrations of MCH. **(A)** Accuracies (mean±SEM; *N*=129–193 flies per data point) as a function of the difficulty of the task. Accuracies of 0.5 correspond to performance at chance level (dotted line). Solid lines depict the psychometric functions predicted by a drift diffusion model (Palmer et al., 2005). **(B)** Reaction times (mean±SEM; *N*=422–857 decisions per data point) as a function of the difficulty of the task. Asterisks indicate significant differences between *FoxP*$^{5\text{-SZ-3955}}$ mutant and wild-type flies (Kolmogorov-Smirnov test; *P*<0.0001, Appendix Table 9). Solid lines depict the chronometric functions predicted by a drift diffusion model (Palmer et al., 2005). **(C, D)** Estimates of drift rates **(C)** and bound heights **(D)** from reaction time measurements (adjusted R^2 > 0.9641, sum of squares due to error < 0.081, standard error < 0.143). Error bars indicate 95% confidence intervals. The residual time was constrained to a value of 1.452 s, determined from wild-type reaction time data in 10^{-4} MCH discrimination tasks (Figure III-2).

In line with model predictions, the decrease in drift rate suggests that *FoxP* mutants are impaired in the accumulation and/or retention of sensory evidence in the build-up to a choice**.** Sensory evidence is therefore less efficient in driving the decision to threshold. A repercussion of this is that the relative influence of noise grows and accuracy declines. However, the increase of the decision bound, which may be compensatory, might counterbalance this effect and allow accurate choices, although at the cost of a further increase in reaction time.

FoxP alleles

To confirm that the *FoxP* phenotype is indeed due to the disruption of the *FoxP* gene, I further analysed flies carrying two independently generated mutant *FoxP* alleles (Figure III-8). These alleles result from transposition events near the P-element insertion site in $FoxP^{5\text{-}SZ\text{-}3955}$: the $FoxP^{GS22100}$ insertion is located 34 bp upstream of the $FoxP^{5\text{-}SZ\text{-}3955}$ insertion, and the insertion in $FoxP^{f03746}$ lies in the 3' untranslated region (UTR) (Figure III-8 A). $FoxP^{GS22100}$ is a strong allele and is homozygous lethal, and could therefore only be examined in trans to $FoxP^{5\text{-}SZ\text{-}3955}$.

Flies heterozygous for these mutant *FoxP* alleles performed like wild-type controls in easy discriminations (concentration ratio 0.1), both in terms of accuracies and reaction times (Figure III-8 B–D; Appendix Table 10). In difficult discriminations (concentration ratio 0.7), however, they displayed prolonged reaction times (Figure III-8 C–D; Appendix Table 10); heterozygous $FoxP^{GS22100}$ flies were also less accurate than wild-type flies (Figure III-8 B; Appendix Table 10).

Homozygous or transheterozygous carriers of two mutant *FoxP* alleles exhibited pronounced reaction time phenotypes for both task difficulties, which equalled or exceeded those of $FoxP^{5\text{-}SZ\text{-}3955}$ homozygotes (Figure III-8 C–D; Appendix Table 10). Furthermore, they also displayed accuracy deficits in difficult discriminations (concentration ratio 0.7) (Figure III-8 B; Appendix Table 10). These results reflect the severity of the decision phenotype: a very strong impairment in accumulation and/or retention of sensory information can

eventually lead to the inability to decide between the reinforced and non-reinforced odour concentration.

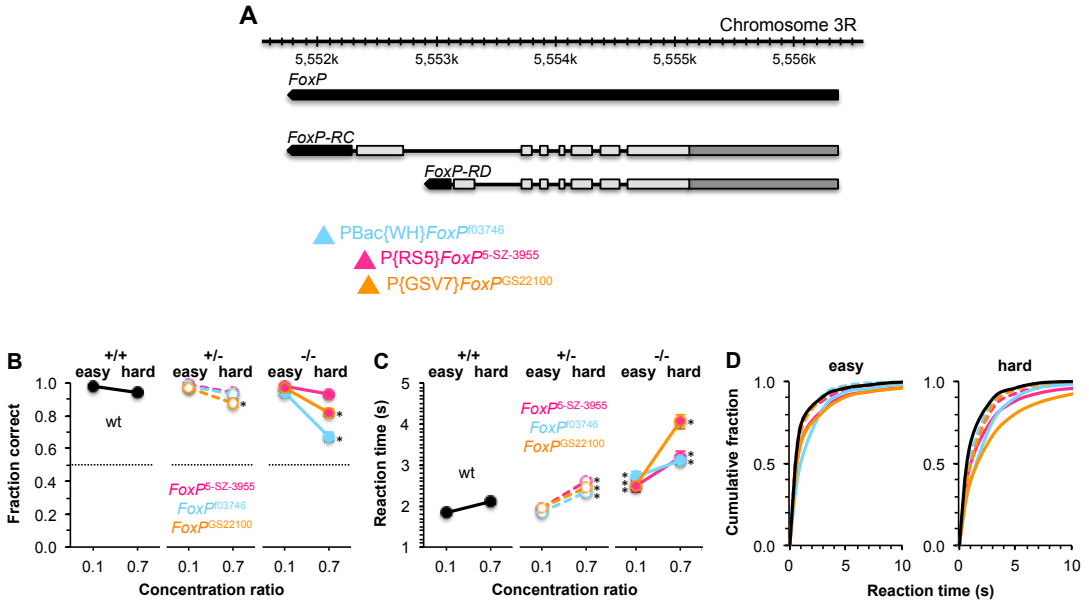


Figure III-8: Allelic interactions of *FoxP* mutations. (A) Organization of the *FoxP* genomic region and insertion sites of P-elements *PBac{WH}FoxP*^{f03746} (blue), *P{RS5}FoxP*$^{5\text{-SZ-}3955}$ (red) and *P{GSV7}FoxP*^{GS22100} (orange). **(B–D)** Flies heterozygous (open symbols, dashed lines), homozygous (filled symbols, solid lines), or transheterozygous (two coloured symbols and lines) for the indicated *FoxP* alleles performed MCH intensity discrimination tasks. **(B)** Accuracies (mean±SEM; *N*=124–190 flies per genotype) as a function of the difficulty of the task. Accuracies of 0.5 correspond to performance at chance level (dotted line). The asterisk indicates a significant difference from wild-type performance (Kruskal-Wallis ANOVA followed by Dunn's test; *P*<0.0035, Appendix Table 10). **(C)** Reaction times (mean±SEM; *N*=394–841 decisions per genotype) as a function of the difficulty of the task. Asterisks indicate significant differences from wild-type performance (Kolmogorov-Smirnov test; *P*<0.0050, Appendix Table 10). **(D)** Cumulative reaction time distributions at easy (left, 0.1 concentration ratio) and hard (right, 0.7 concentration ratio) difficulty levels.

The severity of the *FoxP*^{GS22100} allele could be due to a stronger disruption in the alternatively spliced forkhead domain. *FoxP*^{GS22100} contains the most proximal insertion (Figure III-8 A), and produced a more severe impairment (lethality) in the homozygous than in the transheterozygous *FoxP*^{GS22100}/*FoxP*$^{5\text{-SZ-}3955}$ state. Transheterozygotes displayed a more pronounced behavioural deficit than *FoxP*$^{5\text{-SZ-}3955}$ homozygotes (Figure III-8

B–C; Appendix Table 10). As for *FoxP*^{f03746}, the severity of the phenotype observed could be a direct consequence of disrupting important elements in the 3' UTR, which plays a crucial role in regulating gene expression at the post-transcriptional level (reviewed in Barrett et al., 2012 and Matoulkova et al., 2012).

Overall, the increased reaction times observed with all the *FoxP* mutant alleles studied, and the lack of complementation between them (Figure III-8), firmly tie the defect in decision formation to the *FoxP* locus.

Chapter IV. A neural substrate for trained olfactory decision making

The primary objective of identifying and characterising a mutant with an altered decision making process was to use the gene to gain entry to the decision making circuitry. The ability to use binary systems (reviewed in Venken et al., 2011), in which regulatory elements of a gene can be used to drive the expression of effector molecules for neuronal identification and manipulation, constitutes one of the main advantages of studying decision making in the fruit fly.

Based on the results presented in Chapter III, the establishment of a role for FoxP in evidence accumulation and/or retention during a decision, this Chapter deals with the identification and manipulation of FoxP expressing neurons.

FoxP expression pattern

In order to identify, label, and manipulate the neurons in which *FoxP* is expressed, a 1,373 bp putative promoter fragment immediately upstream of the *FoxP* coding sequence (CDS) was used to direct GAL4 expression.

The *FoxP-GAL4* construct I generated was used to drive GFP transgene expression in adult flies (Figure IV-1). In the central nervous system, *FoxP-GAL4* driven GFP expression was restricted to the mushroom body (MB) (Figure IV-1 A). The MB is an important multisensory structures that receives prominent olfactory inputs and has been proposed to control adaptive behaviours that require extensive information processing, such as learned odour choice (Heisenberg et al., 1985; Pascual and Préat, 2001; McGuire et al., 2003; Qin et al., 2012; Perisse et al., 2013b), mate selection (Keleman et al., 2012), and resolution of visual ambiguity (Liu et al., 1999; Tang and Guo, 2001; Zhang et al., 2007). Within the MB, *FoxP > mCD8::GFP* expression was restricted to specific constituent Kenyon cells (KCs), namely those whose axons project to three of the five lobes (Ito et al., 1997; Crittenden et al., 1998): KCs projecting to the vertical α and horizontal β lobe (αβ KCs) and KCs projecting to the horizontal γ lobe (γ KCs) (Figure IV-1 A and B). Expression in the αβ lobes was further confined to KCs whose axonal projections are restricted to the cores of these lobes (αβc) (Figure IV-1 A and B). *FoxP-GAL4* expression appeared to be limited to ~80 αβc KCs and ~100 γ KCs, small subsets of the estimated 2,000–2,500 KCs that compose each MB. The strength of expression observed was dissimilar in the two subsets: in the lobes and peduncle, expression in γ KCs was weak whereas expression in αβc KCs was strong (Figure IV-1 A and B).

The KCs subsets identified using a putative *FoxP* promoter fragment, αβc and γ KCs, constitute possible sites of FoxP action, which could be involved in the decision making process.

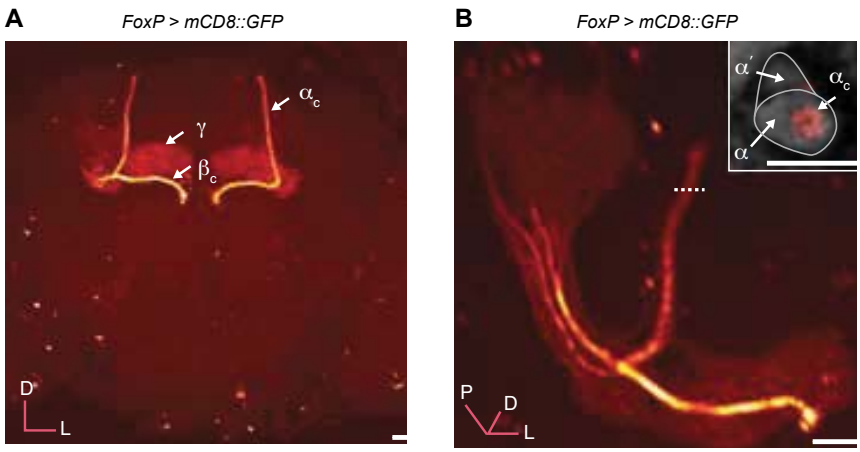


Figure IV-1: Identification of neurons expressing *FoxP-GAL4*. (A, B) *FoxP-GAL4* drives mCD8::GFP expression in $\alpha\beta_c$ and weakly in γ KCs. A cross-section through the α lobe (**B**, inset) shows confinement of *FoxP-GAL4* expression (red) to the core; nc82 staining in grey. Scale bars, 20 µm.

The *FoxP* promoter construct generated included the *Drosophila* synthetic core promoter (DSCP) (Pfeiffer et al., 2008), which contains multiple core promoter motifs, as initial attempts with the putative endogenous *FoxP*-promoter fragment alone failed to drive effector molecules used for visualising neurons. This study did not aim to characterise the promoter structure of the *FoxP* gene, and it is possible that important distal promoter elements (reviewed in Lenhard et al., 2012) were absent from this putative promoter fragment. In line with this, the flybase annotation of the *FoxP* gene has recently changed (FB2014_03, released May 9th, 2014), and the 5' UTR of the gene is now predicted to be as long as 1,246 bp, as opposed to the 10 bp previously identified when the promoter construct was made. The putative promoter site used could have potentially been longer; however, since the region used spans 127 bp over the current presumed 5' UTR sequence, and is only 450 bp away from the putative 3' UTR of the adjacent gene, *alphaTub85E*, increasing the length of the putative promoter might have

included parts of the expression pattern of this neighbouring gene (Figure IV-2).

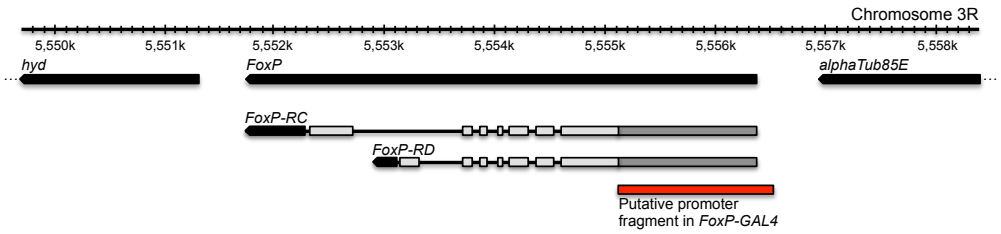


Figure IV-2: The genomic context of *FoxP* locus and location of the putative promoter region used to generate *FoxP-GAL4*. The *FoxP* locus on the right arm of the 3rd chromosome is flanked 5' by the *alphaTub85E* locus and 3' by the *hyd* locus. The putative promoter fragment used to produce the *FoxP-GAL4* construct is represented in red.

Attempts to detect endogenous FoxP and confirm *FoxP* expression patterns using commercially available antibodies (abcam) for vertebrate FoxP1 and FoxP2 failed to yield a signal. Though these antibodies allowed the identification of FoxP expression in humans, mice, rats and birds, the sequence similarities with the *Drosophila* FoxP proteins apparently were insufficient to identify its expression. Potential further strategies to confirm FoxP's endogenous expression are presented in the Discussion.

Despite the requirement of the DSCP in combination with the putative *FoxP* promoter fragment to drive expression of GAL4, and the inability to detect endogenous FoxP expression, the KCs identified with *FoxP-GAL4* constitute sites of potential FoxP action.

Manipulating *FoxP* expression in the mushroom body

To confirm that *FoxP-GAL4* positive neurons are indeed the sites of FoxP action, RNA interference with *FoxP* expression was examined in these neurons, by driving *UAS-FoxP*^{RNAi} with *FoxP-GAL4*. *FoxP-Gal4* is however weak at driving transgene expression, and native GFP fluorescence is only observed in flies homozygous for both *FoxP-GAL4* and *UAS-mCD8::GFP* transgenes. *FoxP* > *FoxP*^{RNAi} flies showed only slightly prolonged reaction times compared with their parental controls, likely due to inadequate levels of *FoxP*^{RNAi} (Figure IV-3 A–C; Appendix Table 11). This could result from natural low expression levels of this transcription factor, the lack of important promoter elements as outlined above, and/or to the possible requirement of enhancers to express appropriate levels of transgenes in a temporally appropriate manner. Indeed in *Drosophila*, the combined action of a range of two to 10 enhancers typically dictates the temporal and spatial patterns of gene expression (reviewed in Levine, 2003). Given this knowledge, it is likely that *FoxP-GAL4* is unable to drive an effective level of *FoxP*^{RNAi} at the required developmental stage.

Consistent with this interpretation, knocking down *FoxP* expression using the strong MB driver *OK107-GAL4* (Connolly et al., 1996), which targets all KCs, recapitulated the *FoxP* mutant phenotype (Figure IV-3 D–F; Appendix Table 11). Accuracy scores for easy (concentration ratio 0.1) and difficult discriminations (concentration ratio 0.9) were similar between *OK107* > *FoxP*^{RNAi} and parental control strains (Figure IV-3 D; Appendix Table 11).

Reaction times, however, differed between *OK107 > FoxP*^{RNAi} and parental control strains: like the effect of mutating *FoxP*, the effect was subtle in easy discriminations (concentration ratio 0.1), but the differences were amplified in difficult tasks (concentration ratio 0.9), where the experimental flies exhibited a disproportionate increase in reaction time (Figure IV-3 E–F; Appendix Table 11).

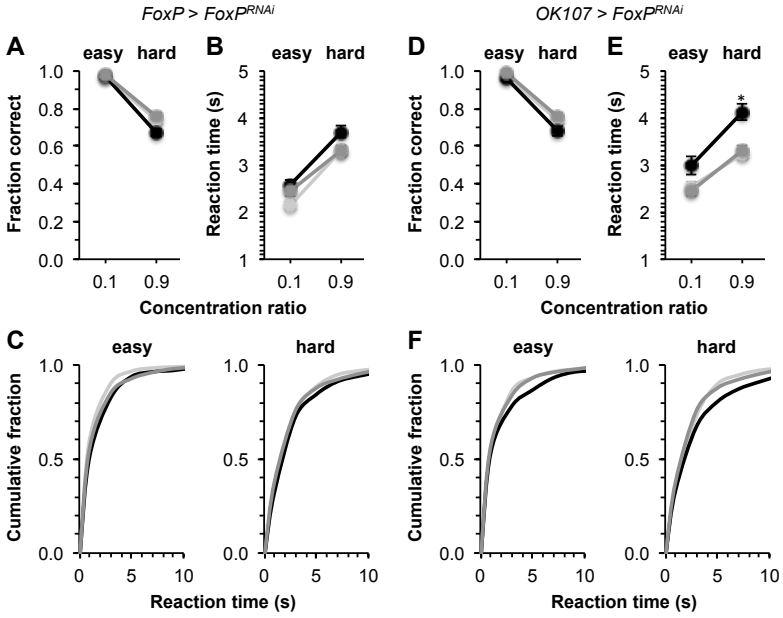


Figure IV-3: Manipulating *FoxP* expression in the mushroom body. (A–C) Flies expressing *FoxP*^{RNAi} under the control of *FoxP-GAL4* performed MCH intensity discrimination tasks. Black and grey symbols and lines denote experimental flies and parental controls, respectively (*FoxP-GAL4*, light grey; *UAS-FoxP*^{RNAi}, dark grey). **(A)** Accuracies (mean±SEM; *N*=98–254 flies per data point) as a function of the difficulty of the task. Accuracies of 0.5 correspond to performance at chance level (dotted line). **(B)** Reaction times (mean±SEM; *N*=455–1187 decisions per data point) as a function of the difficulty of the task. **(C)** Cumulative reaction time distributions at easy (left, 0.1 concentration ratio) and hard (right, 0.9 concentration ratio) difficulty levels. **(D–F)** Flies expressing *FoxP*^{RNAi} under the control of *OK107-GAL4* in all KCs performed MCH intensity discrimination. Black and grey symbols and lines denote experimental flies and parental controls, respectively (*OK107-GAL4*, light grey; *UAS-FoxP*^{RNAi}, dark grey). **(D)** Accuracies (mean±SEM; *N*=116–191 flies per data point) as a function of the difficulty of the task. Accuracies of 0.5 correspond to performance at chance level (dotted line). **(E)** Reaction times (mean±SEM; *N*=323–781 decisions per data point) as a function of the difficulty of the task. The asterisk indicates significant genotype effects (Kolmogorov-Smirnov test; *P*<0.0029, Appendix Table 11). **(F)** Cumulative reaction time distributions at easy (left, 0.1 concentration ratio) and hard (right, 0.9 concentration ratio) difficulty levels.

Although *FoxP-GAL4* driven *UAS-FoxP*^{RNAi} failed to recapitulate the *FoxP* mutant phenotype, interfering with *FoxP* expression in the MB with *OK107-GAL4* mimicked the difficulty dependent prolonged reaction times observed in *FoxP* homozygous mutants. *FoxP* expression in the MB is therefore required for efficient decision-making.

Since using a strong MB driver line *OK107-GAL4* was necessary to drive *FoxP*^{RNAi}, I searched for strong driver lines whose expression domains covered parts of the *FoxP-Gal4* pattern, to test whether they are indeed FoxP expressing neurons integral to the decision making process. This endeavour led to the identification of two lines able to drive strong GFP expression with only one copy of the driver and the effector: *NP6024-GAL4*, which labels αβc KCs (Tanaka et al., 2008; Huang et al., 2012; Perisse et al., 2013b) (Figure IV-4 A), and *NP1131-GAL4*, which labels γ KCs (Tanaka et al., 2008; Qin et al., 2012) (Figure IV-4 E). Both *NP6024* > *FoxP*^{RNAi} and *NP1131* > *FoxP*^{RNAi} showed similar accuracies to parental control strains in easy (concentration ratio 0.1) and difficult (concentration ratio 0.9) discrimination tasks (Figure IV-4 B and F; Appendix Table 12). Interference with *FoxP* expression using these lines showed a selective requirement for FoxP in αβc KCs. Knock-down of FoxP in $\alpha\beta_c$ but not γ KCs replicated the homozygous *FoxP* mutant phenotype: reaction times of experimental flies increased in difficult discriminations (Figure IV-4 B–E and J–L; Appendix Table 12).

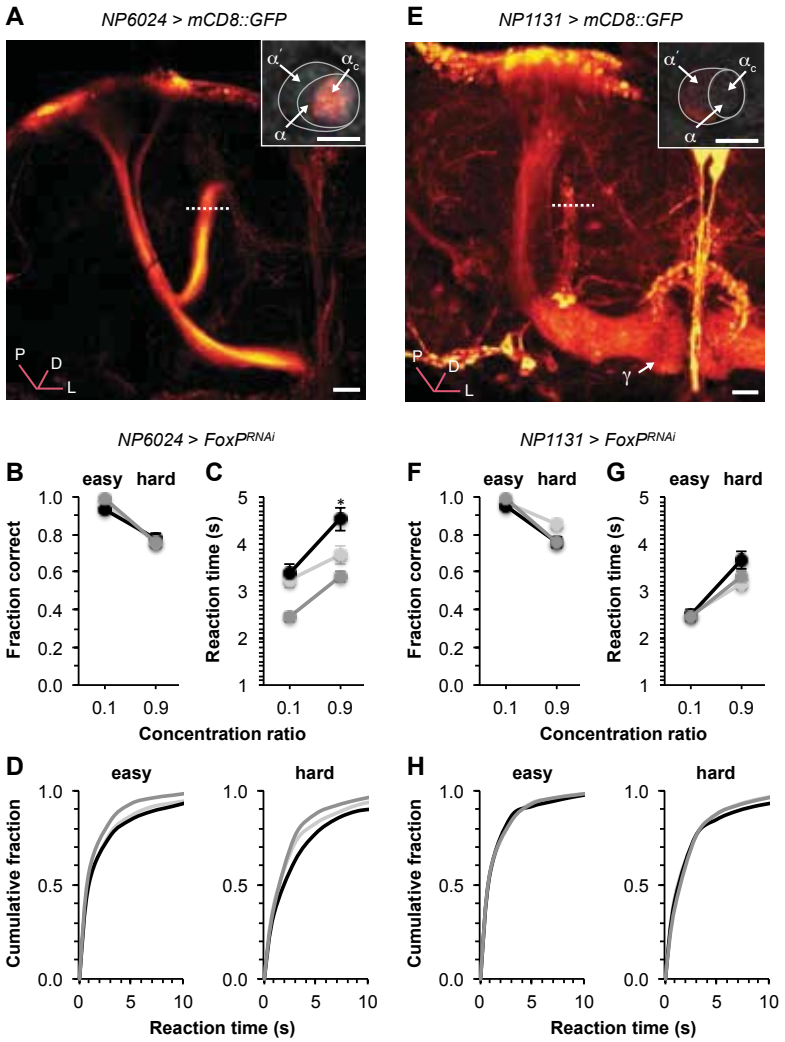


Figure IV-4: Manipulating *FoxP* expression in KC subsets. (A, E) *NP6024-GAL4* **(A)** labels $\alpha\beta_c$ KCs; *NP1131-GAL4* **(E)** labels γ and some α'β' KCs. Insets show cross-sections through the vertical lobes. *GAL4*-driven GFP expression in red; MB staining with *mb247-LexA:LexAop-rCD2::RFP* in grey. Scale bars, 10 µm. **(B–D, F–H)** Flies expressing *FoxP*^{RNAi} in $\alpha\beta_c$ **(B–D)** or γ KCs **(F–H)** performed MCH intensity discrimination tasks. Black and grey symbols and lines denote experimental flies and parental controls, respectively (*X-GAL4*, light grey; *UAS-FoxP*^{RNAi}, dark grey). **(B, F)** Accuracies (mean±SEM; *N*=119–178 flies per genotype) at easy (0.1 concentration ratio) and hard (0.9 concentration ratio) difficulty levels. Accuracies of 0.5 correspond to performance at chance level (dotted line). **(C, G)** Reaction times (mean±SEM; *N*=410–803 decisions per genotype) at easy (0.1 concentration ratio) and hard (0.9 concentration ratio) difficulty levels. The asterisk indicates significant genotype effects (Kolmogorov-Smirnov test; *P*<0.0031, Appendix Table 12). **(D, H)** Cumulative reaction time distributions at easy (left, 0.1 concentration ratio) and hard (right, 0.9 concentration ratio) difficulty levels.

The results obtained by selectively interfering with *FoxP* expression in the MB show that FoxP action within $\alpha\beta_c$ neurons is required for appropriate decision-making processes. Given that the MB is a higher-order olfactory processing

brain centre, the identified KCs might be responsible for: encoding the sensory data that are read and accumulated by downstream integrator circuits; performing the integration operation itself; or combining the functions of representing and accumulating sensory evidence.

Manipulating *FoxP* expressing neurons

Regardless of whether the identified KCs are responsible for the representation and/or accumulation of the sensory evidence that trigger a decision, these processes require externally or recurrently evoked electrical activity (Robinson, 1989; Koulakov et al., 2002). It is therefore predicted that reducing the excitability of these neurons will increase reaction time.

To test if activity in *FoxP* expressing neurons is indeed required for decision-making, the inwardly-rectifying potassium channel Kir2.1 was targeted under *FoxP-GAL4* control to αβc and γ KCs. Overexpression of Kir2.1 decreases a neuron's input resistance by pulling the membrane potential towards the potassium equilibrium potential. This increases the amount of current required to elicit an action potential, without preventing spiking or altering the waveform of an action potential when it occurs (Burrone et al., 2002). The channel expression level was controlled with the help of GAL80, which binds to GAL4 neutralising its transcription-promoting activity (Yun et al., 1991; reviewed in Traven et al., 2006). A temperature sensitive version of this repressor,

GAL80^{ts}, was used, allowing graded transgene expression between 18 and 32 ˚C (McGuire et al., 2003).

Driving low level Kir2.1 expression by raising *FoxP* > *Kir2.1* flies at 25 ˚C had no effect on decision accuracies or reaction times in easy and intermediate discriminations (concentration ratios 0.1 and 0.5, respectively), with the experimental flies' performance matching that of the parental control strains, both in terms of accuracies and reaction times (Figure IV-5 A–C; Appendix Table 13). In difficult tasks (concentration ratio 0.9), *FoxP* > *Kir2.1* flies took significantly longer to decide than the parental control flies (displaying an increase of ~29% and ~22% compared to *FoxP-GAL4* and *UAS-Kir2.1* flies, respectively), while still maintaining comparable decision accuracies (Figure IV-5 A–C; Appendix Table 13).

Driving high-level expression of Kir2.1 in *FoxP-GAL4* positive neurons, by shifting the experimental animals to 30 ˚C for 18 h before training and testing, exacerbated the decision phenotype (Figure IV-5 D–F; Appendix Table 13). *FoxP* > *Kir2.1* flies displayed a further increase in reaction time in difficult tasks (concentration ratio 0.9), taking ~37% and ~44% longer than *FoxP-GAL4* and *UAS-Kir2.1* flies, respectively (Figure IV-5 E–F; Appendix Table 13). At the same time, the experimental flies' performance in difficult tasks (concentration ratio 0.9) dropped to chance level, whereas parental controls maintained a discrimination accuracy of ~70%, similar to that of wild-type flies at the same difficulty level (Figure IV-5 D; Appendix Table 13).

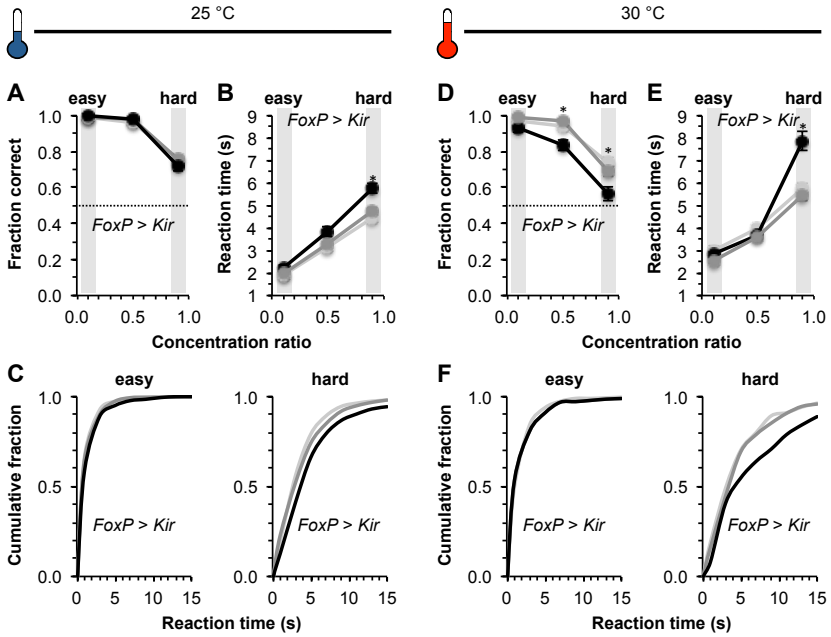


Figure IV-5: Manipulating neurons expressing *FoxP-GAL4*. (A–F) Flies expressing Kir2.1 under *FoxP-GAL4* and *tubP-GAL80^{ts}* control (*FoxP > Kir2.1*, black) and parental controls (*FoxP-GAL4*, light grey; *UAS-Kir2.1*; *tubP-GAL80^{ts}*, dark grey) were maintained at the indicated temperatures for 18 h before performing MCH intensity discrimination tasks. **(A, D)** Accuracies (mean±SEM; *N*=81–175 flies per data point) as a function of the difficulty of the task. Accuracies of 0.5 correspond to performance at chance level (dotted line). The asterisk indicates a significant genotype effect (Kruskal-Wallis ANOVA followed by Dunn's test; *P*<0.0052, Appendix Table 13). **(B, E)** Reaction times (mean±SEM; *N*=255–735 decisions per genotype) as a function of the difficulty of the task. Asterisks indicate significant genotype effects (Kolmogorov-Smirnov test; *P*<0.0005, Appendix Table 13). **(C, F)** Cumulative reaction time distributions of flies maintained at 25 ˚C **(C)** and 30 ˚C **(F)** at easy (left, 0.1 concentration ratio) and hard (right, 0.9 concentration ratio) difficulty levels. Irrespective of temperature, the distributions differ between experimental flies (black) and parental controls (grey) at the hard (*P*<0.0005) but not the easy difficulty level.

Introducing a stabilizing potassium conductance into *FoxP-GAL4* positive neurons thus replicates the behavioural phenotype of homozygous *FoxP* mutants. This manipulation firmly links the activity of *FoxP-GAL4* positive neurons with decision-making, showing that the identified KCs play a central role during this process.

Given that selective interference with *FoxP* expression showed that FoxP action within $\alpha\beta_c$ neurons is required for decision-making, to further test their selective influence, Kir2.1 was expressed in $\alpha\beta_c$ and γ KCs, respectively,

using the same specific driver lines, *NP6024-GAL4* and *NP1131-GAL4* (Figure IV-6). Similarly to the effect of driving Kir2.1 expression with *FoxP-GAL4,* expressing Kir2.1 in $\alpha\beta_c$, but not γ, KCs led to a decrease in accuracy in difficult discriminations (concentration ratio 0.9) compared to parental control strains (Figure IV-6 A and B; Appendix Table 14). Furthermore, this accuracy drop was accompanied by a concomitant increase in reaction times, in a difficulty-dependent manner (Figure IV-6 B–C and E–F; Appendix Table 14). Expressing Kir2.1 in $\alpha\beta_c$ neurons (Figure IV-6 A–C; Appendix Table 14), but not γ KCs (Figure IV-6 A–C; Appendix Table 14) replicated the effect of Kir2.1 expression in *FoxP-GAL4* neurons and recapitulated the *FoxP* homozygous mutant phenotype.

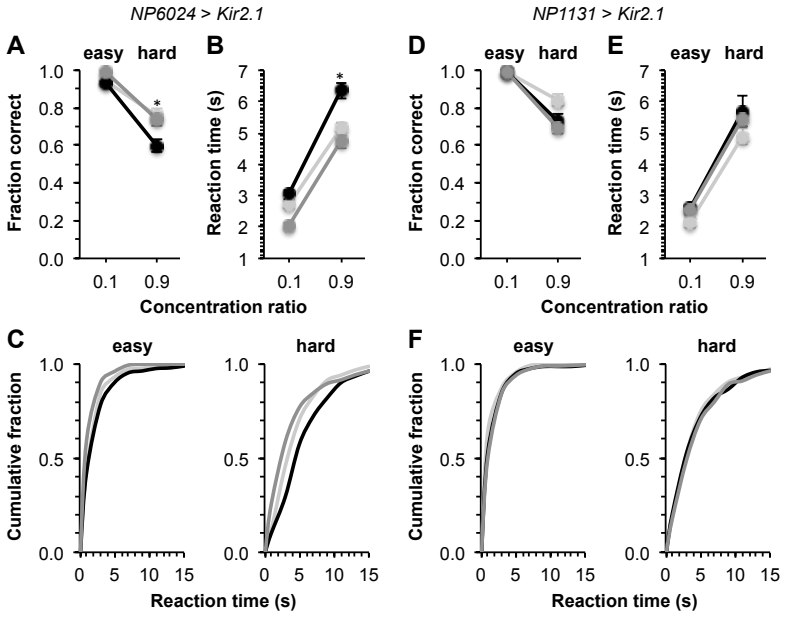


Figure IV-6: Manipulating excitability in KC subsets. (A–C, D–F) Flies expressing Kir2.1 in $\alpha\beta_c$ **(A–C)** or γ KCs **(D–F)** performed MCH intensity discrimination tasks. Black and grey symbols and lines denote experimental flies and parental controls, respectively (*X-GAL4*, light grey; *UAS-Kir2.1*; *tubP-GAL80^{ts}*, dark grey) **(A, D)** Accuracies (mean±SEM; *N*=51–152 flies per genotype) at easy (0.1 concentration ratio) and hard (0.9 concentration ratio) difficulty levels. Accuracies of 0.5 correspond to performance at chance level (dotted line). The asterisk indicates significant genotype effects (Kruskal-Wallis ANOVA followed by Dunn's test; *P*<0.0019, Appendix Table 14). **(B, E)** Reaction times (mean±SEM; *N*=136–414 decisions per genotype) at easy (0.1 concentration ratio) and hard (0.9 concentration ratio) difficulty levels. The asterisk indicates significant genotype effects (Kolmogorov-Smirnov test;

P<0.0007, Appendix Table 14). **(C, F)** Cumulative reaction time distributions at easy (left, 0.1 concentration ratio) and hard (right, 0.9 concentration ratio) difficulty levels.

Both decreasing *FoxP* expression in $\alpha\beta_c$ neurons and reducing their excitability copies the decision-making phenotype observed in *FoxP* homozygous mutants. This clearly pins the site of action of FoxP to $\alpha\beta_c$ neurons and shows that their activity is central to the decision-making process.

These findings open up the possibility of probing neuronal function in a narrowly circumscribed set of neurons during decision-making, and potentially functionally interfering with the decision-making process.

Chapter V. Identifying new molecular players in decision making

A logical research avenue following up from the discovery and description of the role of FoxP in decision-making is to identify downstream molecules affected by this transcription factor. In vertebrates, FoxP affects the developmental specification of neuronal connections and regulates the expression of gene products important for adult neuronal functions (Groszer et al., 2008; Konopka et al., 2009; French et al., 2012; Sia et al., 2013). It is likely that the phenotype observed in *FoxP* mutants results from affecting genes involved in either or both of these processes. Uncovering these genes will allow identifying key molecules in the olfactory decision-making process.

A range of different strategies could be used to identify genes regulated by FoxP. Forward genetic strategies, such as screening transposon insertions, ethylmethane sulfonate induced mutants and deficiencies, have been employed successfully to identify genes involved in different biological processes, ranging from axon guidance to behaviour (reviewed in Venken et al., 2011). This Chapter reports the results of a sensitised screen of deficiency lines to identify genomic regions of interest that might contain genes regulated by FoxP, as well as other genes involved in decision making.

A simplified protocol for initial screening

A simple protocol was optimised to maximise the throughput of the screen. Flies were conditioned with electric shock to avoid 10^{-4} MCH in mineral oil, which was tested against air. In these conditions reaction time differences were clearly detectable between wild-type and *FoxP*$^{5\text{-SZ-}3955}$ mutant flies, while accuracies did not differ (Figure V-1; Appendix Table 15). Although *FoxP*$^{5\text{-SZ-}3955}$ heterozygous mutants showed slightly increased reaction times, these changes fell short of statistical significance (Figure V-1; Appendix Table 15).

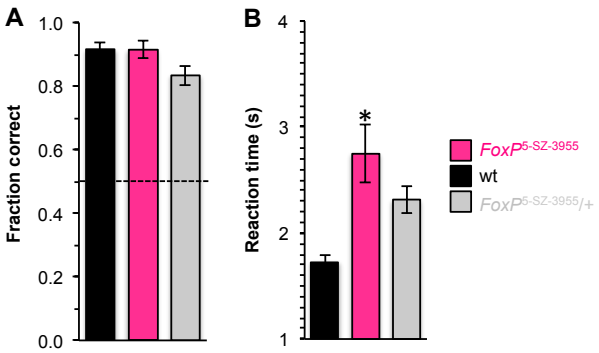


Figure V-1: Decision accuracies and reaction times of wild-type (wt) and *FoxP*$^{5\text{-SZ-}3955}$ heterozygous and homozygous mutant flies performing a trained discrimination task between 10^{-4} MCH and air. (A) Accuracies (mean±SEM; *N*=75–94 flies per genotype). Accuracies of 0.5 correspond to performance at chance level (dotted line). **(B)** Reaction times (mean±SEM; *N*=219–342 decisions per genotype). The asterisk indicates significant differences from wild-type performance (Kolmogorov-Smirnov test; *P*<0.0086, Appendix Table 15).

This simplified protocol therefore seemed suitable for an initial screen of genomic regions that might contain genes involved in decision-making.

Results of the screen

A deficiency screen was the strategy chosen to uncover genomic regions of interest for further pursuit of molecular players central to olfactory decision-making. I used the Bloomington deficiency kit since most of its chromosomal deletions are molecularly defined and globally cover the genome (Cook et al., 2012). These deficiencies were generated primarily by the Bloomington Deletion Project, the DrosDel Project and Exelixis Inc., from FRT-bearing transposable element insertions (Parks et al., 2004; Thibault et al., 2004).

The deficiency lines for the 2nd and 3rd chromosomes were crossed with *FoxP*$^{5\text{-SZ-}3955}$ mutants to obtain a sensitised genetic background, a strategy used to maximise the probability of uncovering genes involved in a particular pathway (reviewed in St Johnston, 2002). This should increase the possibility of ultimately uncovering genes involved in decision-making, potentially those regulated by *FoxP*.

Out of 364 2nd and 3rd chromosomes available deficiency lines, 313 were successfully maintained and non-lethal in the sensitised *FoxP*$^{5\text{-SZ-}3955}$ background. Approximately 3% of the 313 deficiencies screened showed pronounced locomotor impairment and were therefore not analysed (Figure V-2). Seventy-one % of the strains tested produced no phenotype (Figure V-2; Appendix Tables 16–19). The remaining 26% of the deficiencies tested exhibited phenotypes for the following endpoints: ~4% displayed decreased accuracy scores only, ~6% showed decreased accuracies and increased

reaction times, and ~16% presented solely reaction time phenotypes (Figure V-2; Appendix Tables 16–19).

The deficiencies that displayed decreased accuracies were not further analysed. Accuracy defects alone could reflect either olfactory or learning impairments. However, the lines that displayed decreased accuracies and increased reaction times, though not in line with the *FoxP* mutant phenotype, could be of interest for decision-making: they could indicate pronounced impairments in which defects in evidence accumulation and/or retention eventually lead in the failure to commit to a choice.

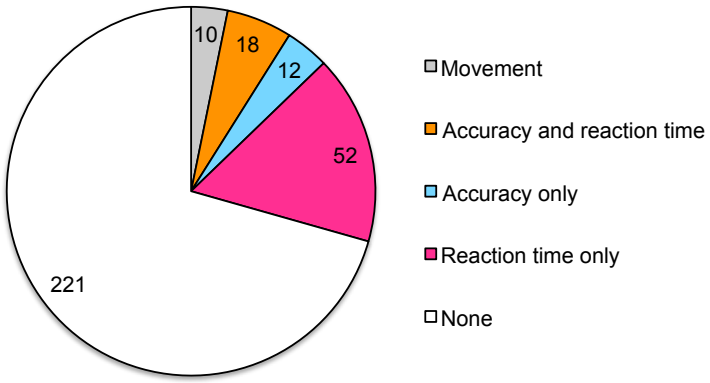


Figure V-2: Results of the sensitised *FoxP*$^{5\text{-SZ-3955}}$ background deficiency screen for the 2nd and 3rd chromosomes. The deficiencies were screened in a trained discrimination task between 10^{-4} MCH and air, in which accuracy and reaction time scores were assessed. Out of the 313 deficiencies tested 71% exhibited no phenotype, 3% showed pronounced locomotor impairment, ~4% displayed decreased accuracy scores, ~6% showed both decreased accuracy and increased reaction times scores and ~16% presented reaction time phenotypes only (Appendix Tables 16–19).

Crucially, as a proof of principle of the soundness of the approach, the deficiency that encompasses the *FoxP* genomic locus, Df(3R)ED5428, did not yield viable progeny when crossed with *FoxP*$^{5\text{-SZ-3955}}$. This is consistent with the fact that the strongest *FoxP* allele (*FoxP*^{GS22100}; data presented in Chapter

III) did not generate homozygous viable progeny. However, when crossed with wild-type flies, *FoxP*$^{5\text{-SZ-3955}}$ and Df(3R)ED5428 heterozygous flies showed similarly increased reaction times, albeit not significantly different from wild-type (Figure V-3; Appendix Table 20).

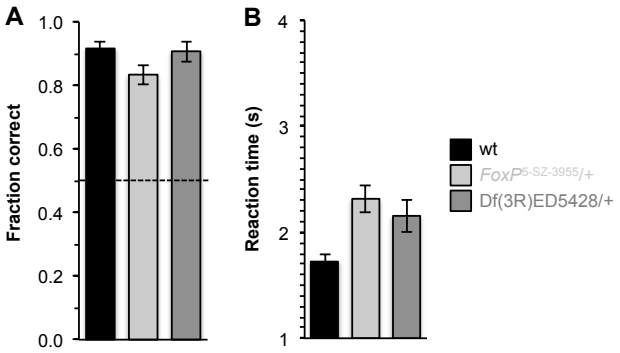


Figure V-3: Decision accuracies and reaction times for a trained discrimination task between 10^{-4} MCH and air of wild-type (wt) flies, *FoxP*$^{5\text{-SZ-3955}}$ heterozygous flies and flies heterozygous for the deficiency in which *FoxP* is deleted (Df(3R)ED5428). (A) Accuracies (mean±SEM; *N*=38–94 flies per genotype). Accuracies of 0.5 correspond to performance at chance level (dotted line). **(B)** Reaction times (mean±SEM; *N*=122–342 decisions per genotype).

Specific deficiencies uncovered for further analysis

Forty-four of the 52 deficiencies that showed a reaction time phenotype took longer to perform the simplified task than control strains; eight showed reduced reaction times. Faster reaction time phenotypes could be interesting, potentially reflecting an increased rate of evidence accumulation and/or a lowering of the choice threshold. However, since the screen was designed to pick up phenotypes consistent with the *FoxP*$^{5\text{-SZ-3955}}$ decision-making impairment, which therefore might include genes regulated by FoxP, only lines displaying increased reaction times were further pursued. Taken

together, the 44 deficiencies disrupt 3,255 genes, with individual deficiencies disrupting between nine and 226 genes (Appendix Table 21). Unfortunately, known homologue genes of the well characterised vertebrate targets *SRPX2* (Roll et al., 2010; Sia et al., 2013), *CNTANP2* (Vernes et al., 2008; O'Roak et al., 2011) and *Pitx3* (Konstantoulas et al., 2010) of FoxP1 and FoxP2, *Hig* (Hoshino et al., 1996; Roll et al., 2006), *Nrx-IV* (Baumgartner et al., 1996; Peles et al., 1997; Zweier et al., 2009) and *Ptx1* (Vorbrüggen et al., 1997; Popovici et al., 2001) are not among this list of genes, as the deficiencies that encompass them, respectively Df(2R)ED1791, Df(3L)E4475 and Df(3R)ED6346, did not display a reaction time phenotype.

The identification of deficiencies that exhibit an increase in reaction time in this simplified discrimination task constitutes a first step for uncovering targets of *FoxP* action relevant for decision-making processes. Immediate further study of these deficiencies will involve analysing performance in easy and difficult intensity discrimination tasks, and identifying deficiencies of smaller genomic regions (and, ultimately, single genes) that show difficulty dependent decision making phenotypes similar to *FoxP* homozygous mutants. Further approaches to uncover the genes involved in decision-making within these chromosomal regions are presented in the Discussion.

Chapter VI. Naive olfactory discrimination

Having shown that *Drosophila melanogaster* displays deliberate decision-making in trained olfactory intensity discrimination tasks, I set out to study the behavioural characteristics of naive intensity discriminations. Since naive and trained olfactory responses are different at the behavioural level and presumed to involve different circuit elements, this Chapter reflects an attempt to study if the same molecules and circuits previously shown to be involved in trained decision making (Chapters III and IV) are involved in naive discriminations.

Behavioural characteristics

The behaviour of wild-type flies was studied in an intensity discrimination task for eight MCH concentration ratios at 10^{-1} absolute odour concentration (Figure VI-1). Naive and trained (using electric shocks as reinforcement) accuracy/choice scores (Figure VI-1 A) and reaction times (Figure VI-1 B) were analysed in a 2 min test period, during which flies discriminated between two concentrations of MCH. These discriminations were easier when the odour concentrations were more distinct (lower concentration ratios) and more difficult for more similar odour concentrations (higher concentration ratios).

Naive discriminations were significantly less reliable than trained ones for all concentration ratios tested: though wild-type flies chose the less concentrated odour (or avoided the more concentrated odour) in both situations, trained choices were more consistent than naive choices (Figure VI-1 A; Appendix Table 22). Reaction times also differed between naive and trained tasks, significantly in more difficult tasks (odour concentration ratios 0.7–0.95) (Figure VI-1 B; Appendix Table 22). Trained reaction times almost doubled from 0.1 to 0.95 concentration ratio, while naive reaction times showed only a ~20% increase between the easiest (0.1 concentration ratio) and most difficult (0.95 concentration ratio) task (Figure VI-1 B). This discrepancy results from the fact that in naive discriminations the stakes associated with a choice are low and therefore in difficult discriminations there is little incentive to perform a consistent choice requiring a longer decision time.

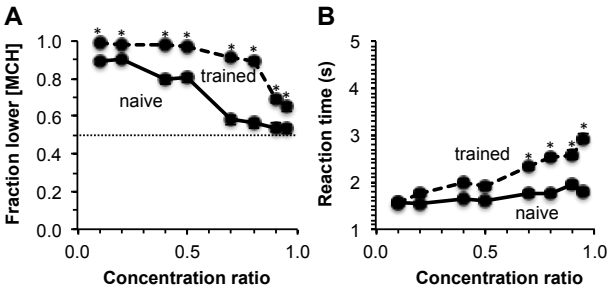


Figure VI-1: Wild-type naive and trained discrimination behaviour. (A–B) Wild-type flies perform naive (solid lines) and trained (dashed lines) intensity discrimination tasks at 10^{-1} concentration of MCH. **(A)** Fraction of choices towards the lower MCH concentration (mean ± SEM; *N*=151–191 flies per data point) as a function of the difficulty of the task. Choices of 0.5 correspond to performance at chance level (dotted line). Asterisks indicate significant differences between naive and trained behaviour (Kruskal-Wallis ANOVA followed by Dunn's test; *P*<0.0423, Appendix Table 22). **(B)** Reaction times (mean ± SEM; *N*=515–857 decisions per data point) as a function of the difficulty of the task. Asterisks indicate significant differences between naive and trained behaviour (Kolmogorov-Smirnov test; *P*<0.0001, Appendix Table 22).

Naive and trained olfactory intensity discrimination tasks differ in the fraction of choices in favour of the lower MCH concentration and in reaction times. Different decision making systems seem to be employed during these tasks: a fast and less consistent naive decision-making system and a slower, more accurate, trained decision-making system.

The role of *FoxP*

Given that *FoxP* mutants exhibited a trained decision-making phenotype, the behaviour of wild-type and $FoxP^{5\text{-}SZ\text{-}3955}$ mutant flies was compared in a naive intensity discrimination task at $10^{-1.5}$ MCH absolute odour concentration (Figure VI-2). This odour concentration was chosen as it constituted an intermediate absolute concentration at which flies were still able to perform discriminations with a high degree of coherence and differences between genotypes became blatantly apparent. Both wild-type and $FoxP^{5\text{-}SZ\text{-}3955}$ mutant flies showed a decrease in consistency of choice with the increase in difficulty of the task (Figure VI-2 A; Appendix Table 23). This was accompanied by an increase in the time they took to commit to a choice(Figure VI-2 B–C; Appendix Table 23). For both wild-type and $FoxP^{5\text{-}SZ\text{-}3955}$ mutant flies, naive choice does not seem to be a purely reflexive behaviour, as there was an increase in reaction time with the difficulty of the task (Figure VI-2 B–C; Appendix Table 23). However, $FoxP^{5\text{-}SZ\text{-}3955}$ mutant flies consistently chose the lower MCH concentration to a higher degree than wild-type flies, being between 10 and 15% more consistent than wild-type up to a concentration

ratio of 0.6 (Figure VI-2 A; Appendix Table 24). Furthermore the mutants' increased consistency was accompanied by a longer reaction time compared to that of wild-type flies (Figure VI-2 B; Appendix Table 24): the reaction times of *FoxP*$^{5\text{-SZ-3955}}$ mutants showed a 73% increase at concentration ratio 0.6 compared to concentration ratio 0.1 while wild-type flies showed only a 26% increase over the same concentration ratio range (Figure VI-2 B). Additionally, although wild-type and mutant reaction times did not differ at easy discriminations, in the most difficult discrimination task (concentration ratio 0.9) *FoxP*$^{5\text{-SZ-3955}}$ mutant's reaction times doubled compared to reaction times in the easiest discrimination (concentration ratio 0.05), while wild-type reaction times displayed only a 22% increase (Figure VI-2 B–C).

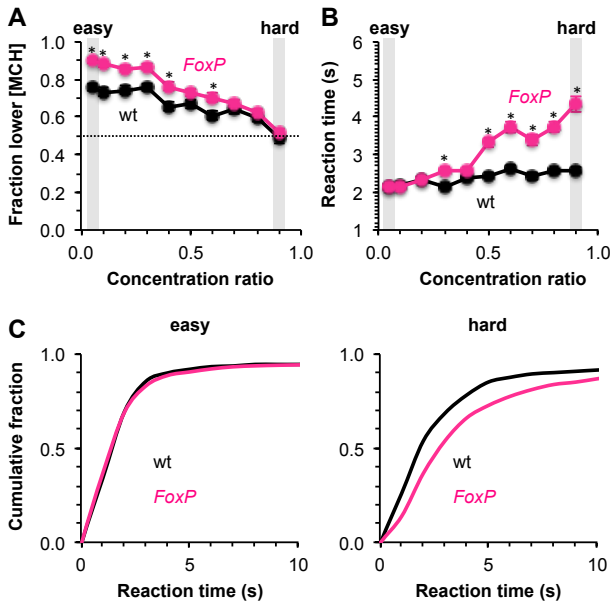


Figure VI-2: Naive performance of wild-type and *FoxP*$^{5\text{-SZ-3955}}$ mutants. (A–B) Wild-type (wt, black) and *FoxP*$^{5\text{-SZ-3955}}$ mutant (*FoxP*, red) flies perform naive intensity discrimination tasks at $10^{-1.5}$ concentration of MCH. **(A)** Fraction of choices towards the lower MCH concentration (mean ± SEM; *N*=84–197 flies per data point) as a function of the difficulty of the task. Choices of 0.5 correspond to performance at chance level (dotted line). Asterisks indicate significant differences between *FoxP*$^{5\text{-SZ-3955}}$ mutant and wild-type flies (Kruskal-Wallis ANOVA followed by Dunn's test; *P*<0.0148, Appendix Table 24). **(B)** Reaction times (mean ± SEM; *N*=559–985 decisions per data point) as a function of the difficulty of the task. Asterisks indicate significant differences between *FoxP*$^{5\text{-SZ-3955}}$ mutant and wild-type flies (Kolmogorov-Smirnov test; *P*<0.0032, Appendix Table 24). **(C)** Cumulative reaction time

distributions at easy (left, 0.1 concentration ratio) and hard (right, 0.7 concentration ratio) difficulty levels.

These data suggest that while wild-type flies engage the faster and less consistent decision-making system for naive intensity discriminations, *FoxP*$^{5\text{-}SZ\text{-}3955}$ mutants seem to engage the slower, more accurate decision system, characteristic of trained decision-making.

As described in Chapter IV, *FoxP* is expressed in the MB, and disrupting its expression in this structure impairs decision-making. It is therefore possible, given the putative role of FoxP in developmentally specifying neuronal connections and/or in regulating important functional neuronal processes (Groszer et al., 2008; Konopka et al., 2009; French et al., 2012; Sia et al., 2013), that impairing *FoxP* expression leads to the inappropriate recruitment of the slower and more accurate decision-making system.

The role of the mushroom body

The first step taken to start to disentangle the circuitry underlying naive intensity discrimination was to assess the role of the MB in this behaviour. As described in the Introduction, the MB is pivotal for olfactory learning and memory, and some studies also suggest it might play a role at least in certain types of naive olfactory behaviours (Wang et al., 2003b; Bräcker et al., 2013).

If the MB is involved in naive intensity discrimination, then blocking its output should impair performance. I tested this prediction by using *OK107-GAL4* to

direct the expression of a dominate-negative temperature-sensitive dynamin, shibire^{ts} (Figure VI-3). Shibire is a protein involved in the process of endocytosis and is essential for synaptic vesicle recycling (Kosaka and Ikeda, 1983); the temperature sensitive allele blocks synaptic transmission at temperatures above 29 °C (Kitamoto, 2001).

Blocking synaptic transmission from the whole MB, by expressing shibire^{ts} at 30 °C for at least 15 min before and during testing, prevented naive intensity discrimination (Figure VI-3 D). This was particularly evident for the easiest intensity discrimination task (concentration ratio 0.1), in which the fraction of choices in favour of the lower MCH concentration made by *OK107* > *shi^{ts}* flies was significantly different from that of parental strains (Figure VI-3 D; Appendix Table 25). Furthermore, the experimental flies performed at chance level for all concentration ratios tested, displaying no modulation with the difficulty of the task (Figure VI-3 D; Appendix Table 26). At 25 °C, when shibire^{ts} is not functional, no differences in performance were observed between experimental and parental control flies (Figure VI-3 A–C; Appendix Table 25).

Reaction times of *OK107* > *shi^{ts}* at 30 °C were increased compared to parental controls (Figure VI-3 E–F; Appendix Table 25); they do not, however, reflect an effect comparable to that observed in *FoxP*$^{5\text{-SZ-}3955}$ mutants, as they were similarly increased for all difficulty levels (Figure VI-3 E–F; Appendix Table 26), rather than exhibiting the characteristic difficulty dependent increase observed at 25 °C for all genotypes (Figure VI-3 B–C; Appendix Table 26). The number of decisions analysed in *OK107* > *shi^{ts}* is significantly lower than that of parental controls: while the experimental flies made 220–

383 decisions, parental control flies made 697–812 and 441–713 decisions, respectively, for *OK107-GAL4* and *UAS-shi^{ts}*. Indeed *OK107 > shi^{ts}* generally paced the entirety of the chamber, consistent with their inability to choose between the two MCH concentrations.

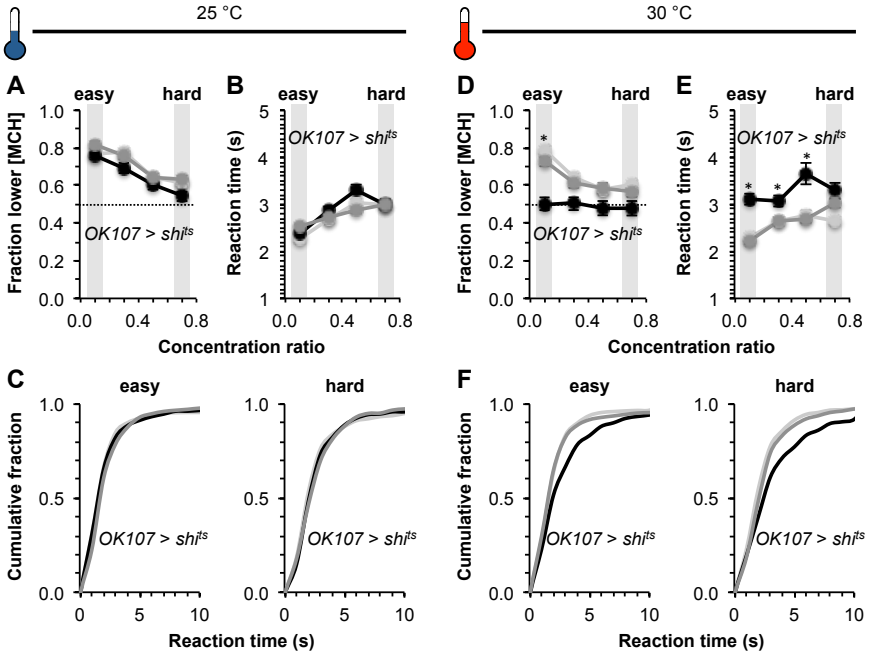


Figure VI-3: Blocking mushroom body output during naive intensity discrimination. (A–F) Flies expressing shibire^{ts} under *OK107-GAL4* (*OK107 > shi^{ts}*, black) and parental controls (*OK107-GAL4*, light grey; *UAS-shibire^{ts}*, dark grey) were maintained at the indicated temperatures for at least 15 min before and during testing in naive intensity discrimination tasks at $10^{-1.5}$ concentration of MCH. **(A, D)** Fraction of choices towards the lower MCH concentration (mean±SEM; *N*=117–198 flies per data point) as a function of the difficulty of the task. Fractions of 0.5 correspond to performance at chance level (dotted line). The asterisk indicates a significant genotype effect (Kruskal-Wallis ANOVA followed by Dunn's test; *P*<0.0001, Appendix Table 25). **(B, E)** Reaction times (mean±SEM; *N*=220–812 decisions per genotype) as a function of the difficulty of the task. Asterisks indicate significant genotype effects (Kolmogorov-Smirnov test; *P*<0.0034, Appendix Table 25). **(C, F)** Cumulative reaction time distributions of flies maintained at 25 ˚C and 30 ˚C **(F)** at easy (left, 0.1 concentration ratio) and hard (right, 0.9 concentration ratio) difficulty levels.

I used a complementary strategy to confirm the role of the MB in naive intensity discrimination: at the same time as directing shibire^{ts} expression with *OK107-GAL4*, a second MB driver line, *247-LexA*, was used to express GAL80, therefore preventing shibire^{ts} expression in the MB at the permissive

temperature, 30 ˚C (Figure VI-4 A–B). *247-MB > GAL80*, *OK107 > shi^{ts}* flies chose the lower MCH concentration with the same consistency as parental controls (Figure VI-4 A; Appendix Table 27). These data show that the naive intensity discrimination impairment observed in *OK107 > shi^{ts}* was due to blocking synaptic transmission, and therefore output, from the MB.

Reaction times were increased at all difficulty levels in *247-MB > GAL80*, *OK107 > shi^{ts}* flies, compared to parental controls (Figure VI-4 B; Appendix Table 27). The fold changes of reaction times between easy (concentration ratio 0.1) and difficult (concentration ratio 0.7) discriminations were however within the same range for all flies tested, 26% for experimental flies and 19% and 37% for parental controls (*247-LexA*, *LexAop-GAL80*; *OK107* and *UAS-shi^{ts}*, respectively). Furthermore, they were also similar to wild-type reaction time fold changes in similar conditions (30%, data not shown). This increased baseline of reaction times observed for *247-MB > GAL80*, *OK107 > shi^{ts}* is likely due to subtle movement defects provoked by the sheer number of transgenes combined in these flies.

To control for potential olfactory detection defects, and also to further see if the MB is recruited in choices between odours and air, I tested the performance of *OK107 > shi^{ts}* and *247-MB > GAL80*, *OK107 > shi^{ts}* in a simple detection task with the presentation of MCH and air (Figure VI-4 C–D). In both cases the performance of the experimental flies was indistinguishable from the parental controls (Figure VI-4 C–D; Appendix Table 28).

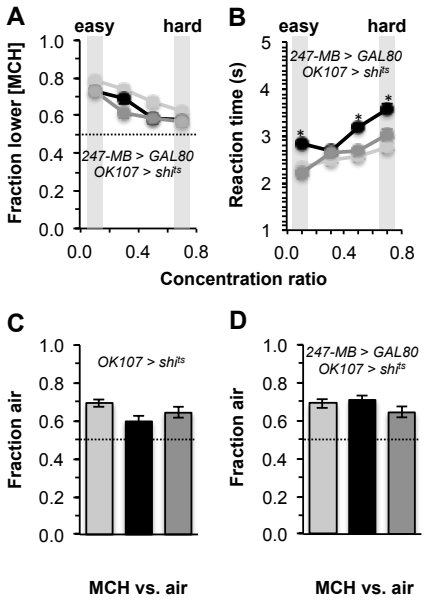


Figure VI-4: The role of mushroom body output in naive intensity discrimination and detection. (A–B) Flies expressing shibire^{ts} under *OK107-GAL4* and GAL80 under mushroom body driver *247-LexA* (*247-MB > GAL80, OK107 > shi^{ts}*, black) and parental controls (*247-LexA, LexAop-GAL80; OK107*, light grey; *UAS-shibire^{ts}*, dark grey) performed naive intensity discrimination tasks. **(A)** Fraction of choices towards the lower MCH concentration (mean±SEM; *N*=171–198 flies per data point) as a function of the difficulty of the task. Choices of 0.5 correspond to performance at chance level (dotted line). **(B)** Reaction times (mean±SEM; *N*=441–1023 decisions per genotype) as a function of the difficulty of the task. Asterisks indicate significant genotype effects (Kolmogorov-Smirnov test; *P*<0.0002, Appendix Table 27). **(C, D)** Fraction of choices towards air (mean±SEM; *N*=171–198 flies per data point) for flies expressing shibire^{ts} under *OK107-GAL4* (OK107 > shi^{ts}, black) **(C)** and also GAL80 under mushroom body driver *247-LexA* (*247-MB > GAL80, OK107 > shi^{ts}*, black) **(D),** performing naive MCH detection against air. Grey symbols denote parental controls: *O107-GAL4* alone or in conjunction with *247-LexA*, *LexAop-GAL80* (light grey) and *UAS-shibire^{ts}* (dark grey). Choices of 0.5 correspond to performance at chance level (dotted line).

Since the MB seems to be employed in naive discriminations and *FoxP*$^{5\text{-}SZ\text{-}3955}$ mutants displayed altered performance in these tasks, it is likely that *FoxP* expression in the MB is required for appropriate naive discrimination. To confirm this expectation, *OK107-GAL4* was used to drive *UAS-FoxP*^{RNAi} (Figure VI-5). Knocking down *FoxP* expression in the MB significantly increased reaction times, specifically in difficult discrimination tasks (concentration ratio 0.7) (Figure VI-5 B; Appendix Table 29). While *OK107 > FoxP*^{RNAi} displayed a 43% increase in reaction time between concentration

ratios 0.1 and 0.7, *OK107-GAL4* and *UAS-FoxP*^{RNAi} controls showed only an increase of 14% and 23%, respectively.

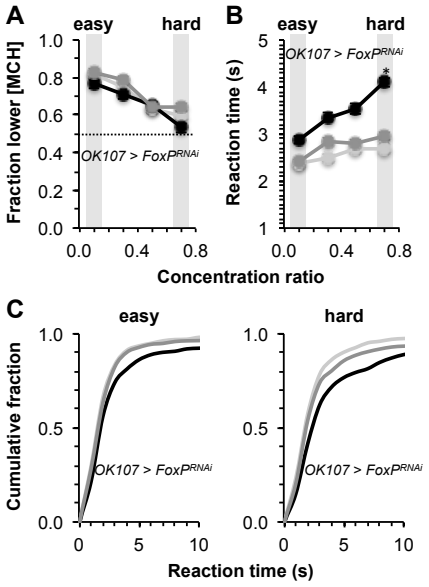


Figure VI-5: Manipulating *FoxP* expression in the mushroom body. (A–C) Flies expressing *FoxP*^{RNAi} under the control of *OK107-GAL4* performed naive intensity discrimination tasks. Black and grey symbols and lines denote experimental flies and parental controls, respectively (*OK107-GAL4*, light grey; *UAS-FoxP*^{RNAi}, dark grey) **(A)** Fraction of choices towards the lower MCH concentration (mean±SEM; *N*=162–191 flies per data point) as a function of the difficulty of the task. Choices of 0.5 correspond to performance at chance level (dotted line). **(B)** Reaction times (mean±SEM; *N*=507–806 decisions per data point) as a function of the difficulty of the task. The asterisk indicates significant genotype effects (Kolmogorov-Smirnov test; *P*<0.0001, Appendix Table 29). **(C)** Cumulative reaction time distributions at easy (left, 0.1 concentration ratio) and hard (right, 0.7 concentration ratio) difficulty levels.

The data presented in this Chapter seem to point to the fact that the MB is an integral part of the circuitry responsible for naive intensity discrimination tasks. Furthermore, *FoxP* expression within this structure seems to mediate which type of decision-making system is engaged.

Chapter VII. Discussion

The work presented in this thesis entailed using trained olfactory discriminations in two-alternative forced-choice tasks to characterise the involvement of the transcription factor FoxP in decision-making. Analysing this molecule's expression pattern together with targeted neuronal excitation and FoxP expression manipulation permitted the identification of a subset of mushroom body (MB) neurons, Kenyon cells (KCs), projecting to the cores of the α and β lobes (αβc), as critical for decision-making. Additionally, an initial screen for gene products potentially regulated by FoxP yielded candidate genomic regions of interest for further study. Finally, a characterisation of naive olfactory discrimination was also performed and future work will allow disentangling the commonalities and differences between the circuits and computations involved in trained and naive olfactory choice behaviours.

This Chapter comprises a discussion of the results obtained, pinpointing open questions and future avenues of research.

Trained decision making behaviour

The work presented in Chapter III showed that trained adult fruit flies engage an active decision-making process when performing olfactory discriminations of varying difficulty (Figure III-2 and Figure III-3). These studies were

performed using a previously developed two-choice single fly assay (Claridge-Chang et al., 2009) which, unlike commonly used traditional population assays (Quinn et al., 1974; Tully and Quinn, 1985; Woodard et al., 1989; Park et al., 2002; Larsson et al., 2004; Ruebenbauer et al., 2008), or low throughput individual fly setups (Budick and Dickinson, 2006; Duistermars et al., 2009; Bhandawat et al., 2010), allowed analysing the subtleties of trained odour discrimination tasks in several individual flies simultaneously. Other studies involving multiple single fly tracking setups (Steck et al., 2012), identified differences in olfactory detection responses to different odorants in finer endpoints such as response latency and temporal dynamics of sensitivity. The assay and tasks used in this thesis assessed, however, for the first time, simultaneous measurements of accuracy and reaction time in discrimination tasks of varying difficulty.

The results obtained by analysing the fly's performance in discrimination tasks of increasing difficulty (Figure III-2) showed that its behaviour is consistent with human (Vickers, 1970; Vickers and Packer, 1982; Palmer et al., 2005), non-human primate (Shadlen and Newsome, 2001; Roitman and Shadlen, 2002; Heitz and Schall, 2012) and rodent (Uchida and Mainen, 2003; Abraham et al., 2004; Rinberg et al., 2006) behaviour in perceptual two-alternative forced-choice tasks: increasing task difficulty by decreasing stimulus contrast leads to an increase in reaction times and eventually a decline in accuracy. These results together with the positive skew of reaction time distributions, considered indicative of deliberate decision making, are consistent with sequential analysis framework models (reviewed in Ratcliff and Smith, 2004; Gold and Shadlen, 2007). In these models, evidence is

accrued in favour of a choice until a response criterion is met and behaviour is discharged; the weaker the sensory evidence, the longer the integration process takes with the consequent increase in reaction times.

Indeed, the fruit fly's olfactory discrimination psychometric and chronometric data are consistent with a simple drift diffusion model (Figure III-2) (Palmer et al., 2005) of the type extensively used to model vertebrate decision making behaviour. This type of model, by assuming a single integrator accumulates net evidence, does not make assumptions of how independent evidence integrators interact in order to yield a single outcome of the decision-making process. Furthermore, the minimal number of the free estimated parameters in the coupled analytical expressions for reaction time and accuracy (Palmer et al., 2005), residual time, bound height and drift rate (which is also constant), make it the most parsimonious model to use. In line with this, many other models can be reduced to drift-diffusion models (Bogacz et al., 2006). Further cellular and circuit level studies of decision-making will allow developing and testing biologically based decision-making models.

Unlike previous attempts to study decision making in the fruit fly using tasks with alternative courses of action (Certel et al., 2007, 2010; Maimon et al., 2008; reviewed in Dickson, 2008) or choices between different stimuli (Tanimura et al., 1982; Tang and Guo, 2001; Yang et al., 2008a; reviewed in Itskov and Ribeiro, 2013), this study conclusively showed that the fruit fly exhibits deliberate decision making. Studies in the bumble bee (Chittka and Dyer, 2003; Kulahci et al., 2008; reviewed in Chittka et al., 2009) had shown that at least some invertebrates displayed characteristics of deliberate decision making, namely speed-accuracy trade-offs, but did not provide

insights into the circuit mechanisms used to construct and act upon decision variables.

The establishment of a trained two-alternative forced-choice olfactory discrimination task with the characteristics of evidence integration to threshold in a multiple fly, individual testing assay lays the ground to uncover the molecular and neuronal basis of decision-making in detail (further discussed below). At the behavioural level alone this study is also the starting point for several avenues of research. Given that deliberate decision-making is a characteristic of at least three different trained olfactory tasks (intensity discrimination, masking odour and mixture discrimination), it would be interesting to determine if this process generalises to choices between two alternatives of other sensory stimuli or even combinations of different sensory stimuli.

In terms of the behavioural analysis itself, developing a setup that allows a finer examination at higher resolution could prove informative, and ultimately allow a electrophysiological characterisation of the progression of the integration process, as well as manipulation of the neuronal circuits responsible, as a decision progresses toward commitment (further discussed below). This could be done by adapting the previously described air-supported ball setup for *Drosophila melanogaster* (Buchner, 1976) used for studying osmotropotaxis (Borst and Heisenberg, 1982), particularly incorporating higher precision movement detection features of more recent designs (Chiappe et al., 2010; Gaudry et al., 2013), together with shock and odour delivery systems. In order to simulate the virtual movement of the fly the two air streams would ideally be susceptible of being quickly displaced.

This type of setup, similar to one used to study auditory discriminations in mice (Sanders and Kepecs, 2012), would allow a more detailed description of the behaviour than the current tracking of the fly's silhouette, by simultaneously recording its movements on the ball and imaging the antennae.

The fly requires both antennae to show normal osmotropotaxis (Borst and Heisenberg, 1982) and uses bilateral, albeit asymmetrical, olfactory and mechanosensory signals to track odour gradients in tethered flight conditions (Duistermars et al., 2009). Furthermore, odour lateralisation is also encoded by increased neurotransmitter release in bilaterally projecting olfactory sensing neurons on the ipsilateral axon branch, which results in a shorter latency and/or higher firing rates in projection neurons (Gaudry et al., 2013). It would be interesting to study the fine behaviour of the fly at the spatial location where it has access to the information concerning the two odour streams for the different task difficulties. This would provide insight into the sampling mechanism used by the fly during evidence integration.

Another interesting line of research to pursue, possible if the experimenter can control the time the fly is exposed to the two odour streams, would be to further test the speed-accuracy interplay and the limits of olfactory decision making. By forcing the fly to integrate evidence for different periods of time and analysing accuracies, it should be possible, for each concentration ratio, to determine the integration time that allows maximal performance and determine the minimum integration time for performance above chance. This knowledge could be useful for further studies of neuronal function and in

comparisons between wild-type and mutant flies with impaired decision-making.

Molecular players in trained decision making

As previously mentioned, the main advantage of studying decision-making in the fruit fly is the possibility of uncovering genes involved in this process. This constitutes a platform for determining the neuronal mechanisms responsible for the integration process and imposing the criterion for commitment to a choice, as well as the delineation of the neuronal circuits involved.

Mutating *FoxP* impairs decision making

The results presented in Chapter IV showed that mutating the *FoxP* gene impaired decision-making, leading to increased reaction times, particularly in difficult discriminations (Figure III-6). Taking into account the drift diffusion modelling exercise of the mutant data, the transcription factor FoxP seems to be involved in the progression of neural activity from a choice-neutral to a choice-specific state, and mutating the gene slows this progression. The exact mechanisms behind FoxP's action are still unknown.

The FoxP subfamily of forkhead box transcription factors consists of four members in vertebrates FoxP1–4 (reviewed in Hannenhalli and Kaestner,

2009; Takahashi and Takahashi, 2009). Distinguishing features of the FoxP subfamily include a carboxy-terminal DNA-binding domain (leucine zipper) and a zinc finger motif located at the N-terminus of this domain (Li et al., 2004). Each of these FoxP members encompasses several isoforms, which result from highly regulated tissue-specific alternative splicing, but only FoxP1 seems to show alternative splicing of the forkhead domain (Santos et al., 2011). While FoxP1, FoxP2 and FoxP4 are expressed in the brain and other organs such as the heart, lung and gut, FoxP3 is expressed in the immune system (reviewed in Takahashi and Takahashi, 2009).

Drosophila melanogaster has a single *FoxP* gene comprised of six constitutively and two alternatively spliced exons that give rise to protein isoforms FoxP-A and FoxP-B (Santos et al., 2011). Both isoforms are expressed in the central nervous system (CNS) from embryonic stage 8, share a N-terminal zinc finger domain but possess different C-terminal forkhead domains (Santos et al., 2011). FoxP-A is additionally expressed in hemocytes (Santos et al., 2011) and could therefore play a role in immunity.

The alternative splicing of the forkhead domain of *Drosophila melanogaster*'s *FoxP* gene is a feature though to be reminiscent of the ancestral bilaterian *FoxP* gene, which has been maintained only in the *FoxP1* orthologue and lost in *FoxP2–4* (Santos et al., 2011). A phylogenetic analysis of the sequences of forkhead and zinc finger domains further supports the fact that *FoxP* is closer to *FoxP1* than any other orthologue (Santos et al., 2011); the forkhead domains of *FoxP* and *FoxP2* are furthermore also very similar (Santos et al., 2011), and FoxP2 is the closest relative of FoxP1 (reviewed in Bacon and Rappold, 2012).

Impairments in vertebrate FoxP1 and FoxP2 have been implicated in cognitive development, and display some similar phenotypes (reviewed in Bacon and Rappold, 2012). These transcription factors potentially even act together in the CNS, in certain instances (Teramitsu et al., 2004; Konopka et al., 2012), through the formation of heterodimers (Li et al., 2004) to facilitate DNA binding for transcriptional regulation, and/or are expressed in different neuronal components of circuits involved in cognitive functions (Hisaoka et al., 2010). The *FoxP2* gene has been implicated in the development of speech and language (Lai et al., 2001; reviewed in Fisher and Scharff, 2009; Enard, 2011; Nudel and Newbury, 2013), birdsong (Haesler et al., 2007), vocalisations in mice (Shu et al., 2005), and has also been shown to impact motor learning in rodents (Groszer et al., 2008; French et al., 2012). *FoxP1* has also been implicated in the development of speech and motor control (Pariani et al., 2009; Carr et al., 2010; Horn et al., 2010; O'Roak et al., 2011; Talkowski et al., 2012; Le Fevre et al., 2013). Both genes have further been associated with cognitive disorders (Vargha-Khadem et al., 1995; Fisher et al., 1998; Carr et al., 2010; Hamdan et al., 2010; Horn et al., 2010; O'Roak et al., 2011; Talkowski et al., 2012; Le Fevre et al., 2013).

Drosophila melanogaster's *FoxP* gene has been less extensively characterised than its vertebrate homologues. Nevertheless, two recent studies investigated the effect of impairing *FoxP* expression on motor coordination (Lawton et al., 2014) and operant motor learning (Mendoza et al., 2014). Pan-neuronal expression of $FoxP^{RNAi}$ decreased male courtship behaviour, altered the structure of the courtship song, and impaired flight escape and walking in both sexes (Lawton et al., 2014). These results are in

line with the observed movement defect produced by pan-neuronally expressing *FoxP*^{RNAi} (data not shown), and a role for FoxP in movement initiation and/or coordination seems plausible.

Another study showed that three *FoxP* mutants exhibit decreased flight performance and analysed the behaviour of *FoxP*^{3955} mutants and flies with pan-neuronally expressed *FoxP*^{RNAi} in different types of operant learning tasks (Mendoza et al., 2014). Homozygosity for the *FoxP*^{3955} mutation and pan-neuronal disruption of *FoxP* expression only impaired an operant learning task where the fly's flight movement alone is associated with heat punishment and had no effect on tasks in which a colour was also predictive of punishment (Mendoza et al., 2014). These data show that FoxP might also have a role in motor learning, similarly to vertebrate FoxP1 and FoxP2.

FoxP and the vertebrate FoxP1 and FoxP2 appear to have a common role in processing through ordered activity sequences as required for the appropriate representation of trains of thought, strings of syllables, sequences of motor commands or evidence accumulation. Given that *Drosophila melanogaster*'s *FoxP* gene potentially closely represents the ancestral bilateria gene (Santos et al., 2011), studying its function could provide insight into the basis of temporal processing (Mauk and Buonomano, 2004).

Targets of FoxP action

As transcription factors, members of the FoxP subfamily regulate the expression of other genes. To understand their effect on cognitive processes, it is therefore essential to identify and classify target genes to determine the pathways and networks they regulate. FoxP2 has been more extensively studied than FoxP1, and several genome wide *in vivo* chromatin immunoprecipitation studies (ChIP; technique for assaying protein–DNA binding in vivo) (Solomon et al., 1988) with microarray use (ChIP-chip) (Blat and Kleckner, 1999; Ren et al., 2000), coupled to expression profiling, have identified many transcriptional targets mainly in humans and mice (Spiteri et al., 2007; Vernes et al., 2007, 2011).

These studies, together with other target discovery studies (Groszer et al., 2008; Vernes et al., 2008; Konopka et al., 2009; Sia et al., 2013), have implicated FoxP2 in the development of neuronal connections and adult neuronal functions. FoxP2 has been shown to play a role in: CNS patterning, by regulating, for example, members of homeotic (HOX) and paired box (PAX) genes (Spiteri et al., 2007; Vernes et al., 2007); CNS development, through the control of Wnt members (Spiteri et al., 2007; Vernes et al., 2007); neurite outgrowth and axonal morphology, including calcium-mediated growth cone dynamics (Spiteri et al., 2007; Vernes et al., 2007, 2011; Enard et al., 2009; Konopka et al., 2012); activity-based networks involved in plasticity, including branching of dendrites, mobilization of calcium, and learning (Spiteri et al., 2007; Vernes et al., 2007, 2011; Groszer et al., 2008; Enard et al.,

2009; French et al., 2012); synaptogenesis through the regulation of sushi repeat–containing protein X-linked 2 (SRPX2) gene (Roll et al., 2010; Sia et al., 2013); intracellular signalling cascades and cation homeostasis (Spiteri et al., 2007); neural recognition and cell adhesion via regulation of genes such as neurexin family member contactin-associated protein-like 2 (*CNTNAP2*) (Vernes et al., 2008). Identified FoxP1 targets in the brain are more restricted; nevertheless, it has been established that FoxP1 regulates *CNTNAP2* expression (O'Roak et al., 2011), similarly to FoxP2, and *Pitx3* transcription, that is involved in neuronal differentiation and development (Konstantoulas et al., 2010).

Since *Drosophila melanogaster*'s *FoxP* gene is similar to the vertebrate *FoxP1*, which in turn is very similar to *FoxP2*, it is likely that the role and mode of action of the proteins, including the nature of the genes they regulate, exhibit some commonalities. Therefore, FoxP potentially modulates synaptic plasticity, neurodevelopment, neurotransmission, and/or axon guidance, and defects due to mutations in the *FoxP* gene likely result from disrupting the expression of genes involved in developmentally specifying neuronal connections and/or regulating adult neuronal function. $FoxP^{3955}$ mutants have no clear neuroanatomical defect (data not shown), further corroborated by a recent study in which only reduced volume of the optic glomeruli was reported (Mendoza et al., 2014). Impairing *FoxP* expression produces no obvious gross morphological disruption and more subtle effects that could account for the phenotypes observed are yet to be uncovered.

In order to start to uncover potential targets of FoxP action, while potentially maximising the discovery of genes in other cascades involved in decision

making, a sensitised deficiency screen was performed for the 2nd and 3rd chromosomes within a *FoxP* mutant background (Chapter V). This strategy was chosen over other types of commonly used forward genetic strategies, such as transposon insertions or ethylmethane sulfonate mutagenesis (EMS) (reviewed Venken et al., 2011), mainly because it presented a feasible approach to scan virtually the whole genome, using molecularly defined deficiencies, and maximised the chances of finding FoxP regulated gene products and/or interacting partners. Sensitised screens have been extensively used in developmental studies where heterozygote loss-of-function mutations are recessive and 50% of the wild-type level of a protein is sufficient for normal development; partially disrupting a particular process with another mutation exposes the inadequacy of heterozygous protein levels and allows the identification of other genes in the pathway of the sensitised genetic background (St Johnston, 2002).

Screening the deficiency set within a sensitised genetic background, albeit a more targeted, systematic and high throughput approach than screening EMS lines or transposon insertion collections (reviewed in Venken et al., 2011), may present some caveats. Some deficiencies might modify the phenotype by altering the expression of the allele or construct used to generate the sensitized background, rather than constituting an actual player within the molecular cascade of the sensitized allele (reviewed in St Johnston, 2002). Furthermore, since not all of the components of a pathway will necessarily be dosage sensitive (reviewed in St Johnston, 2002), this type of screen can potentially overlook important targets involved in decision-making.

Despite these caveats, the strategy used constitutes a good first approach to uncover genomic regions of interest that might contain downstream targets of FoxP. By analogy with the closely related FoxP1 and FoxP2, which interact with various proteins to regulate gene expression in different tissues (reviewed in Bacon and Rappold, 2012), it is likely that *Drosophila* FoxP also interacts with other proteins that could be picked up in the deficiency screen. Uncovering both types of molecules will provide insight into the molecular mechanisms underlying decision-making.

Using a simplified protocol, 313 deficiencies were analysed. Reassuringly, the majority of the deficiencies tested (227) did not exhibit a phenotype (Figure V-2), and out of the ones that did, only 44 displayed increased reaction times, similar to the performance of $FoxP^{3955}$ homozygous mutants. These deficiencies disrupt a total of 3,255 genes, which constitutes an impractical number of genes for which to test individual mutants even if they were immediately available.

The first step to further pursue this line of research should be to confirm that the severity of the reaction time phenotypes observed, as in the case of *FoxP* mutant flies, is dependent on stimulus contrast. Therefore, the behaviour of each of these deficiencies should be analysed in at least two different concentration ratios, an easy and a difficult task. Once deficiencies that actually replicate the mutant phenotype have been identified, further smaller deficiencies can be tested to increasingly narrow down the genomic regions of interest.

A useful parallel approach to develop, similarly to what has been done to uncover networks regulated by FoxP2 in vertebrates (Spiteri et al., 2007; Vernes et al., 2007, 2011), would be to use whole genome ChIP-chip or ChIP-seq (chromatin immunoprecipitation with massively parallel DNA sequencing) (Barski et al., 2007; Johnson et al., 2007; Robertson et al., 2007; reviewed in Park, 2009 and Furey, 2012). As described in Chapter IV, however, attempts to confirm FoxP expression using commercially available antibodies did not yield conclusive results. A recent study developed a FoxP antibody that supposedly detects a region common to both FoxP isoforms (Lawton et al., 2014). If this antibody indeed effectively binds to FoxP, or if a working antibody can be raised, these strategies would be feasible. It would furthermore be interesting to disentangle the role of each FoxP isoform. The *FoxP* mutants used in this study resulted from P element insertions either in the 8th alternatively spliced exon, that gives rise to part of the C-terminal present only in isoform B, or in the 3'UTR region (Figure III-5 and Figure III-8). Attempts to detect levels of FoxP expression with real time/quantitative PCR (qPCR) were inconclusive (data not shown), potentially because the level of transcription was too low to produce reliable and reproducible results. It is therefore unknown if the source of the defects in decision-making observed in strains with a disrupted *FoxP* locus is the impairment of the expression of either FoxP-B or both isoforms. Uncovering genes regulated by each isoform (by raising specific antibodies), together with other strategies further discussed in the next section, would allow determining their involvement in decision making.

In the case appropriate antibodies can not be raised against FoxP and each isoform, whole genome microarray expression data comparisons between wild-type and *FoxP* mutant flies could also be cross-referenced with the deficiency screen to determine genes whose expression is regulated by FoxP.

Since FoxP's binding site(s) has/have yet to be characterised despite many initiatives to characterize transcriptions factors and their target domains in the fruit fly (see for example Shazman et al., 2014)), further parallel strategies could involve specifically identifying this/these sites. *In vitro* strategies could include employing selex (Tuerk & Gold, 1990; reviewed in Gold, 1995; protocol available in Ogawa & Biggin, 2012;), protein-binding microarrays (Mukherjee et al., 2004; Berger et al., 2006) and microfluidics platforms such as MITOMI (mechanically induced trapping of molecular interactions) (Maerkl and Quake, 2007; protocol available in Rockel et al., 2012), or the bacterial one-hybrid system (Meng et al., 2005; reviewed in Bulyk, 2005; protocols available in Noyes et al., 2008; Noyes, 2012). *In silico* computational approaches could also be used to search for the binding sites associated with vertebrate FoxP1 and FoxP2, given their evolutionary conservation with FoxP, and/or also to identify statistically overrepresented sequence motifs within genomic segments identified using other techniques.

The intersection between the results obtained with these strategies will yield a number of genes of interest, whose involvement in decision-making can further be confirmed using other approaches such as screening existing mutants and also driving RNAi for these genes (Mohr, 2014) in the neurons in which FoxP is expressed (further discussed in the next section).

Directing GAL4 expression using *FoxP*'s putative promoter allowed the identification of subsets of the MB as potential sites of FoxP action (Chapter IV). The *FoxP-GAL4* line I constructed displayed very restricted expression, labelling ~80 αβc KCs and ~100 γ KCs out of the 2,000–2,500 KCs present in the MB (Technau, 1984; Balling et al., 1987; Tanaka et al., 2008; Aso et al., 2009) (Figure IV-1). A line produced in another study showed a broader expression pattern encompassing approximately 420 neurons, distributed throughout a wide area of the CNS, including the protocerebral bridge and other smaller clusters, such as in the abdominal and thoracic ganglions, but not the MB, according to the authors (Lawton et al., 2014). The line I generated was weak at driving transgene expression, and expression was analysed using two copies of both the driver and the effector to allow strong GFP visualisation; the expression pattern of the other *FoxP-GAL4* line, however, was assessed with a single copy of both transgenes, which could account for the lack of MB expression. The differences between the two lines could be due to the way they were generated: the putative promoter region used in the construct I developed was smaller (1,411 bp from 3R: 5,555,156..5,556,528 versus 1,542 bp from 3R: 5,555,155..5,556,697), and the *FoxP-GAL4* strain was produced through site-directed insertion through ΦC31 integration (Groth et al., 2004) into the *attP40* site, while the other line was randomly inserted in the genome. Being bigger, the putative promoter region used for the other *FoxP-GAL4* could potentially encompass unrelated

regulatory elements from the upstream gene (Figure IV-2). As for the insertion method, both strategies are susceptible to influences on expression strength; however, randomly inserted driver lines are particularly prone to be affected by regulatory elements of other genes in unpredicted ways, unlike the well characterised ΦC31 integration sites (Markstein et al., 2008; Pfeiffer et al., 2010), whose expression levels have been studied with some detail.

It is perfectly possible that the line I generated only partially identifies the expression of *FoxP*. The expression of the other *FoxP-GAL4* strain (Lawton et al., 2014) reportedly coincides with that identified with the FoxP antibody developed in the same study, though background expression levels were found to be high. This broader expression pattern seems quite plausible as both pan-neuronally decreasing *FoxP* expression and preventing synaptic transmission from FoxP positive neurons (Lawton et al., 2014) produced motor impairments. It would however be useful, in order to unambiguously confirm the regions in which FoxP and particularly each isoform is expressed, to perform *in situ* hybridisations.

Consistent with the possibility that the *FoxP-GAL4* I developed does not encompass all FoxP-positive neurons, it was found to be weak at driving transgene expression and was inefficient at driving $FoxP^{RNAi}$ (Figure IV-3). Attempts to develop stronger driver lines for FoxP neurons are underway by combining the putative promoter and sequences corresponding to the last intron; adding intronic regions, common sites for enhancers that can dictate aspects of the expression of a gene (reviewed in Maeda and Karch, 2011), should boost expression levels. Indeed a putative *FoxP* 406 bp enhancer element corresponding to a region of the last intron (3R:5553319..5553725),

common to both isoforms, was used to develop a strain (*P{GMR95A01-GAL4}attP2*, Rubin laboratory at Janelia Farm) that also shows expression mainly in the MB (data not shown). Homologous recombination (HR) approaches (reviewed in Maggert et al., 2008) could further be used to directly insert driver and effector genes in the *FoxP* locus, specifically through optimised ends-out HR (Huang et al., 2008, 2009). Developing a driver line with stronger expression levels would be useful for further studies.

Despite the fact that FoxP's expression is likely broader than the expression pattern observable with the *FoxP-GAL4* here described, selectively impairing *FoxP* expression in αβc KCs using a stronger driver line (Figure IV-4) mimicked the *FoxP* homozygous mutant phenotype. Furthermore, both decreasing neuronal excitability by expressing Kir 2.1 in FoxP-positive neurons (Figure IV-5), or specifically in αβc KCs (Figure IV-6) also replicated the mutant's impairment. These data point to a previously unassigned role of αβc KCs as possible integrators involved in evidence accumulation in decision-making.

Previous studies showed that γ KCs are involved in both appetitive and aversive short-term memory (STM) (Trannoy et al., 2011; Knapek et al., 2013; Zars et al., 2000; McGuire et al., 2003; Blum et al., 2009; Qin et al., 2012; Boto et al., 2014), and that their selective inhibition is essential for discriminative learning (Zhang and Roman, 2013). αβ KCs were previously shown to be involved in middle and long term memory (LTM) retrieval (McGuire et al., 2001; Schwaerzel et al., 2002; Isabel et al., 2004; Krashes et al., 2007; Trannoy et al., 2011), with a segregated role of each subdivision: output from αβs is required for appetitive and aversive LTM retrieval and αβc

output is specifically required for the retrieval of consolidated appetitive memory (Perisse et al., 2013b). While these results are in apparent contradiction with my results, the investigations of the role of αβ KCs focused on retrieval of memories mostly after 3 h, some after 30 min, while my experiments were performed immediately after training. The role of αβ KCs and particularly its subdivisions in STM has not been thoroughly analysed and, in fact, one study has reported that besides a role for γ KCs, αβ KCs also have a effect on STM, depending on the odour combinations used during training (Akalal et al., 2006). Consistent with this idea, though aversive reinforcing PPL1 cluster MP1 and PAM cluster M3 DA afferent neurons preferentially arborize in the αβs layer, their innervation in αβc is not inexistent (Perisse et al., 2013b). Furthermore αβc neurons have been implicated in value-based decisions, more specifically in choices between odours associated with punishments of differing severity (Perisse et al., 2013b). It could be possible that this type of value judgment also exhibits a difficulty dependent increase in reaction time, which could easily be tested and help to further understand the role of αβc KCs.

My results suggest that in addition to the early role of γ KCs in memory processes and the role of αβc in longer-term memories, αβc KCs are also required immediately after training for an appropriate evidence accumulation process underlying discrimination choices. It would be interesting to trace the circuit from the neurons responsible for evidence integration all the way to the motor output centres. Some efferent neurons involved in approach and avoidance behaviour have been identified: MB-V3 neurons that arborise throughout both βs and βc regions (Perisse et al., 2013b) and are required for

appetitive and some types of aversive LTM (Pai et al., 2013; Plaçais et al., 2013); MB-V2α aversive memory specific output neurons (Séjourné et al., 2011) whose dendrites are most pronounced in the αs region, but not absent from the αc region (Perisse et al., 2013b). The studies are also not necessarily in contradiction with my results, as there are still open questions regarding these output neurons: the role of MB-V3 neurons immediately after training has not be assessed and they could potentially be involved at this time point; the fact that MB-V2α neurons are not absent from the αc region also still leaves open the possibly of their involvement in aversive STM.

It seems clear that the population assays used over the past four decades may have overlooked nuances of the role of the MB. Indeed other studies have shown that traditional learning and memory mutants (whose impaired genes are required in the MB) show defects in attention in the optomotor maze and in working memory in spatial orientation tasks (van Swinderen and Flores, 2007; van Swinderen and Brembs, 2010). Other studies have also found that inactivating the MB impairs the fly's ability to perform clear cut decisions in a saliency based paradigm in the flight simulator (Tang and Guo, 2001; Zhang et al., 2007). The evidence presented in Chapter IV of this thesis clearly points to a more subtle function of the ~80 FoxP-positive αβc KCs in evidence accumulation in intensity discrimination tasks. Studying decision-making after the formation of aversive memories of different lengths and after appetitive conditioning should additionally shed light on the role of αβc KCs.

How exactly FoxP affects αβc KC function is still unknown. Since the neurons in which FoxP function is required for appropriate decision making have been identified, downstream targets could be uncovered by direct analysis of the

transcription profiles of wild-type and *FoxP*^{3955} mutant αβc KC. This could be done, for example, by fluorescence-activated cell sorting (FACS) followed by either ChIP-chip/-seq or mRNA sequencing, depending on the successful development of antibodies. Additionally, αβc KCs with RNAi-mediated *FoxP* expression disruption could also be analysed.

FoxP expression using the *FoxP-GAL4* I generated (data not shown) and in an independent study (Lawton et al., 2014) is also observable throughout development. Furthermore, only RNAi mediated disruption of *FoxP* expression during development and not in the adult stage (Lawton et al., 2014), impairs movement. It would be interesting to study in which developmental stage *FoxP* expression is necessary for appropriate decision making, which would also provide insight into the type of processes that this transcription factor regulates. This could be done by using GAL80^{ts} (McGuire et al., 2003) to control the expression of *UAS-FoxP*^{RNAi} in αβc KCs.

It is currently unknown if the integration impairment observed in *FoxP* mutants or by driving *UAS-FoxP*^{RNAi} in αβc KCs results from disrupting both or only one of the two FoxP isoforms. The RNAi line used, *v15732* (Dietzl et al., 2007), is a 305 bp hairpin whose sequence corresponds to a region within the first *FoxP* exon (3R: 5.554.703–5.555.007), similarly transcribed and translated in both isoforms. Further studies using fly strains that specifically rescue FoxP-A or FoxP-B, as well as both isoforms, in the mutant background, will allow further elucidation. Preliminary attempts were made in this direction (data not shown), although the results were inconclusive. FoxP levels are probably highly regulated and the developmental timing of expression extremely sensitive; rescue experiments are therefore potentially

complicated as they could very easily fail due to under- or overexpression of the transcription factor in the appropriate period. Another strategy to disentangle the role of each isoform in decision-making could include developing dominant-negative constructs for the differentially spliced forkhead domains of each isoform.

Given that impairing *FoxP* expression in αβc KCs and decreasing their excitability leads to increased reaction times, it seems plausible that the slower accruement of olfactory evidence is at least partially due to changes in activity patterns. In order to test this prediction the olfactory responses of αβc KCs are currently being studied by imaging calcium responses in the mutant. Ultimately it would also be useful to obtain electrophysiological data, which could provide more detailed information about the properties of these neurons.

Since at least part of the decision-making circuitry involved in olfactory discriminations is now known, the involvement of the same molecules and neurons could be probed in other discrimination tasks. The MB is a higher order multisensory structure, with proposed roles, beyond olfactory learning and memory, in controlling behaviours that require extensive information processing, such as sleep/wake cycles (Joiner et al., 2006; Pitman et al., 2006), courtship conditioning and mate selection (McBride et al., 1999; Keleman et al., 2012), motor activity fine tuning (Serway et al., 2009), resolution of visual ambiguity (Liu et al., 1999; Tang and Guo, 2001; Zhang et al., 2007) and stabilisation of visual memories against context changes (Brembs and Wiener, 2006). It is therefore possible that it is an integral part of the evidence integration circuitry in multiple stimuli discrimination tasks.

Compared with the previously alluded limited possibility to probe circuit function in vertebrates, the fruit fly should allow a much more detailed study of biophysical mechanisms underlying the decision-making process, as well as tracing and manipulating the circuit all the way from the neurons responsible for sensory encoding to the neurons responsible for the behavioural outcome reflecting a choice. Fine behavioural analysis assays have been optimised to allow electrophysiological recordings (Maimon et al., 2010), functional imaging (Chiappe et al., 2010; Seelig and Jayaraman, 2013) and neuronal activation and inactivation (Gaudry et al., 2013; Bath et al., 2014) in behaving flies. Similarly, the previously mentioned air-supported ball setup with coupled olfactory delivery setup could allow, in the long run, studying neuronal activity and decreasing or increasing activity in αβc KCs at specific steps of evidence integration before the commitment to a choice. Optogenetic activation studies will however be most useful for unravelling the downstream circuits responsible for conveying the result of the decision process to the motor output centres responsible for the manifestation of the choice rather than for attempting to activate αβc KCs. Even though a recent study managed to induce learning by thermogenetically activating a random subset of KCs paired with a shock (Vasmer et al., 2014), the sparseness of KC responses (Wang et al., 2004; Turner et al., 2008; Honegger et al., 2011) means that finding the subset of αβc KCs that respond specifically in the discrimination tasks studied, and activating them to bias the decision process is at the moment impractical.

Naive olfactory discrimination

Naive discrimination behaviour, characterised in Chapter VI, is, compared to trained discrimination behaviour, faster and less consistent, especially for smaller concentration ratios, i.e., lower stimulus contrast (Figure VI-1). This distinction seems obvious: in trained tasks stakes are higher, due to the reinforcement of the higher MCH concentration, increasing the motivation to perform difficult discriminations; conversely, in naive tasks, the lack of reinforcement makes the motivation to perform a difficult discrimination weak. However, naive choice does not seem to be a purely reflexive behaviour as reaction times display a slight increase in difficult discriminations. Despite this fact, the behavioural signature of naive and trained performance is unquestionably different and the discrepancies seem to point to the existence of two decision making systems: a slower, more accurate, trained decision making system, and a faster, less consistent, naive discrimination system. In vertebrates, dual systems with slower/faster, accurate/less accurate dichotomies have been identified and their interplay modelled (Trimmer et al., 2008); further studies in the fruit fly could help shed light into circuit and neuronal mechanism underlying these systems.

Once again the behaviour of *FoxP* mutants differs from that of wild-type flies (Figure VI-2), being more consistent and slower. It seems possible that disrupting *FoxP* expression leads to an inappropriate recruitment of the circuitry normally involved in trained discriminations, given its potential role in regulating genes involved in the development of neuronal connections and of

importance for mature neuronal functions. Indeed the MB seems to also be engaged in naive olfactory discrimination and FoxP expression within it appears to be required for appropriate naive discrimination: blocking MB output using a strong and broad line *OK107-GAL4* (Figure VI-3) prevented flies from discriminating the two MCH concentrations; RNAi-mediated down-regulation of *FoxP* expression in the MB replicated the reaction time phenotype observed in the *FoxP* mutant (Figure VI-5), but not the enhanced consistency of choice – the decrease of FoxP levels is likely not sufficient for a full recapitulation of the mutant phenotype.

While it is widely assumed that the LH (Suh et al., 2004, 2007; Kurtovic et al., 2007; van der Goes van Naters and Carlson, 2007; Datta et al., 2008; Ruta et al., 2010; Kohl et al., 2013; Lin et al., 2013a; Min et al., 2013), but not the MB (Heisenberg et al., 1985; de Belle and Heisenberg, 1994; Dubnau et al., 2001; McGuire et al., 2001; Parnas et al., 2013), mediate naive olfactory behaviour, some studies showed that the MB is required, in certain contexts, for at least selected innate responses (Wang et al., 2003b; Bräcker et al., 2013).

Most studies of LH function dealt with environmentally or socially relevant dedicated olfactory processing channels, while their role in the processing of general odours and particularly of odour discriminations has not been extensively studied. A recent study, however, used *247-LexA*, another MB line that drives transgene expression in all KCs, and showed that the fly's spontaneous discrimination behaviour for several sets of two odours was MB independent (Parnas et al., 2013). It is possible that the expression patterns of *OK107-GAL4* and *247-LexA* vary on a fine scale or that the strength of expression of the effector shibire^{ts} using these two binary systems

differentially impacts discriminations. Given the broadness of the driver *OK107-GAL4*, which further encompasses the antennal lobe (Aso et al., 2009), this driver could also be responsible for producing an effect at earlier stages of olfactory processing. However, using *247-LexA* to drive *LexAop-GAL80*, while *OK107-GAL4* drives *UAS-shibire*^{ts} (preventing shibire expression in the MB using another MB driver), thereby leaving MB function intact, did not affect naive discrimination. Furthermore, MCH detection in *OK107 > shi*^{ts} (Figure VI-4) was not impaired suggesting that these flies are able to process olfactory information appropriately. Finally, the data presented in this other olfactory discrimination study (Parnas et al., 2013) is not necessarily in contradiction with my own as the tasks were substantially different: I used different intensities of the same odour, while only discriminations between different odours had been previously studied.

It is important to further confirm the results presented in Chapter VI using another MB line, preferentially one that drives GAL4 expression as well, for cross reference with the data already obtained and for the expression of *UAS-FoxP*^{RNAi}. A *247-GAL4* exists (Zars et al., 2000) but does not cover the entire MB, leaving out α'β' and αβc (Tanaka et al., 2008). A possible way around this constrain would be to combine two lines with partial non-overlapping MB coverage in order to target all KCs. It would furthermore be interesting to determine if a specific subset of KCs or rather the whole MB is required for naive discrimination.

The encouraging results here discussed beget many follow-up studies. First of all, it is necessary to determine which KC subset is responsible for this FoxP-mediated naive phenotype. This can be probed by driving *FoxP*^{RNAi}

expression with the same lines used for the trained experiments, *NP6024-GAL4* and *NP1131-GAL4*. Targeted expression of shibire^{ts} in the mutant background in the required neurons could further allow restoring wild-type behaviour. As in the case of the trained behaviour, to confirm that it is the integration step in the lead up to a choice that is impaired, Kir2.1 will be expressed in the different subsets to decrease the neurons' excitability; this should reproduce the mutant phenotype.

Summary of future work

Many future avenues of research have been presented in this Discussion, as have the specific steps through which different hypotheses could be tested and the decision-making field advanced. In short the main follow-up strategies from this research project are:

1. Develop a high resolution behavioural assay that allows:
    a. finer behavioural characterisation of decision-making
    b. measuring neuronal activity
    c. activating and inactivating circuit components during decision-making and choice;
2. Use parallel approaches to discover genes regulated by FoxP and ultimately gene products that are important for the integration of information in the lead up to a choice;
3. Determine the role of each FoxP isoform in decision making;

4. Determine if FoxP is acting throughout development and/or in the adult;
5. Study how ubiquitous the deliberate decision making process is;
6. Study the circuit logic and computational differences between naive and trained olfactory discrimination behaviours.

Conclusions

The project depicted in this thesis initiated a systems neuroscience approach to perceptual decision-making research in *Drosophila melanogaster*, and, through the identification of molecules and neuronal components involved in decision-making processes, displays the vast potential of performing these studies in the fruit fly. Pursuing the research avenues opened up with this work will allow studying decision-making processes to a level of detail currently unattainable in vertebrates, unravelling not only the underlying biophysical processes, but also studying the whole circuitry from sensory neurons to motor output.

Bibliography

Abraham NM, Spors H, Carleton A, Margrie TW, Kuner T, Schaefer AT (2004) Maintaining accuracy at the expense of speed: stimulus similarity defines odor discrimination time in mice. Neuron 44:865–876.

Abuin L, Bargeton B, Ulbrich MH, Isacoff EY, Kellenberger S, Benton R (2011) Functional architecture of olfactory ionotropic glutamate receptors. Neuron 69:44–60.

Adams GK, Watson KK, Pearson J, Platt ML (2012) Neuroethology of decision-making. Curr Opin Neurobiol 22:982–989.

Ai M, Min S, Grosjean Y, Leblanc C, Bell R, Benton R, Suh GSB (2010) Acid sensing by the *Drosophila* olfactory system. Nature 468:691–695.

Akalal D-BG, Wilson CF, Zong L, Tanaka NK, Ito K, Davis RL (2006) Roles for *Drosophila* mushroom body neurons in olfactory learning and memory. Learn Mem 13:659–668.

Akalal D-BG, Yu D, Davis RL (2010) A late-phase, long-term memory trace forms in the γ neurons of *Drosophila* mushroom bodies after olfactory classical conditioning. J Neurosci 30:16699–16708.

Andersen RA, Cui H (2009) Intention, action planning, and decision making in parietal-frontal circuits. Neuron 63:568–583.

Asahina K, Louis M, Piccinotti S, Vosshall LB (2009) A circuit supporting concentration-invariant odor perception in *Drosophila*. J Biol 8:9.

Ashraf SI, McLoon AL, Sclarsic SM, Kunes S (2006) Synaptic protein synthesis associated with memory is regulated by the RISC pathway in *Drosophila*. Cell 124:191–205.

Aso Y, Grübel K, Busch S, Friedrich AB, Siwanowicz I, Tanimoto H (2009) The mushroom body of adult *Drosophila* characterized by GAL4 drivers. J Neurogenet 23:156–172.

Aso Y, Herb A, Ogueta M, Siwanowicz I, Templier T, Friedrich AB, Ito K, Scholz H, Tanimoto H (2012) Three dopamine pathways induce aversive odor memories with different stability. PLoS Genet 8:e1002768.

Aso Y, Siwanowicz I, Bräcker L, Ito K, Kitamoto T, Tanimoto H (2010) Specific dopaminergic neurons for the formation of labile aversive memory. Curr Biol 20:1445–1451.

Azanchi R, Kaun KR, Heberlein U (2013) Competing dopamine neurons drive oviposition choice for ethanol in *Drosophila*. Proc Natl Acad Sci U S A 110:21153–21158.

Bacon C, Rappold GA (2012) The distinct and overlapping phenotypic spectra of FOXP1 and FOXP2 in cognitive disorders. Hum Genet 131:1687–1698.

Baines R a, Uhler JP, Thompson a, Sweeney ST, Bate M (2001) Altered electrical properties in *Drosophila* neurons developing without synaptic transmission. J Neurosci 21:1523–1531.

Balling A, Technau GM, Heisenberg M (1987) Are the structural changes in adult *Drosophila* mushroom bodies memory traces? Studies on biochemical learning mutants. J Neurogenet 21:209–217.

Barrett LW, Fletcher S, Wilton SD (2012) Regulation of eukaryotic gene expression by the untranslated gene regions and other non-coding elements. Cell Mol Life Sci 69:3613–3634.

Barski A, Cuddapah S, Cui K, Roh T-Y, Schones DE, Wang Z, Wei G, Chepelev I, Zhao K (2007) High-resolution profiling of histone methylations in the human genome. Cell 129:823–837.

Bartelt R, Schaner A, Jackson L (1985) cis-vaccenyl acetate as an aggregation pheromone in *Drosophila melanogaster*. J Chem Ecol 11.

Bath DE, Stowers JR, Hörmann D, Poehlmann A, Dickson BJ, Straw AD (2014) FlyMAD: rapid thermogenetic control of neuronal activity in freely walking *Drosophila*. Nat Methods 11:756–762.

Baumgartner S, Littleton JT, Broadie K, Bhat M a, Harbecke R, Lengyel J a, Chiquet-Ehrismann R, Prokop a, Bellen HJ (1996) A *Drosophila* neurexin is required for septate junction and blood-nerve barrier formation and function. Cell 87:1059–1068.

Becher PG, Bengtsson M, Hansson BS, Witzgall P (2010) Flying the fly: long-range flight behavior of *Drosophila melanogaster* to attractive odors. J Chem Ecol 36:599–607.

Beck JM, Ma WJ, Kiani R, Hanks T, Churchland AK, Roitman J, Shadlen MN, Latham PE, Pouget A (2008) Probabilistic population codes for Bayesian decision making. Neuron 60:1142–1152.

Benton R, Sachse S, Michnick SW, Vosshall LB (2006) Atypical membrane topology and heteromeric function of *Drosophila* odorant receptors in vivo. PLoS Biol 4:e20.

Benton R, Vannice KS, Gomez-Diaz C, Vosshall LB (2009) Variant ionotropic glutamate receptors as chemosensory receptors in *Drosophila*. Cell 136:149–162.

Berger MF, Philippakis A a, Qureshi AM, He FS, Estep PW, Bulyk ML (2006) Compact, universal DNA microarrays to comprehensively determine transcription-factor binding site specificities. Nat Biotechnol 24:1429–1435.

Berry JA, Cervantes-Sandoval I, Nicholas EP, Davis RL (2012) Dopamine is required for learning and forgetting in *Drosophila*. Neuron 74:530–542.

Beshel J, Zhong Y (2013) Graded encoding of food odor value in the *Drosophila* brain. J Neurosci 33:15693–15704.

Bhandawat V, Maimon G, Dickinson MH, Wilson RI (2010) Olfactory modulation of flight in *Drosophila* is sensitive, selective and rapid. J Exp Biol 213:3625–3635.

Bhandawat V, Olsen SR, Gouwens NW, Schlief ML, Wilson RI (2007) Sensory processing in the *Drosophila* antennal lobe increases reliability and separability of ensemble odor representations. Nat Neurosci 10:1474–1482.

Billeter J-C, Atallah J, Krupp JJ, Millar JG, Levine JD (2009) Specialized cells tag sexual and species identity in *Drosophila melanogaster*. Nature 461:987–991.

Bischof J, Maeda RK, Hediger M, Karch F, Basler K (2007) An optimized transgenesis system for *Drosophila* using germ-line-specific phiC31 integrases. Proc Natl Acad Sci U S A 104:3312–3317.

Blat Y, Kleckner N (1999) Cohesins bind to preferential sites along yeast chromosome III, with differential regulation along arms versus the centric region. Cell 98:249–259.

Blum AL, Li W, Cressy M, Dubnau J (2009) Short- and long-term memory in *Drosophila* require cAMP signaling in distinct neuron types. Curr Biol 19:1341–1350.

Bogacz R, Brown E, Moehlis J, Holmes P, Cohen JD (2006) The physics of optimal decision making: a formal analysis of models of performance in two-alternative forced-choice tasks. Psychol Rev 113:700–765.

Bogacz R, Wagenmakers E-J, Forstmann BU, Nieuwenhuis S (2010) The neural basis of the speed-accuracy tradeoff. Trends Neurosci 33:10–16.

Borst A, Heisenberg M (1982) Osmotropotaxis in *Drosophila melanogaster*. J Comp Physiol 147:479–484.

Boto T, Louis T, Jindachomthong K, Jalink K, Tomchik SM (2014) Dopaminergic modulation of cAMP drives nonlinear plasticity across the *Drosophila* mushroom body lobes. Curr Biol 24:822–831.

Bowman N, Kording K, Gottfried J (2012) Temporal integration of olfactory perceptual evidence in human orbitofrontal cortex. Neuron 75:916–927.

Bräcker LB, Siju KP, Varela N, Aso Y, Zhang M, Hein I, Vasconcelos ML, Grunwald Kadow IC (2013) Essential role of the mushroom body in context-dependent CO_2 avoidance in *Drosophila*. Curr Biol 23:1228–1234.

Brand AH, Perrimon N (1993) Targeted gene expression as a means of altering cell fates and generating dominant phenotypes. Development 118:401–415.

Brembs B, Wiener J (2006) Context and occasion setting in *Drosophila* visual learning. Learn Mem 13:618–628.

Britten K, Newsome W, Shadlen M, Celebrini S, Movshon J (1996) A relationship between behavioral choice and the visual responses of neurons in macaque MT. Vis Neurosci 13:87–100.

Britten K, Shadlen M (1993) Responses of neurons in macaque MT to stochastic motion signals. Vis Neurosci 10:1157–1169.

Britten K, Shadlen M, Newsome W, Movshon J (1992) The analysis of visual motion: a comparison of neuronal and psychophysical performance. J Neurosci 12:4745–4765.

Brunton BW, Botvinick MM, Brody CD (2013) Rats and humans can optimally accumulate evidence for decision-making. Science 340:95–98.

Buchner E (1976) Elementary movement detectors in an insect visual system. Biol Cybern 24:85–101.

Budick SA, Dickinson MH (2006) Free-flight responses of *Drosophila melanogaster* to attractive odors. J Exp Biol 209:3001–3017.

Bulyk ML (2005) Discovering DNA regulatory elements with bacteria. Nat Biotechnol 23:942–944.

Burke CJ, Huetteroth W, Owald D, Perisse E, Krashes MJ, Das G, Gohl D, Silies M, Certel S, Waddell S (2012) Layered reward signalling through octopamine and dopamine in *Drosophila*. Nature 492:433–437.

Burrone J, O'Byrne M, Murthy V (2002) Multiple forms of synaptic plasticity triggered by selective suppression of activity in individual neurons. Nature 420:414–418.

Busch S, Selcho M, Ito K, Tanimoto H (2009) A map of octopaminergic neurons in the *Drosophila* brain. J Comp Neurol 513:643–667.

Busemeyer JR, Townsend JT (1993) Decision field theory: a dynamic-cognitive approach to decision making in an uncertain environment. Psychol Rev 100:432–459.

Busse L, Ayaz A, Dhruv NT, Katzner S, Saleem AB, Schölvinck ML, Zaharia AD, Carandini M (2011) The detection of visual contrast in the behaving mouse. J Neurosci 31:11351–11361.

Butcher NJ, Friedrich AB, Lu Z, Tanimoto H, Meinertzhagen IA (2012) Different classes of input and output neurons reveal new features in microglomeruli of the adult *Drosophila* mushroom body calyx. J Comp Neurol 520:2185–2201.

Carandini M, Churchland AK (2013) Probing perceptual decisions in rodents. Nat Neurosci 16:824–831.

Caron SJC, Ruta V, Abbott LF, Axel R (2013) Random convergence of olfactory inputs in the *Drosophila* mushroom body. Nature 497:113–117.

Carr CW, Moreno-De-Luca D, Parker C, Zimmerman HH, Ledbetter N, Martin CL, Dobyns WB, Abdul-Rahman OA (2010) Chiari I malformation, delayed gross motor skills, severe speech delay, and epileptiform discharges in a child with FOXP1 haploinsufficiency. Eur J Hum Genet 18:1216–1220.

Certel SJ, Leung A, Lin C-Y, Perez P, Chiang A-S, Kravitz EA (2010) Octopamine neuromodulatory effects on a social behavior decision-making network in *Drosophila* males. PLoS One 5:e13248.

Certel SJ, Savella MG, Schlegel DCF, Kravitz EA (2007) Modulation of *Drosophila* male behavioral choice. Proc Natl Acad Sci U S A 104:4706–4711.

Cervantes-Sandoval I, Davis RL (2012) Distinct traces for appetitive versus aversive olfactory memories in DPM neurons of *Drosophila*. Curr Biol 22:1247–1252.

Chiappe ME, Seelig JD, Reiser MB, Jayaraman V (2010) Walking modulates speed sensitivity in *Drosophila* motion vision. Curr Biol 20:1470–1475.

Chittka L, Dyer AG (2003) Bees trade off foraging speed for accuracy. Nature 424:388.

Chittka L, Skorupski P, Raine NE (2009) Speed-accuracy tradeoffs in animal decision making. Trends Ecol Evol 24:400–407.

Chou Y-H, Spletter ML, Yaksi E, Leong JCS, Wilson RI, Luo L (2010) Diversity and wiring variability of olfactory local interneurons in the *Drosophila* antennal lobe. Nat Neurosci 13:439–449.

Christiansen F, Zube C, Andlauer TFM, Wichmann C, Fouquet W, Owald D, Mertel S, Leiss F, Tavosanis G, Luna AJF, Fiala A, Sigrist SJ (2011) Presynapses in Kenyon cell dendrites in the mushroom body calyx of *Drosophila*. J Neurosci 31:9696–9707.

Churchland AK, Ditterich J (2012) New advances in understanding decisions among multiple alternatives. Curr Opin Neurobiol 22:920–926.

Claridge-Chang A, Roorda RD, Vrontou E, Sjulson L, Li H, Hirsh J, Miesenböck G (2009) Writing memories with light-addressable reinforcement circuitry. Cell 139:405–415.

Clyne P, Grant A, O'Connell R, Carlson JR (1997) Odorant response of individual sensilla on the antenna. Invert Neurosci 3:127–135.

Clyne PJ, Warr CG, Carlson JR (2000) Candidate taste receptors in *Drosophila*. Science (80-) 287:1830–1834.

Clyne PJ, Warr CG, Freeman MR, Lessing D, Kim J, Carlson JR (1999) A novel family of divergent seven-transmembrane proteins: candidate odorant receptors in *Drosophila*. Neuron 22:327–338.

Connolly JB, Roberts IJ, Armstrong JD, Kaiser K, Forte M, Tully T, O'Kane CJ (1996) Associative learning disrupted by impaired Gs signaling in *Drosophila* mushroom bodies. Science 274:2104–2107.

Cook RK, Christensen SJ, Deal JA, Coburn RA, Deal ME, Gresens JM, Kaufman TC, Cook KR (2012) The generation of chromosomal deletions to provide extensive coverage and subdivision of the *Drosophila melanogaster* genome. Genome Biol 13:R21.

Couto A, Alenius M, Dickson BJ (2005) Molecular, anatomical, and functional organization of the *Drosophila* olfactory system. Curr Biol 15:1535–1547.

Crittenden J, Skoulakis E, Han K-A, Kalderon D, Davis RL (1998) Tripartite mushroom body architecture revealed by antigenic markers. Learn Mem 5:38–51.

Croset V, Rytz R, Cummins SF, Budd A, Brawand D, Kaessmann H, Gibson TJ, Benton R (2010) Ancient protostome origin of chemosensory ionotropic glutamate receptors and the evolution of insect taste and olfaction. PLoS Genet 6:e1001064.

Das A, Chiang A, Davla S, Priya R, Reichert H, Vijayraghavan K, Rodrigues V (2011) Identification and analysis of a glutamatergic local interneuron lineage in the adult *Drosophila* olfactory system. Neural Syst Circuits 1:4.

Das A, Sen S, Lichtneckert R, Okada R, Ito K, Rodrigues V, Reichert H (2008) Drosophila olfactory local interneurons and projection neurons derive from a common neuroblast lineage specified by the empty spiracles gene. Neural Dev 3:33.

DasGupta S, Ferreira CH, Miesenbock G (2014) FoxP influences the speed and accuracy of a perceptual decision in *Drosophila*. Science 344:901–904.

Datta SR, Vasconcelos ML, Ruta V, Luo S, Wong A, Demir E, Flores J, Balonze K, Dickson BJ, Axel R (2008) The *Drosophila* pheromone cVA activates a sexually dimorphic neural circuit. Nature 452:473–477.

De Belle J, Heisenberg M (1994) Associative odor learning in *Drosophila* abolished by chemical ablation of mushroom bodies. Science 263:692–695.

De Bruyne M, Clyne P, Carlson J (1999) Odor coding in a model olfactory organ: the *Drosophila* maxillary palp. J Neurosci 19:4520–4532.

De Bruyne M, Foster K, Carlson JR (2001) Odor coding in the *Drosophila* antenna. Neuron 30:537–552.

Deco G, Rolls ET (2006) Decision-making and Weber's law: a neurophysiological model. Eur J Neurosci 24:901–916.

Deco G, Scarano L, Soto-Faraco S (2007) Weber's law in decision making: integrating behavioral data in humans with a neurophysiological model. J Neurosci 27:11192–11200.

Devaud JM, Acebes A, Ferrús A (2001) Odor exposure causes central adaptation and morphological changes in selected olfactory glomeruli in *Drosophila*. J Neurosci 21:6274–6282.

Dickson BJ (2008) Wired for sex: the neurobiology of *Drosophila* mating decisions. Science 322:904–909.

Dietzl G, Chen D, Schnorrer F, Su K-C, Barinova Y, Fellner M, Gasser B, Kinsey K, Oppel S, Scheiblauer S, Couto A, Marra V, Keleman K, Dickson BJ (2007) A genome-wide transgenic RNAi library for conditional gene inactivation in *Drosophila*. Nature 448:151–156.

Ditterich J, Mazurek ME, Shadlen MN (2003) Microstimulation of visual cortex affects the speed of perceptual decisions. Nat Neurosci 6:891–898.

Dobritsa AA, van der Goes van Naters W, Warr CG, Steinbrecht RA, Carlson JR (2003) Integrating the molecular and cellular basis of odor coding in the *Drosophila* antenna. Neuron 37:827–841.

Donders FC (1969) On the speed of mental processes. Acta Psychol (Amst) 30:412–431.

Dubnau J, Chiang A-S, Tully T (2003) Neural substrates of memory: from synapse to system. J Neurobiol 54:238–253.

Dubnau J, Grady L, Kitamoto T, Tully T (2001) Disruption of neurotransmission in *Drosophila* mushroom body blocks retrieval but not acquisition of memory. Nature 411:476–480.

Duistermars BJ, Chow DM, Frye MA (2009) Flies require bilateral sensory input to track odor gradients in flight. Curr Biol 19:1301–1307.

Dunipace L, Meister S, McNealy C, Amrein H (2001) Spatially restricted expression of candidate taste receptors in the *Drosophila* gustatory system. Curr Biol 11:822–835.

Dweck H, Ebrahim S, Kromann S, Bown D, Hillbur Y, Sachse S, Hansson BS, Stensmyr MC (2013) Olfactory preference for egg laying on citrus substrates in *Drosophila*. Curr Biol 23:2472–2480.

Ejima A, Smith BPC, Lucas C, van der Goes van Naters W, Miller CJ, Carlson JR, Levine JD, Griffith LC (2007) Generalization of courtship learning in *Drosophila* is mediated by cis-vaccenyl acetate. Curr Biol 17:599–605.

Elmore T, Ignell R, Carlson JR, Smith DP (2003) Targeted mutation of a *Drosophila* odor receptor defines receptor requirement in a novel class of sensillum. J Neurosci 23:9906–9912.

Enard W et al. (2009) A humanized version of Foxp2 affects cortico-basal ganglia circuits in mice. Cell 137:961–971.

Enard W (2011) FOXP2 and the role of cortico-basal ganglia circuits in speech and language evolution. Curr Opin Neurobiol 21:415–424.

Endo K, Aoki T, Yoda Y, Kimura K, Hama C (2007) Notch signal organizes the *Drosophila* olfactory circuitry by diversifying the sensory neuronal lineages. Nat Neurosci 10:153–160.

Fahrbach SE (2006) Structure of the mushroom bodies of the insect brain. Annu Rev Entomol 51:209–232.

Faisal AA, Selen LPJ, Wolpert DM (2008) Noise in the nervous system. Nat Rev Neurosci 9:292–303.

Faucher C, Forstreuter M, Hilker M, de Bruyne M (2006) Behavioral responses of *Drosophila* to biogenic levels of carbon dioxide depend on life-stage, sex and olfactory context. J Exp Biol 209:2739–2748.

Faucher CP, Hilker M, de Bruyne M (2013) Interactions of carbon dioxide and food odours in *Drosophila*: olfactory hedonics and sensory neuron properties. PLoS One 8:e56361.

Fechner G (1966) Elements of psychophysics. Holt, Rinehart and Winston.

Fişek M, Wilson RI (2014) Stereotyped connectivity and computations in higher-order olfactory neurons. Nat Neurosci 17:280–288.

Fisher SE, Scharff C (2009) FOXP2 as a molecular window into speech and language. Trends Genet 25:166–177.

Fisher SE, Vargha-Khadem F, Watkins KE, Monaco AP, Pembrey ME (1998) Localisation of a gene imlicated in a severe speech and language disorder. Nature 18:168–170.

Fishilevich E, Vosshall LB (2005) Genetic and functional subdivision of the *Drosophila* antennal lobe. Curr Biol 15:1548–1553.

Folkers E, Drain P, Quinn WG (1993) Radish, a *Drosophila* mutant deficient in consolidated memory. Proc Natl Acad Sci U S A 90:8123–8127.

French CA, Jin X, Campbell TG, Gerfen E, Groszer M, Fisher SE, Costa RM (2012) An aetiological Foxp2 mutation causes aberrant striatal activity and alters plasticity during skill learning. Mol Psychiatry 17:1077–1085.

Frye MA (2004) Motor output reflects the linear superposition of visual and olfactory inputs in *Drosophila*. J Exp Biol 207:123–131.

Frye MA, Tarsitano M, Dickinson MH (2003) Odor localization requires visual feedback during free flight in *Drosophila melanogaster*. J Exp Biol 206:843–855.

Furey TS (2012) ChIP-seq and beyond: new and improved methodologies to detect and characterize protein-DNA interactions. Nat Rev Genet 13:840–852.

Furman M, Wang X-J (2008) Similarity effect and optimal control of multiple-choice decision making. Neuron 60:1153–1168.

Gao Q, Chess A (1999) Identification of candidate *Drosophila* olfactory receptors from genomic DNA sequence. Genomics 60:31–39.

Gao Q, Yuan B, Chess A (2000) Convergent projections of *Drosophila* olfactory neurons to specific glomeruli in the antennal lobe. Nat Neurosci 3:780–785.

Gaudry Q, Hong EJ, Kain J, de Bivort BL, Wilson RI (2013) Asymmetric neurotransmitter release enables rapid odour lateralization in *Drosophila*. Nature 493:424–428.

Gaudry Q, Nagel KI, Wilson RI (2012) Smelling on the fly: sensory cues and strategies for olfactory navigation in *Drosophila*. Curr Opin Neurobiol 22:216–222.

Getahun MN, Wicher D, Hansson BS, Olsson SB (2012) Temporal response dynamics of *Drosophila* olfactory sensory neurons depends on receptor type and response polarity. Front Cell Neurosci 6:54.

Gifford AM, Cohen YE, Stocker AA (2014) Characterizing the impact of category uncertainty on human auditory categorization behavior. PLoS Comput Biol 10:e1003715.

Gold JI, Shadlen MN (2003) The influence of behavioral context on the representation of a perceptual decision in developing oculomotor commands. J Neurosci 23:632–651.

Gold JI, Shadlen MN (2007) The neural basis of decision making. Annu Rev Neurosci 30:535–574.

Gold L (1995) Oligonucleotides as research, diagnostic, and therapeutic agents. J Biol Chem 270:113581–113584.

Goldman AL, van der Goes van Naters W, Lessing D, Warr CG, Carlson JR (2005) Coexpression of two functional odor receptors in one neuron. Neuron 45:661–666.

Gomez-Marin A, Stephens GJ, Louis M (2011) Active sampling and decision making in *Drosophila* chemotaxis. Nat Commun 2:441.

Grosjean Y, Rytz R, Farine J, Abuin L (2011) An olfactory receptor for food-derived odours promotes male courtship in *Drosophila*. Nature 478:236–240.

Groszer M et al. (2008) Impaired synaptic plasticity and motor learning in mice with a point mutation implicated in human speech deficits. Curr Biol 18:354–362.

Groth A, Fish M, Nusse R, Calos M (2004) Construction of transgenic *Drosophila* by using the site-specific integrase from phage φC31. Genetics 1782:1775–1782.

Gruntman E, Turner GC (2013) Integration of the olfactory code across dendritic claws of single mushroom body neurons. Nat Neurosci 16:1821–1829.

Ha TS, Smith DP (2006) A pheromone receptor mediates 11-cis-vaccenyl acetate-induced responses in *Drosophila*. J Neurosci 26:8727–8733.

Haesler S, Rochefort C, Georgi B, Licznerski P, Osten P, Scharff C (2007) Incomplete and inaccurate vocal imitation after knockdown of FoxP2 in songbird basal ganglia nucleus Area X. PLoS Biol 5:e321.

Hallem E, Ho MG, Carlson JR (2004) The molecular basis of odor coding in the *Drosophila* antenna. Cell 117:965–979.

Hallem EA, Carlson JR (2004) The odor coding system of *Drosophila*. Trends Genet 20:453–459.

Hallem EA, Carlson JR (2006) Coding of odors by a receptor repertoire. Cell 125:143–160.

Hamdan FF, Daoud H, Rochefort D, Piton A, Gauthier J, Langlois M, Foomani G, Dobrzeniecka S, Krebs M-O, Joober R, Lafrenière RG, Lacaille J-C, Mottron L, Drapeau P, Beauchamp MH, Phillips MS, Fombonne E, Rouleau GA, Michaud JL (2010) De novo mutations in FOXP1 in cases with intellectual disability, autism, and language impairment. Am J Hum Genet 87:671–678.

Han KA, Millar NS, Grotewiel MS, Davis RL (1996) DAMB, a novel dopamine receptor expressed specifically in *Drosophila* mushroom bodies. Neuron 16:1127–1135.

Hanes DP, Schall JD (1996) Neural control of voluntary movement initiation. Science 274:427–430.

Hanks TD, Ditterich J, Shadlen MN (2006) Microstimulation of macaque area LIP affects decision-making in a motion discrimination task. Nat Neurosci 9:682–689.

Hannenhalli S, Kaestner KH (2009) The evolution of Fox genes and their role in development and disease. Nat Rev Genet 10:233–240.

Hayashi S, Ito K, Sado Y, Taniguchi M, Akimoto A, Takeuchi H, Aigaki T, Matsuzaki F, Nakagoshi H, Tanimura T, Ueda R, Uemura T, Yoshihara M, Goto S (2002) GETDB, a database compiling expression patterns and molecular locations of a collection of Gal4 enhancer traps. Genesis 34:58–61.

Heekeren HR, Marrett S, Ungerleider LG (2008) The neural systems that mediate human perceptual decision making. Nat Rev Neurosci 9:467–479.

Heimbeck G, Bugnon V, Gendre N, Keller A, Stocker RF (2001) A central neural circuit for experience-independent olfactory and courtship behavior in *Drosophila melanogaster*. Proc Natl Acad Sci U S A 98:15336–15341.

Heisenberg M (2003) Mushroom body memoir: from maps to models. Nat Rev Neurosci 4:266–275.

Heisenberg M, Borst A, Wagner S, Byers D (1985) *Drosophila* mushroom body mutants are deficient in olfactory learning. J Neurogenet 2:1–30.

Heitz RP (2014) The speed-accuracy tradeoff: history, physiology, methodology, and behavior. Front Neurosci 8:1–19.

Heitz RP, Schall JD (2012) Neural mechanisms of speed-accuracy tradeoff. Neuron 76:616–628.

Hinke W (1961) Das relative postembryonale wachstum der hirnteile von culex pipiens, drosophila melanogaster und drosophila-mutaten. Z Morph Okol Tiere 50:81–118.

Hisaoka T, Nakamura Y, Senba E, Morikawa Y (2010) The forkhead transcription factors, Foxp1 and Foxp2, identify different subpopulations of projection neurons in the mouse cerebral cortex. Neuroscience 166:551–563.

Honegger KS, Campbell RAA, Turner GC (2011) Cellular-resolution population imaging reveals robust sparse coding in the *Drosophila* mushroom body. J Neurosci 31:11772–11785.

Horn D, Kapeller J, Rivera-Brugués N (2010) Identification of FOXP1 deletions in three unrelated patients with mental retardation and significant speech and language deficits. Hum Mutat 31:1851–1860.

Hoshino M, Suzuki E, Nabeshima Y, Hama C (1996) Hikaru genki protein is secreted into synaptic clefts from an early stage of synapse formation in *Drosophila*. Development 122:589–597.

Hoskins RA et al. (2000) A BAC-based physical map of the major autosomes of *Drosophila melanogaster*. Science (80-) 287:2271–2274.

Howard RA (1966) Decision analysis: applied decision theory. Proc 4th Int Conf Oper Res:55–77.

Huang C, Zheng X, Zhao H, Li M, Wang P, Xie Z, Wang L, Zhong Y (2012) A permissive role of mushroom body α/β core neurons in long-term memory consolidation in *Drosophila*. Curr Biol 22:1981–1989.

Huang J, Zhang W, Qiao W, Hu A, Wang Z (2010) Functional connectivity and selective odor responses of excitatory local interneurons in *Drosophila* antennal lobe. Neuron 67:1021–1033.

Huang J, Zhou W, Dong W, Watson AM, Hong Y (2009) Directed, efficient, and versatile modifications of the *Drosophila* genome by genomic engineering. Proc Natl Acad Sci U S A 106:8284–8289.

Huang J, Zhou W, Watson AM, Jan Y-N, Hong Y (2008) Efficient ends-out gene targeting in *Drosophila*. Genetics 180:703–707.

Isabel G, Pascual A, Preat T (2004) Exclusive consolidated memory phases in *Drosophila*. Science 304:1024–1027.

Ito K, Awano W, Suzuki K, Hiromi Y, Yamamoto D (1997) The *Drosophila* mushroom body is a quadruple structure of clonal units each of which contains a virtually identical set of neurones and glial cells. Development 124:761–771.

Ito K, Suzuki K, Estes P (1998) The organization of extrinsic neurons and their implications in the functional roles of the mushroom bodies in *Drosophila melanogaster* Meigen. Learn Mem 5:52–77.

Itskov PM, Ribeiro C (2013) The dilemmas of the gourmet fly: the molecular and neuronal mechanisms of feeding and nutrient decision making in *Drosophila*. Front Neurosci 7:12.

Jefferis G, Marin E, Stocker R, Luo L (2001) Target neuron prespecification in the olfactory map of *Drosophila*. Nature 414:204–208.

Jefferis GSXE, Potter CJ, Chan AM, Marin EC, Rohlfing T, Maurer CR, Luo L (2007) Comprehensive maps of *Drosophila* higher olfactory centers: spatially segregated fruit and pheromone representation. Cell 128:1187–1203.

Jefferis GSXE, Vyas RM, Berdnik D, Ramaekers A, Stocker RF, Tanaka NK, Ito K, Luo L (2004) Developmental origin of wiring specificity in the olfactory system of *Drosophila*. Development 131:117–130.

Johard H, Enell L (2008) Intrinsic neurons of *Drosophila* mushroom bodies express short neuropeptide F: relations to extrinsic neurons expressing different neurotransmitters. J Comp Neurol 1496:1479–1496.

Johnson DS, Mortazavi A, Myers RM, Wold B (2007) Genome-wide mapping of in vivo protein-DNA interactions. Science 316:1497–1502.

Joiner WJ, Crocker A, White BH, Sehgal A (2006) Sleep in *Drosophila* is regulated by adult mushroom bodies. Nature 441:757–760.

Jones W, Cayirlioglu P, Kadow I, Vosshall L (2006) Two chemosensory receptors together mediate carbon dioxide detection in *Drosophila*. Nature 445:86–90.

Kazama H, Wilson RI (2008) Homeostatic matching and nonlinear amplification at identified central synapses. Neuron 58:401–413.

Kazama H, Wilson RI (2009) Origins of correlated activity in an olfactory circuit. Nat Neurosci 12:1136–1144.

Keene AC, Krashes MJ, Leung B, Bernard JA, Waddell S (2006) *Drosophila* dorsal paired medial neurons provide a general mechanism for memory consolidation. Curr Biol 16:1524–1530.

Keene AC, Stratmann M, Keller A, Perrat PN, Vosshall LB, Waddell S (2004) Diverse odor-conditioned memories require uniquely timed dorsal paired medial neuron output. Neuron 44:521–533.

Keene AC, Waddell S (2007) *Drosophila* olfactory memory: single genes to complex neural circuits. Nat Rev Neurosci 8:341–354.

Keleman K, Krüttner S, Alenius M, Dickson BJ (2007) Function of the *Drosophila* CPEB protein Orb2 in long-term courtship memory. Nat Neurosci 10:1587–1593.

Keleman K, Vrontou E, Krüttner S, Yu JY, Kurtovic-Kozaric A, Dickson BJ (2012) Dopamine neurons modulate pheromone responses in *Drosophila* courtship learning. Nature 489:145–149.

Keller A, Vosshall LB (2007) Influence of odorant receptor repertoire on odor perception in humans and fruit flies. Proc Natl Acad Sci U S A 104:5614–5619.

Kim AJ, Lazar AA, Slutskiy YB (2011) System identification of *Drosophila* olfactory sensory neurons. J Comput Neurosci 30:143–161.

Kim Y-C, Lee H-G, Han K-A (2007) D1 dopamine receptor dDA1 is required in the mushroom body neurons for aversive and appetitive learning in *Drosophila*. J Neurosci 27:7640–7647.

Kim Y-C, Lee H-G, Seong C-S, Han K-A (2003) Expression of a D1 dopamine receptor dDA1/DmDOP1 in the central nervous system of *Drosophila melanogaster*. Gene Expr Patterns 3:237–245.

Kitamoto T (2001) Conditional modification of behavior in *Drosophila* by targeted expression of a temperature-sensitive shibire allele in defined neurons. J Neurobiol 47:81–92.

Knaden M, Strutz A, Ahsan J, Sachse S, Hansson B (2012) Spatial representation of odorant valence in an insect brain. Cell Rep 1:392–399.

Knapek S, Kahsai L, Winther AME, Tanimoto H, Nässel DR (2013) Short neuropeptide F acts as a functional neuromodulator for olfactory memory in Kenyon cells of *Drosophila* mushroom bodies. J Neurosci 33:5340–5345.

Kohl J, Ostrovsky A, Frechter S, Jefferis G (2013) A bidirectional circuit switch reroutes pheromone signals in male and female brains. Cell 155:1610–1623.

Konopka G, Bomar JM, Winden K, Coppola G, Jonsson ZO, Gao F, Peng S, Preuss TM, Wohlschlegel JA, Geschwind DH (2009) Human-specific transcriptional regulation of CNS development genes by FOXP2. Nature 462:213–217.

Konopka G, Friedrich T, Davis-Turak J, Winden K, Oldham MC, Gao F, Chen L, Wang G-Z, Luo R, Preuss TM, Geschwind DH (2012) Human-specific transcriptional networks in the brain. Neuron 75:601–617.

Konstantoulas CJ, Parmar M, Li M (2010) FoxP1 promotes midbrain identity in embryonic stem cell-derived dopamine neurons by regulating Pitx3. J Neurochem 113:836–847.

Kosaka T, Ikeda K (1983) Possible temperature-dependent blockage of synaptic vesicle recycling induced by a single gene mutation in *Drosophila*. J Neurobiol 14:207–225.

Koulakov AA, Raghavachari S, Kepecs A, Lisman JE (2002) Model for a robust neural integrator. Nat Neurosci 5:775–782.

Krashes MJ, DasGupta S, Vreede A, White B, Armstrong JD, Waddell S (2009) A neural circuit mechanism integrating motivational state with memory expression in *Drosophila*. Cell 139:416–427.

Krashes MJ, Keene AC, Leung B, Armstrong JD, Waddell S (2007) Sequential use of mushroom body neuron subsets during *Drosophila* odor memory processing. Neuron 53:103–115.

Krashes MJ, Waddell S (2008) Rapid consolidation to a radish and protein synthesis-dependent long-term memory after single-session appetitive olfactory conditioning in *Drosophila*. J Neurosci 28:3103–3113.

Kreher SA, Mathew D, Kim J, Carlson JR (2008) Translation of sensory input into behavioral output via an olfactory system. Neuron 59:110–124.

Kulahci IG, Dornhaus A, Papaj DR (2008) Multimodal signals enhance decision making in foraging bumble-bees. Proc Biol Sci 275:797–802.

Kurtovic A, Widmer A, Dickson BJ (2007) A single class of olfactory neurons mediates behavioural responses to a *Drosophila* sex pheromone. Nature 446:542–546.

Kwon JY, Dahanukar A, Weiss LA, Carlson JR (2007) The molecular basis of CO2 reception in *Drosophila*. Proc Natl Acad Sci U S A 104:3574–3578.

LaBerge D (1962) A recruitment theory of simple behaviour. Psychometrika 27:375–396.

Lai CSL, Fisher SE, Hurst JA, Vargha-khadem F, Monaco AP (2001) A forkhead-domain gene is mutated in a severe speech and language disorder. Nature 413:519–523.

Lai S-L, Awasaki T, Ito K, Lee T (2008) Clonal analysis of *Drosophila* antennal lobe neurons: diverse neuronal architectures in the lateral neuroblast lineage. Development 135:2883–2893.

Laissue PP, Reiter C, Hiesinger PR, Halter S, Fischbach KF, Stocker RF (1999) Three-dimensional reconstruction of the antennal lobe in *Drosophila melanogaster*. J Comp Neurol 405:543–552.

Laming DRJ (1968) Information theory of choice-reaction times. Oxford: Academic Press.

Larsson MC, Domingos AI, Jones WD, Chiappe ME, Amrein H, Vosshall LB (2004) Or83b encodes a broadly expressed odorant receptor essential for *Drosophila* olfaction. Neuron 43:703–714.

Lawton KJ, Wassmer TL, Deitcher DL (2014) Conserved role of *Drosophila melanogaster* FoxP in motor coordination and courtship song. Behav Brain Res 268:213–221.

Le Fevre AK, Taylor S, Malek NH, Horn D, Carr CW, Abdul-Rahman OA, O'Donnell S, Burgess T, Shaw M, Gecz J, Bain N, Fagan K, Hunter MF (2013) FOXP1 mutations cause intellectual disability and a recognizable phenotype. Am J Med Genet A 161A:3166–3175.

Lee D, Seo H, Jung MW (2012) Neural basis of reinforcement learning and decision making. Annu Rev Neurosci 35:287–308.

Lee P, Lin H, Chang Y (2011) Serotonin–mushroom body circuit modulating the formation of anesthesia-resistant memory in *Drosophila*. Proc Natl Acad Sci U S A 108:13794–13799.

Lee T, Lee A, Luo L (1999) Development of the *Drosophila* mushroom bodies: sequential generation of three distinct types of neurons from a neuroblast. Development 126:4065–4076.

Lei Z, Chen K, Li H, Liu H, Guo A (2013) The GABA system regulates the sparse coding of odors in the mushroom bodies of *Drosophila*. Biochem Biophys Res Commun 436:35–40.

Leiss F, Groh C, Butcher NJ, Meinertzhagen IA, Tavosanis G (2009) Synaptic organization in the adult *Drosophila* mushroom body calyx. J Comp Neurol 517:808–824.

Lenhard B, Sandelin A, Carninci P (2012) Metazoan promoters: emerging characteristics and insights into transcriptional regulation. Nat Rev Genet 13:233–245.

Levin LR, Han P-L, Hwang PM, Feinstein PG, Davis RL, Reed RR (1992) The *Drosophila* learning and memory gene rutabaga encodes a adenylyl cyclase. Cell 68:479–489.

Levine M, Tjian R (2003) Transcription regulation and animal diversity. Nature 424:147–151.

Li S, Weidenfeld J, Morrisey EE (2004) Transcriptional and DNA binding activity of the Foxp1/2/4 family is modulated by heterotypic and homotypic protein interactions. 24:809–822.

Liang L, Li Y, Potter CJ, Yizhar O, Deisseroth K, Tsien RW, Luo L (2013) GABAergic projection neurons route selective olfactory inputs to specific higher-order neurons. Neuron 79:917–931.

Lin AC, Bygrave AM, de Calignon A, Lee T, Miesenböck G (2014) Sparse, decorrelated odor coding in the mushroom body enhances learned odor discrimination. Nat Neurosci 17:559–568.

Lin H, Lai J, Chin A, Chen Y, Chiang A-S (2007) A Map of Olfactory Representation in the *Drosophila* Mushroom Body. Cell 128:1205–1217.

Lin H-H, Chu L-A, Fu T-F, Dickson BJ, Chiang A-S (2013) Parallel neural pathways mediate CO2 avoidance responses in *Drosophila*. Science 340:1338–1341.

Link S (1975) The relative judgment theory of two choice response time. J Math Psychol 12:114–135.

Link S, Heath R (1975) A sequential theory of psychological discrimination. Psychometrika 40:77–105.

Liu C, Plaçais P-Y, Yamagata N, Pfeiffer BD, Aso Y, Friedrich AB, Siwanowicz I, Rubin GM, Preat T, Tanimoto H (2012) A subset of dopamine neurons signals reward for odour memory in *Drosophila*. Nature 488:512–516.

Liu F, Wang X-J (2008) A common cortical circuit mechanism for perceptual categorical discrimination and veridical judgment. PLoS Comput Biol 4:e1000253.

Liu L, Wolf R, Ernst R, Heisenberg M (1999) Context generalization in *Drosophila* visual learning requires the mushroom bodies. Nature 400:753–756.

Liu W, Wilson R (2013) Glutamate is an inhibitory neurotransmitter in the *Drosophila* olfactory system. Proc Natl Acad Sci U S A 110:10294–10299.

Liu X, Davis RL (2009) The GABAergic anterior paired lateral neuron suppresses and is suppressed by olfactory learning. Nat Neurosci 12:53–59.

Livingstone MS, Sziber PP, Quinn WG (1984) Loss of calcium/calmodulin responsiveness in adenylate cyclase of rutabaga, a *Drosophila* learning mutant. Cell 37:205–215.

Lo C-C, Wang X-J (2006) Cortico-basal ganglia circuit mechanism for a decision threshold in reaction time tasks. Nat Neurosci 9:956–963.

Luce RD (1986) Response times: Their role in inferring elementary mental organization. Oxford: Oxford University Press.

Lundin C, Käll L, Kreher SA, Kapp K, Sonnhammer EL, Carlson JR, Heijne G Von, Nilsson I (2007) Membrane topology of the *Drosophila* OR83b odorant receptor. FEBS Lett 581:5601–5604.

Luo SX, Axel R, Abbott LF (2010) Generating sparse and selective third-order responses in the olfactory system of the fly. Proc Natl Acad Sci U S A 107:10713–10718.

Machens CK, Romo R, Brody CD (2005) Flexible control of mutual inhibition: a neural model of two-interval discrimination. Science 307:1121–1124.

Maeda RK, Karch F (2011) Gene expression in time and space: additive vs hierarchical organization of cis-regulatory regions. Curr Opin Genet Dev 21:187–193.

Maerkl SJ, Quake SR (2007) A systems approach to measuring the binding energy landscapes of transcription factors. Science 315:233–237.

Maggert KA, Gong WJ, Golic KG (2008) Methods for homologous recombination in *Drosophila*. Methods Mol Biol 420:155–174.

Maimon G, Straw AD, Dickinson MH (2008) A simple vision-based algorithm for decision making in flying *Drosophila*. Curr Biol 18:464–470.

Maimon G, Straw AD, Dickinson MH (2010) Active flight increases the gain of visual motion processing in *Drosophila*. Nat Neurosci 13:393–399.

Mao Z, Davis RL (2009) Eight different types of dopaminergic neurons innervate the *Drosophila* mushroom body neuropil: anatomical and physiological heterogeneity. Front Neural Circuits 3:5.

Mao Z, Roman G, Zong L, Davis RL (2004) Pharmacogenetic rescue in time and space of the rutabaga memory impairment by using Gene-Switch. Proc Natl Acad Sci U S A 101:198–203.

Marin EC, Jefferis GSXE, Komiyama T, Zhu H, Luo L (2002) Representation of the glomerular olfactory map in the *Drosophila* brain. Cell 109:243–255.

Markstein M, Pitsouli C, Villalta C, Celniker SE, Perrimon N (2008) Exploiting position effects and the gypsy retrovirus insulator to engineer precisely expressed transgenes. Nat Genet 40:476–483.

Matoulkova E, Michalova E, Vojtesek B, Hrstka R (2012) The role of the 3′ untranslated region in post-transcriptional regulation of protein expression in mammalian cells. RNA Biol 9:563–576.

Mauk MD, Buonomano D V (2004) The neural basis of temporal processing. Annu Rev Neurosci 27:307–340.

Mazurek ME, Roitman JD, Ditterich J, Shadlen MN (2003) A role for neural integrators in perceptual decision making. Cereb Cortex 13:1257–1269.

McBride SM, Giuliani G, Choi C, Krause P, Correale D, Watson K, Baker G, Siwicki KK (1999) Mushroom body ablation impairs short-term memory and long-term memory of courtship conditioning in *Drosophila melanogaster*. Neuron 24:967–977.

McGuire SE, Le PT, Davis RL (2001) The role of *Drosophila* mushroom body signaling in olfactory memory. Science 293:1330–1333.

McGuire SE, Le PT, Davis RL, Osborn AJ, Matsumoto K (2003) Spatiotemporal rescue of memory dysfunction in *Drosophila*. Science 302:1765–1768.

McPeek RM, Keller EL (2004) Deficits in saccade target selection after inactivation of superior colliculus. Nat Neurosci 7:757–763.

Mendoza E, Colomb J, Rybak J, Pflüger H-J, Zars T, Scharff C, Brembs B (2014) *Drosophila* FoxP mutants are deficient in operant self-learning. PLoS One 9:e100648.

Meng X, Brodsky MH, Wolfe S a (2005) A bacterial one-hybrid system for determining the DNA-binding specificity of transcription factors. Nat Biotechnol 23:988–994.

Min S, Ai M, Shin SA, Suh GSB (2013) Dedicated olfactory neurons mediating attraction behavior to ammonia and amines in *Drosophila*. Proc Natl Acad Sci U S A 110:E1321–E1329.

Mohr SE (2014) RNAi screening in *Drosophila* cells and *in vivo*. Methods 68:82–88.

Morgan M, Ward R (1980) Conditions for motion flow in dynamic visual noise. Vision Res 20:431–435.

Mountcastle V, Steinmetz M, Romo R (1990) Frequency discrimination in the sense of flutter: psychophysical measurements correlated with postcentral events in behaving monkeys. J Neurosci 10:3032–3044.

Mountcastle VB, Talbot WH, Darian-Smith I, Kornhuber HH (1967) Neural basis of the sense of flutter-vibration. Science 155:597–600.

Mukherjee S, Berger MF, Jona G, Wang XS, Muzzey D, Snyder M, Young R a, Bulyk ML (2004) Rapid analysis of the DNA-binding specificities of transcription factors with DNA microarrays. Nat Genet 36:1331–1339.

Murthy M, Fiete I, Laurent G (2008) Testing odor response stereotypy in the *Drosophila* mushroom body. Neuron 59:1009–1023.

Nagel KI, Wilson RI (2011) Biophysical mechanisms underlying olfactory receptor neuron dynamics. Nat Neurosci 14:208–216.

Neuhaus EM, Gisselmann G, Zhang W, Dooley R, Störtkuhl K, Hatt H (2005) Odorant receptor heterodimerization in the olfactory system of *Drosophila melanogaster*. Nat Neurosci 8:15–17.

Newsome W, Paré E (1988) A selective impairment of motion perception following lesions of the middle temporal visual area (MT). J Neurosci 8:2201–2211.

Ng M, Roorda RD, Lima SQ, Zemelman B V, Morcillo P, Miesenböck G (2002) Transmission of olfactory information between three populations of neurons in the antennal lobe of the fly. Neuron 36:463–474.

Noveen A, Daniel A, Hartenstein V (2000) Early development of the *Drosophila* mushroom body: the roles of eyeless and dachshund. Development 3488:3475–3488.

Noyes MB (2012) Analysis of specific protein–DNA interactions by bacterial one-hybrid assay. In: Gene regulatory networks: Methods and Protocols, Methods in Molecular Biology (Deplancke B, Gheldof N, eds), pp 79–95 Methods in Molecular Biology. Totowa, NJ: Humana Press.

Noyes MB, Meng X, Wakabayashi A, Sinha S, Brodsky MH, Wolfe S (2008) A systematic characterization of factors that regulate *Drosophila* segmentation via a bacterial one-hybrid system. Nucleic Acids Res 36:2547–2560.

Nudel R, Newbury DF (2013) FOXP2. Wiley Interdiscip Rev Cogn Sci 4:547–560.

O'Roak BJ, Deriziotis P, Lee C, Vives L, Schwartz JJ, Girirajan S, Karakoc E, Mackenzie AP, Ng SB, Baker C, Rieder MJ, Nickerson DA, Bernier R, Fisher SE, Shendure J, Eichler EE (2011) Exome sequencing in sporadic

autism spectrum disorders identifies severe de novo mutations. Nat Genet 43:585–589.

Ogawa N, Biggin MD (2012) High-throughput SELEX determination of DNA sequences bound by transcription factors *in vitro*. In: Gene Regulatory Networks: Methods and Protocols, Methods in Molecular Biology (Deplancke B, Gheldof N, eds), pp 51–63 Methods in Molecular Biology. Totowa, NJ: Humana Press.

Okada R, Awasaki T, Ito K (2009) Gamma-aminobutyric acid (GABA)-mediated neural connections in the *Drosophila* antennal lobe. J Comp Neurol 514:74–91.

Olsen SR, Bhandawat V, Wilson RI (2007) Excitatory interactions between olfactory processing channels in the *Drosophila* antennal lobe. Neuron 54:89–103.

Olsen SR, Bhandawat V, Wilson RI (2010) Divisive normalization in olfactory population codes. Neuron 66:287–299.

Olsen SR, Wilson RI (2008) Lateral presynaptic inhibition mediates gain control in an olfactory circuit. Nature 452:956–960.

Pai T, Chen C, Lin H (2013) *Drosophila* ORB protein in two mushroom body output neurons is necessary for long-term memory formation. Proc Natl Acad Sci U S A 110:7898–7903.

Palmer J, Huk AC, Shadlen MN (2005) The effect of stimulus strength on the speed and accuracy of a perceptual decision. J Vis 5:376–404.

Pariani MJ, Spencer A, Graham JM, Rimoin DL (2009) A 785kb deletion of 3p14.1p13, including the FOXP1 gene, associated with speech delay, contractures, hypertonia and blepharophimosis. Eur J Med Genet 52:123–127.

Park PJ (2009) ChIP-seq: advantages and challenges of a maturing technology. Nat Rev Genet 10:669–680.

Park S-K, Shanbhag SR, Dubin AE, de Bruyne M, Wang Q, Yu P, Shimoni N, D'Mello S, Carlson JR, Harris GL, Steinbrecht RA, Pikielny CW (2002) Inactivation of olfactory sensilla of a single morphological type differentially affects the response of *Drosophila* to odors. J Neurobiol 51:248–260.

Parks AL et al. (2004) Systematic generation of high-resolution deletion coverage of the *Drosophila melanogaster* genome. Nat Genet 36:288–292.

Parnas M, Lin AC, Huetteroth W, Miesenböck G (2013) Odor discrimination in *Drosophila*: from neural population codes to behavior. Neuron 79:932–944.

Pascual A, Préat T (2001) Localization of long-term memory within the *Drosophila* mushroom body. Science 294:1115–1117.

Pasternak T, Merigan WH (1994) Motion perception following lesions of the superior temporal sulcus in the monkey. Cereb Cortex 4:247–259.

Peles E, Joho K, Plowman GD, Schlessinger J (1997) Close similarity between *Drosophila* neurexin IV and mammalian Caspr protein suggests a conserved mechanism. Cell 88:745–746.

Perazzona B, Isabel G, Preat T, Davis RL (2004) The role of cAMP response element-binding protein in *Drosophila* long-term memory. J Neurosci 24:8823–8828.

Perisse E, Burke C, Huetteroth W, Waddell S (2013a) Shocking revelations and saccharin sweetness in the study of *Drosophila* olfactory memory. Curr Biol 23:R752–R763.

Perisse E, Yin Y, Lin AC, Lin S, Huetteroth W, Waddell S (2013b) Different Kenyon cell populations drive learned approach and avoidance in *Drosophila*. Neuron 79:945–956.

Pfeiffer BD, Jenett A, Hammonds AS, Ngo T-TB, Misra S, Murphy C, Scully A, Carlson JW, Wan KH, Laverty TR, Mungall C, Svirskas R, Kadonaga JT, Doe CQ, Eisen MB, Celniker SE, Rubin GM (2008) Tools for neuroanatomy and neurogenetics in *Drosophila*. Proc Natl Acad Sci U S A 105:9715–9720.

Pfeiffer BD, Ngo T-TB, Hibbard KL, Murphy C, Jenett A, Truman JW, Rubin GM (2010) Refinement of tools for targeted gene expression in *Drosophila*. Genetics 186:735–755.

Pfeiffer BD, Truman JW, Rubin GM (2012) Using translational enhancers to increase transgene expression in *Drosophila*. Proc Natl Acad Sci U S A 109:6626–6631.

Pike AR (1966) Stochastic models of choice behaviour: response probabilities and latencies of finite markov chain systems. Br J Math Stat Psychol 19:15–32.

Pitman JL, Huetteroth W, Burke CJ, Krashes MJ, Lai S-L, Lee T, Waddell S (2011) A pair of inhibitory neurons are required to sustain labile memory in the *Drosophila* mushroom body. Curr Biol 21:855–861.

Pitman JL, McGill JJ, Keegan KP, Allada R (2006) A dynamic role for the mushroom bodies in promoting sleep in *Drosophila*. Nature 441:753–756.

Plaçais P-Y, Preat T (2013) To favor survival under food shortage, the brain disables costly memory. Science 339:440–442.

Plaçais P-Y, Trannoy S, Friedrich AB, Tanimoto H, Preat T (2013) Two pairs of mushroom body efferent neurons are required for appetitive long-term memory retrieval in *Drosophila*. Cell Rep 5:769–780.

Plaçais P-Y, Trannoy S, Isabel G, Aso Y, Siwanowicz I, Belliart-Guérin G, Vernier P, Birman S, Tanimoto H, Preat T (2012) Slow oscillations in two pairs of dopaminergic neurons gate long-term memory formation in *Drosophila*. Nat Neurosci 15:592–599.

Popovici C, Leveugle M, Birnbaum D, Coulier F (2001) Homeobox gene clusters and the human paralogy map. FEBS Lett 491:237–242.

Qin H, Cressy M, Li W, Coravos JS, Izzi SA, Dubnau J (2012) Gamma neurons mediate dopaminergic input druing aversive olfactory memory formation. Curr Biol 22:608–614.

Quinn W, Dudai Y (1976) Memory phases in *Drosophila* a. Nature 262:576–577.

Quinn W, Harris W, Benzer S (1974) Conditioned behaviour in *Drosophila melanogaster*. Proc Natl Acad Sci U S A 71:708–712.

Ratcliff R (1978) A theory of memory retrieval. Psychol Rev 85:59–108.

Ratcliff R, Cherian A, Segraves M (2003) A comparison of macaque behavior and superior colliculus neuronal activity to predictions from models of two-choice decisions. J Neurophysiol 90:1392–1407.

Ratcliff R, Smith PL (2004) A comparison of sequential sampling models for two-choice reaction time. Psychol Rev 111:333–367.

Ren B, Robert F, Wyrick JJ, Aparicio O, Jennings EG, Simon I, Zeitlinger J, Schreiber J, Hannett N, Kanin E, Volkert TL, Wilson CJ, Bell SP, Young R a (2000) Genome-wide location and function of DNA binding proteins. Science 290:2306–2309.

Rinberg D, Koulakov A, Gelperin A (2006) Speed-accuracy tradeoff in olfaction. Neuron 51:351–358.

Robertson G, Hirst M, Bainbridge M, Bilenky M, Zhao Y, Zeng T, Euskirchen G, Bernier B, Varhol R, Delaney A, Thiessen N, Griffith OL, He A, Marra M, Snyder M, Jones S (2007) Genome-wide profiles of STAT1 DNA association using chromatin immunoprecipitation and massively parallel sequencing. Nature 4:651–657.

Robertson HM, Warr CG, Carlson JR (2003) Molecular evolution of the insect chemoreceptor gene superfamily in *Drosophila melanogaster*. Proc Natl Acad Sci U S A 100:14537–14542.

Robinson DA (1989) Integrating with neurons. Annu Rev Neurosci 12:33–45.

Rockel S, Geertz M, Maerkl SJ (2012) MITOMI: A Microfluidic Platform for In Vitro Characterization of Transcription Factor–DNA Interaction. In: Gene Regulatory Networks: Methods and Protocols, Methods in Molecular Biology (Deplancke B, Gheldof N, eds), pp 97–114 Methods in Molecular Biology. Totowa, NJ: Humana Press.

Roitman JD, Shadlen MN (2002) Response of neurons in the lateral intraparietal area during a combined visual discrimination reaction time task. J Neurosci 22:9475–9489.

Roll P et al. (2006) SRPX2 mutations in disorders of language cortex and cognition. Hum Mol Genet 15:1195–1207.

Roll P, Vernes S, Bruneau N (2010) Molecular networks implicated in speech-related disorders: FOXP2 regulates the SRPX2/uPAR complex. Hum Mol … 19:4848–4860.

Root CM, Masuyama K, Green DS, Enell LE, Nässel DR, Lee C-H, Wang JW (2008) A presynaptic gain control mechanism fine-tunes olfactory behavior. Neuron 59:311–321.

Root CM, Semmelhack JL, Wong AM, Flores J, Wang JW (2007) Propagation of olfactory information in *Drosophila*. Proc Natl Acad Sci U S A 104:11826–11831.

Roy B, Singh AP, Shetty C, Chaudhary V, North A, Landgraf M, Vijayraghavan K, Rodrigues V (2007) Metamorphosis of an identified serotonergic neuron in the *Drosophila* olfactory system. Neural Dev 2:20.

Ruebenbauer A, Schlyter F, Hansson BS, Löfstedt C, Larsson MC (2008) Genetic variability and robustness of host odor preference in *Drosophila melanogaster*. Curr Biol 18:1438–1443.

Ruta V, Datta SR, Vasconcelos ML, Freeland J, Looger LL, Axel R (2010) A dimorphic pheromone circuit in *Drosophila* from sensory input to descending output. Nature 468:686–690.

Ryder E et al. (2004) The DrosDel collection: a set of P-element insertions for generating custom chromosomal aberrations in *Drosophila melanogaster*. Genetics 167:797–813.

Rytz R, Croset V, Benton R (2013) Ionotropic receptors (IRs): chemosensory ionotropic glutamate receptors in *Drosophila* and beyond. Insect Biochem Mol Biol 43:888–897.

Sachse S, Rueckert E, Keller A, Okada R, Tanaka NK, Ito K, Vosshall LB (2007) Activity-dependent plasticity in an olfactory circuit. Neuron 56:838–850.

Salzman C, Murasugi C, Britten K, Newsome W (1992) Microstimulation in visual area MT: effects on direction discrimination performance. J Neurosci 12:2331–2355.

Sanders JI, Kepecs A (2012) Choice ball: a response interface for two-choice psychometric discrimination in head-fixed mice. J Neurophysiol 108:3416–3423.

Santos ME, Athanasiadis A, Leitão AB, DuPasquier L, Sucena E (2011) Alternative splicing and gene duplication in the evolution of the FoxP gene subfamily. Mol Biol Evol 28:237–247.

Sato K, Pellegrino M, Nakagawa T, Nakagawa T, Vosshall LB, Touhara K (2008) Insect olfactory receptors are heteromeric ligand-gated ion channels. Nature 452:1002–1006.

Savage L (1954) The foundations of statistics. John Wiley & Sons, Inc.

Schlief ML, Wilson RI (2007) Olfactory processing and behavior downstream from highly selective receptor neurons. Nat Neurosci 10:623–630.

Schuckel J, Meisner S, Torkkeli PH, French AS (2008) Dynamic properties of *Drosophila* olfactory electroantennograms. J Comp Physiol A Neuroethol Sens Neural Behav Physiol 194:483–489.

Schuckel J, Torkkeli P, French AS (2009) Two interacting olfactory transduction mechanisms have linked polarities and dynamics in *Drosophila melanogaster* antennal basiconic sensilla neurons. J Neurophysiol 102:214–223.

Schwaerzel M, Heisenberg M, Zars T (2002) Extinction antagonizes olfactory memory at the subcellular level. Neuron 35:951–960.

Schwaerzel M, Monastirioti M, Scholz H, Friggi-Grelin F, Birman S, Heisenberg M (2003) Dopamine and octopamine differentiate between aversive and appetitive olfactory memories in *Drosophila*. J Neurosci 23:10495–10502.

Scott K, Brady R, Cravchik a, Morozov P, Rzhetsky a, Zuker C, Axel R (2001) A chemosensory gene family encoding candidate gustatory and olfactory receptors in *Drosophila*. Cell 104:661–673.

Seelig JD, Jayaraman V (2013) Feature detection and orientation tuning in the *Drosophila* central complex. Nature 503:262–266.

Séjourné J, Plaçais P-Y, Aso Y, Siwanowicz I, Trannoy S, Thoma V, Tedjakumala SR, Rubin GM, Tchénio P, Ito K, Isabel G, Tanimoto H, Preat T (2011) Mushroom body efferent neurons responsible for aversive olfactory memory retrieval in *Drosophila*. Nat Neurosci 14:903–910.

Seki Y, Rybak J, Wicher D (2010) Physiological and morphological characterization of local interneurons in the *Drosophila* antennal lobe. J Neurophysiol 104:1007–1019.

Semmelhack JL, Wang JW (2009) Select *Drosophila* glomeruli mediate innate olfactory attraction and aversion. Nature 459:218–223.

Serway CN, Kaufman RR, Strauss R, de Belle JS (2009) Mushroom bodies enhance initial motor activity in *Drosophila*. J Neurogenet 23:173–184.

Shadlen MN, Newsome WT (1996) Motion perception: seeing and deciding. Proc Natl Acad Sci U S A 93:628–633.

Shadlen MN, Newsome WT (2001) Neural basis of a perceptual decision in the parietal cortex (area LIP) of the rhesus monkey. J Neurophysiol 86:1916–1936.

Shanbhag S, Müller B, Steinbrecht R (1999) Atlas of olfactory organs of *Drosophila melanogaster*: 1. Types, external organization, innervation and distribution of olfactory sensilla. Int J Insect Morphol Embryol 28:377–397.

Shanbhag SR, Müller B, Steinbrecht RA (2000) Atlas of olfactory organs of *Drosophila melanogaster* 2. Internal organization and cellular architecture of olfactory sensilla. Arthropod Struct Dev 29:211–229.

Shang Y, Claridge-Chang A, Sjulson L, Pypaert M, Miesenböck G (2007) Excitatory local circuits and their implications for olfactory processing in the fly antennal lobe. Cell 128:601–612.

Shazman S, Lee H, Socol Y, Mann RS, Honig B (2014) OnTheFly: a database of *Drosophila melanogaster* transcription factors and their binding sites. Nucleic Acids Res 42:D167–71.

Shinomiya K, Matsuda K, Oishi T, Otsuna H, Ito K (2011) Flybrain neuron database: a comprehensive database system of the *Drosophila* brain neurons. J Comp Neurol 519:807–833.

Shu W, Cho JY, Jiang Y, Zhang M, Weisz D, Elder GA, Schmeidler J, De Gasperi R, Sosa MAG, Rabidou D, Santucci A, Perl D, Morrisey E, Buxbaum JD (2005) Altered ultrasonic vocalization in mice with a disruption in the Foxp2 gene. Proc Natl Acad Sci U S A 102:9643–9648.

Sia GM, Clem RL, Huganir RL (2013) The human language-associated gene SRPX2 regulates synapse formation and vocalization in mice. Science 342:987–991.

Silbering A, Okada R, Ito K, Galizia CG (2008) Olfactory information processing in the *Drosophila* antennal lobe: anything goes? J Neurosci 28:13075–13087.

Silbering AF, Galizia CG (2007) Processing of odor mixtures in the *Drosophila* antennal lobe reveals both global inhibition and glomerulus-specific interactions. J Neurosci 27:11966–11977.

Silbering AF, Rytz R, Grosjean Y, Abuin L, Ramdya P, Jefferis GSXE, Benton R (2011) Complementary function and integrated wiring of the evolutionarily distinct *Drosophila* olfactory subsystems. J Neurosci 31:13357–13375.

Sinakevitch I, Strausfeld NJ (2006) Comparison of octopamine-like immunoreactivity in the brains of the fruit fly and blow fly. J Comp Neurol 494:460–475.

Singh R, Nayak S (1985) Fine structure and primary sensory projections of sensilla on the maxillary palp of *Drosophila melanogaster* Meigen (Diptera: Drosophilidae). Int J insect Morphol Embryol 14:291–306.

Smith PL, Ratcliff R (2004) Psychology and neurobiology of simple decisions. Trends Neurosci 27:161–168.

Solomon MJ, Larsen PL, Varshavsky a (1988) Mapping protein-DNA interactions *in vivo* with formaldehyde: evidence that histone H4 is retained on a highly transcribed gene. Cell 53:937–947.

Spiteri E, Konopka G, Coppola G, Bomar J, Oldham M, Ou J, Vernes SC, Fisher SE, Ren B, Geschwind DH (2007) Identification of the transcriptional targets of FOXP2, a gene linked to speech and language, in developing human brain. Am J Hum Genet 81:1144–1157.

St Johnston D (2002) The art and design of genetic screens: *Drosophila melanogaster*. Nat Rev Genet 3:176–188.

Steck K, Veit D, Grandy R, Badia SBI, Badia SBI, Mathews Z, Verschure P, Hansson BS, Knaden M (2012) A high-throughput behavioral paradigm for *Drosophila* olfaction - The Flywalk. Sci Rep 2:361.

Stensmyr M, Dweck H, Farhan A, Ibba I (2012) A conserved dedicated olfactory circuit for detecting harmful microbes in *Drosophila*. Cell 151:1345–1357.

Stocker R (1994) The organization of the chemosensory system in *Drosophila melanogaster*: a review. Cell Tissue Res:3–26.

Stocker R, Lienhard M, Borst A, Fischbach KF (1990) Neuronal architecture of the antennal lobe in *Drosophila melanogaster*. Cell Tissue Res 262:9–34.

Stocker RF, Heimbeck G, Gendre N, de Belle JS (1997) Neuroblast ablation in *Drosophila* P[GAL4] lines reveals origins of olfactory interneurons. J Neurobiol 32:443–456.

Stocker RF, Singh RN, Schorderet M, Siddiqi O (1983) Projection patterns of different types of antennal sensilla in the antennal glomeruli of *Drosophila melanogaster*. Cell Tissue Res 232:237–248.

Stökl J, Strutz A, Dafni A, Svatos A, Doubsky J, Knaden M, Sachse S, Hansson BS, Stensmyr MC (2010) A deceptive pollination system targeting drosophilids through olfactory mimicry of yeast. Curr Biol 20:1846–1852.

Stone M (1960) Models for choice-reaction time. Psychometrika 25:251–260.

Strausfeld N, Hansen L, Li Y, Gomez RS, Ito K (1998) Evolution, discovery, and interpretations of arthropod mushroom bodies. Learn Mem:11–37.

Strausfeld NJ, Sinakevitch I, Vilinsky I (2003) The mushroom bodies of *Drosophila melanogaster*: an immunocytological and golgi study of Kenyon cell organization in the calyces and lobes. Microsc Res Tech 62:151–169.

Strauss R (2002) The central complex and the genetic dissection of locomotor behaviour. Curr Opin Neurobiol 12:633–638.

Su C-Y, Wang JW (2014) Modulation of neural circuits: how stimulus context shapes innate behavior in *Drosophila*. Curr Opin Neurobiol 29:9–16.

Suh GSB, de Leon SB-T, Tanimoto H, Fiala A, Benzer S, Anderson DJ (2007) Light activation of an innate olfactory avoidance response in *Drosophila*. Curr Biol 17:905–908.

Suh GSB, Wong AM, Hergarden AC, Wang JW, Simon AF, Benzer S, Axel R, Anderson DJ (2004) A single population of olfactory sensory neurons mediates an innate avoidance behaviour in *Drosophila*. Nature 431:854–859.

Takahashi H, Takahashi K (2009) FOXP genes, neural development, speech and language disorders. In: Forkhead transcription factors: vital elements in Biology and Medicine (Kenneth Maiese, ed), pp 117–129. Landes Bioscience and Springer Science+Business Media.

Talkowski ME et al. (2012) Sequencing chromosomal abnormalities reveals neurodevelopmental loci that confer risk across diagnostic boundaries. Cell 149:525–537.

Tanaka N, Awasaki T, Shimada T, Ito K (2004) Integration of chemosensory pathways in the *Drosophila* second-order olfactory centers. Curr Biol 14:449–457.

Tanaka NK, Endo K, Ito K (2012a) Organization of antennal lobe-associated neurons in adult *Drosophila melanogaster* brain. J Comp Neurol 520:4067–4130.

Tanaka NK, Ito K, Stopfer M (2009) Odor-evoked neural oscillations in *Drosophila* are mediated by widely branching interneurons. J Neurosci 29:8595–8603.

Tanaka NK, Suzuki E, Dye L, Ejima A, Stopfer M (2012b) Dye fills reveal additional olfactory tracts in the protocerebrum of wild-type *Drosophila*. J Comp Neurol 520:4131–4140.

Tanaka NK, Tanimoto H, Ito K (2008) Neuronal assemblies of the *Drosophila* mushroom body. J Comp Neurol 508:711–755.

Tang S, Guo A (2001) Choice behavior of *Drosophila* facing contradictory visual cues. Science 294:1543–1547.

Tanimura T, Isono K, Takamura T, Shimada I (1982) Genetic dimorphism in the taste sensitivity to trehalose in *Drosophila melanogaster*. J Comp Physiol 147:433–437.

Technau GM (1984) Fiber number in the mushroom bodies of adult *Drosophila melanogaster* depends on age, sex and experience. J Neurogenet 21:183–196.

Tempel BL, Bonini N, Dawson DR, Quinn WG (1983) Reward learning in normal and mutant *Drosophila*. Proc Natl Acad Sci U S A 80:1482–1486.

Teramitsu I, Kudo LC, London SE, Geschwind DH, White SA (2004) Parallel FoxP1 and FoxP2 expression in songbird and human brain predicts functional interaction. J Neurosci 24:3152–3163.

Thibault ST et al. (2004) A complementary transposon tool kit for *Drosophila melanogaster* using P and piggyBac. Nat Genet 36:283–287.

Thistle R, Cameron P, Ghorayshi A, Dennison L, Scott K (2012) Contact chemoreceptors mediate male-male repulsion and male-female attraction during *Drosophila* courtship. Cell 149:1140–1151.

Thum AS, Jenett A, Ito K, Heisenberg M, Tanimoto H (2007) Multiple memory traces for olfactory reward learning in *Drosophila*. J Neurosci 27:11132–11138.

Trannoy S, Redt-Clouet C, Dura J-M, Preat T (2011) Parallel processing of appetitive short- and long-term memories in *Drosophila*. Curr Biol 21:1647–1653.

Traven A, Jelicic B, Sopta M (2006) Yeast Gal4: a transcriptional paradigm revisited. EMBO Rep 7:496–499.

Trimmer PC, Houston AI, Marshall JAR, Bogacz R, Paul ES, Mendl MT, McNamara JM (2008) Mammalian choices: combining fast-but-inaccurate and slow-but-accurate decision-making systems. Proc Biol Sci 275:2353–2361.

Tuerk C, Gold L (1990) Systematic Evolution of Ligands by Exponential Enrichment: RNA Ligands to Bacteriophage T4 DNA Polymerase. Science 249:505–510.

Tully T, Preat T, Boynton S, Del Vecchio M (1994) Genetic dissection of consolidated memory in *Drosophila*. Cell 79:35–47.

Tully T, Quinn WG (1985) Classical conditioning and retention in normal and mutant *Drosophila melanogaster*. J Comp Physiol A 157:263–277.

Turner GCG, Bazhenov M, Laurent G (2008) Olfactory representations by *Drosophila* mushroom body neurons. J Neurophysiol 99:734–746.

Turner SL, Ray A (2009) Modification of CO2 avoidance behaviour in *Drosophila* by inhibitory odorants. Nature 461:277–281.

Uchida N, Mainen ZF (2003) Speed and accuracy of olfactory discrimination in the rat. Nat Neurosci 6:1224–1229.

Usher M, McClelland JL (2001) The time course of perceptual choice: the leaky, competing accumulator model. Psychol Rev 108:550–592.

Van der Goes van Naters W, Carlson JR (2007) Receptors and neurons for fly odors in *Drosophila*. Curr Biol 17:606–612.

Van Swinderen B, Brembs B (2010) Attention-like deficit and hyperactivity in a *Drosophila* memory mutant. J Neurosci 30:1003–1014.

Van Swinderen B, Flores KA (2007) Attention-Like Processes Underlying Optomotor Performance in a *Drosophila* Choice Maze. Dev Neurobiol 67:129–145.

Vargha-Khadem F, Watkins K, Alcock K, Fletcher P, Passingham R (1995) Praxic and nonverbal cognitive deficits in a large family with a genetically transmitted speech and language disorder. Proc Natl Acad Sci U S A 92:930–933.

Vasmer D, Pooryasin A, Riemensperger T, Fiala A (2014) Induction of aversive learning through thermogenetic activation of Kenyon cell ensembles in *Drosophila*. Front Behav Neurosci 8:174.

Venkatesh S, Singh RN (1984) Sensilla on the third antennal segment of *Drosophila melanogaster* Meigen (Diptera: Drosophilidae). Int J Insect Morphol Embryol 13:51–63.

Venken KJT, Simpson JH, Bellen HJ (2011) Genetic manipulation of genes and cells in the nervous system of the fruit fly. Neuron 72:202–230.

Vernes SC, Newbury DF, Abrahams BS, Winchester L, Nicod J, Groszer M, Alarcón M, Oliver PL, Davies KE, Geschwind DH, Monaco AP, Fisher SE (2008) A functional genetic link between distinct developmental language disorders. N Engl J Med 359:2337–2345.

Vernes SC, Oliver PL, Spiteri E, Lockstone HE, Puliyadi R, Taylor JM, Ho J, Mombereau C, Brewer A, Lowy E, Nicod J, Groszer M, Baban D, Sahgal N, Cazier J-B, Ragoussis J, Davies KE, Geschwind DH, Fisher SE (2011) Foxp2 regulates gene networks implicated in neurite outgrowth in the developing brain. PLoS Genet 7:e1002145.

Vernes SC, Spiteri E, Nicod J, Groszer M, Taylor JM, Davies KE, Geschwind DH, Fisher SE (2007) High-throughput analysis of promoter occupancy reveals direct neural targets of FOXP2, a gene mutated in speech and language disorders. Am J Hum Genet 81:1232–1250.

Vet LEM, Van Lenteren JC, Heymans M, Meelis E (1983) An airflow olfactometer for measuring olfactory responses of hymenopterous parasitoids and other small insects. Physiol Entomol 8:97–106.

Vickers D (1970) Evidence for an accumulator model of psychophysical discrimination. Ergonomics 13:37–58.

Vickers D, Packer J (1982) Effects of aletrnating set for speed or accuracy on response time, accuracy and confidence in a unidimensional discrimination task. Acta Psychol (Amst) 50:179–197.

Von Neumann J, Morgenstern O (1947) Theory of games and economic behavior. Princeton: Princeton University Press.

Vorbrüggen G, Constien R, Zilian O, Wimmer E a, Dowe G, Taubert H, Noll M, Jäckle H (1997) Embryonic expression and characterization of a Ptx1 homolog in *Drosophila*. Mech Dev 68:139–147.

Vosshall LB, Amrein H, Morozov PS, Rzhetsky A, Axel R (1999) A spatial map of olfactory receptor expression in the *Drosophila* antenna. Cell 96:725–736.

Vosshall LB, Wong AM, Axel R (2000) An olfactory sensory map in the fly brain. Cell 102:147–159.

Waddell S, Armstrong JD, Kitamoto T, Kaiser K, Quinn WG (2000) The amnesiac gene product is expressed in two neurons in the *Drosophila* brain that are critical for memory. Cell 103:805–813.

Wald A (1947) Sequential analysis. New York: John Wiley.

Wang JW, Wong AM, Flores J, Vosshall LB, Axel R (2003a) Two-photon calcium imaging reveals an odor-evoked map of activity in the fly brain. Cell 112:271–282.

Wang K, Gong J, Wang Q, Li H, Cheng Q, Liu Y, Zeng S, Wang Z (2014) Parallel pathways convey olfactory information with opposite polarities in *Drosophila*. Proc Natl Acad Sci U S A 111:3164–3169.

Wang L, Anderson DJ (2010) Identification of an aggression-promoting pheromone and its receptor neurons in *Drosophila*. Nature 463:227–231.

Wang X-J (2002) Probabilistic decision making by slow reverberation in cortical circuits. Neuron 36:955–968.

Wang X-J (2008) Decision making in recurrent neuronal circuits. Neuron 60:215–234.

Wang X-J (2012) Neural dynamics and circuit mechanisms of decision-making. Curr Opin Neurobiol 22:1039–1046.

Wang Y, Chiang A-S, Xia S, Kitamoto T, Tully T, Zhong Y (2003b) Blockade of neurotransmission in *Drosophila* mushroom bodies impairs odor attraction, but not repulsion. Curr Biol 13:1900–1904.

Wang Y, Guo H-F, Pologruto TA, Hannan F, Hakker I, Svoboda K, Zhong Y (2004) Stereotyped odor-evoked activity in the mushroom body of *Drosophila* revealed by green fluorescent protein-based Ca2+ imaging. J Neurosci 24:6507–6514.

Wang Y, Mamiya A, Chiang A, Zhong Y (2008) Imaging of an early memory trace in the *Drosophila* mushroom body. J Neurosci 28:4368–4376.

Watson A (1979) Probability summation over time. Vision Res 19:515–522.

Wicher D, Schäfer R, Bauernfeind R, Stensmyr MC, Heller R, Heinemann SH, Hansson BS (2008) Drosophila odorant receptors are both ligand-gated and cyclic-nucleotide-activated cation channels. Nature 452:1007–1011.

Wickelgren W (1977) Speed-accuracy tradeoff and information processing dynamics. Acta Psychol (Amst) 41:67–85.

Wilson RI, Laurent G (2005) Role of GABAergic inhibition in shaping odor-evoked spatiotemporal patterns in the *Drosophila* antennal lobe. J Neurosci 25:9069–9079.

Wilson RI, Turner GC, Laurent G (2004) Transformation of olfactory representations in the *Drosophila* antennal lobe. Science 303:366–370.

Wise PM, Cain WS (2000) Latency and accuracy of discriminations of odor quality between binary mixtures and their components. Chem Senses 25:247–265.

Wistrand M, Käll L, Sonnhammer E (2006) A general model of G protein-coupled receptor sequences and its application to detect remote homologs. Protein Sci:509–521.

Wolf FW, Rodan AR, Tsai LT, Heberlein U (2002) High-resolution analysis of ethanol-induced locomotor stimulation in *Drosophila*. J Neurosci 22:11035–11044.

Wong AM, Wang JW, Axel R (2002) Spatial representation of the glomerular map in the *Drosophila* protocerebrum. Cell 109:229–241.

Wong K-F, Wang X-J (2006) A recurrent network mechanism of time integration in perceptual decisions. J Neurosci 26:1314–1328.

Woodard C, Huang T, Sun H, Helfand SL, Carlson J (1989) Genetic analysis of olfactory behavior in *Drosophila*: a new screen yields the ota mutants. Genetics 123:315–326.

Wu C-L, Shih M-FM, Lai JS-Y, Yang H-T, Turner GC, Chen L, Chiang A-S (2011) Heterotypic gap junctions between two neurons in the *Drosophila* brain are critical for memory. Curr Biol 21:848–854.

Wu C-L, Xia S, Fu T-F, Wang H, Chen Y-H, Leong D, Chiang A-S, Tully T (2007) Specific requirement of NMDA receptors for long-term memory consolidation in *Drosophila* ellipsoid body. Nat Neurosci 10:1578–1586.

Xu P, Atkinson R, Jones DNM, Smith DP (2005) *Drosophila* OBP LUSH is required for activity of pheromone-sensitive neurons. Neuron 45:193–200.

Yaksi E, Wilson RI (2010) Electrical coupling between olfactory glomeruli. Neuron 67:1034–1047.

Yang C-H, Belawat P, Hafen E, Jan LY, Jan Y-N (2008a) *Drosophila* egg-laying site selection as a system to study simple decision-making processes. Science 319:1679–1683.

Yang MY, Armstrong JD, Vilinsky I, Strausfeld NJ, Kaiser K (1995) Subdivision of the *Drosophila* mushroom bodies by enhancer-trap expression patterns. Neuron 15:45–54.

Yang Y, DeWeese MR, Otazu GH, Zador AM (2008b) Millisecond-scale differences in neural activity in auditory cortex can drive decisions. Nat Neurosci 11:1262–1263.

Yao CA, Ignell R, Carlson JR (2005) Chemosensory coding by neurons in the coeloconic sensilla of the *Drosophila* antenna. J Neurosci 25:8359–8367.

Yapici N, Zimmer M, Domingos AI (2014) Cellular and molecular basis of decision-making. EMBO Rep:1–13.

Yasuyama K (2002) Synaptic organization of the mushroom body calyx in *Drosophila melanogaster*. J Comp Neurol 445:211–226.

Yasuyama K, Meinertzhagen IA, Schürmann F-W (2003) Synaptic connections of cholinergic antennal lobe relay neurons innervating the lateral horn neuropile in the brain of *Drosophila melanogaster*. J Comp Neurol 466:299–315.

Yasuyama K, Salvaterra PM (1999) Localization of choline acetyltransferase-expressing neurons in *Drosophila* nervous system. Microsc Res Tech 45:65–79.

Yin J, Wallach J (1995) A *Drosophila* CREB/CREM homolog encodes multiple isoforms, including a cyclic AMP-dependent protein kinase-responsive transcriptional activator and antagonist. Mol Cell Biol 15:5123–5130.

Yin JC, Wallach JS, Del Vecchio M, Wilder EL, Zhou H, Quinn WG, Tully T (1994) Induction of a dominant negative CREB transgene specifically blocks long-term memory in *Drosophila*. Cell 79:49–58.

Yu D, Akalal D-BG, Davis RL (2006) *Drosophila* alpha/beta mushroom body neurons form a branch-specific, long-term cellular memory trace after spaced olfactory conditioning. Neuron 52:845–855.

Yu D, Keene AC, Srivatsan A, Waddell S, Davis RL (2005) *Drosophila* DPM neurons form a delayed and branch-specific memory trace after olfactory classical conditioning. Cell 123:945–957.

Yu D, Ponomarev A, Davis RL (2004) Altered representation of the spatial code for odors after olfactory classical conditioning: memory trace formation by synaptic recruitment. Neuron 42:437–449.

Yun S-J, Hiraoka Y, Nishizawa M, Takio K, Titani K, Nogi Y, Fukasawas T (1991) Purification and characterization of the yeast negative regulatory protein GAL8O. J Biol Chem 266:693–697.

Zars T, Fischer M, Schulz R, Heisenberg M (2000) Localization of a short-term memory in *Drosophila*. Science 288:672–675.

Zhang K, Guo JZ, Peng Y, Xi W, Guo A (2007) Dopamine-mushroom body circuit regulates saliency-based decision-making in *Drosophila*. Science 316:1901–1904.

Zhang S, Roman G (2013) Presynaptic inhibition of gamma lobe neurons is required for olfactory learning in *Drosophila*. Curr Biol 23:2519–2527.

Zhu J, Park K, Baker T (2003a) Identification of odors from overripe mango that attract vinegar flies, *Drosophila melanogaster*. J Chem Ecol 29:899–909.

Zhu S, Chiang A-S, Lee T (2003b) Development of the *Drosophila* mushroom bodies: elaboration, remodeling and spatial organization of dendrites in the calyx. Development 130:2603–2610.

Zweier C, de Jong EK, Zweier M, Orrico A, Ousager LB, Collins AL, Bijlsma EK, Oortveld M a W, Ekici AB, Reis A, Schenck A, Rauch A (2009) CNTNAP2 and NRXN1 are mutated in autosomal-recessive Pitt-Hopkins-like mental retardation and determine the level of a common synaptic protein in *Drosophila*. Am J Hum Genet 85:655–666.

Zylberberg A, Fernández Slezak D, Roelfsema PR, Dehaene S, Sigman M (2010) The brain's router: a cortical network model of serial processing in the primate brain. PLoS Comput Biol 6:e1000765.

Appendix

Table 1: Statistical comparisons of wild-type behaviour between 0.1 and 0.3–0.9 MCH concentration ratios at 10^{-4} absolute odour intensity. *P* values of pairwise comparisons of accuracies (Kruskal-Wallis ANOVA, KW, followed by Dunn's test) and reaction times (Kolmogorov-Smirnov test, KS; Bonferroni-corrected significance level is 0.0062).

Comparison	KW test *P* value Fraction correct	KS test *P* value Reaction time
0.1 vs. 0.2	> 0.9999	0.0005
0.1 vs. 0.3	> 0.9999	< 0.0001
0.1 vs. 0.4	0.3942	< 0.0001
0.1 vs. 0.5	0.0111	< 0.0001
0.1 vs. 0.6	< 0.0001	< 0.0001
0.1 vs. 0.7	< 0.0001	< 0.0001
0.1 vs. 0.8	< 0.0001	< 0.0001
0.1 vs. 0.9	< 0.0001	< 0.0001

Table 2: Statistical comparisons of wild-type reaction and transit times between easy (0.1 concentration ratio), intermediate (0.5 concentration ratio) and difficult (0.9 concentration ratio) tasks at 10^{-4} absolute odour intensity. *P* values of pairwise comparisons of accuracies (Kruskal-Wallis ANOVA, KW, followed by Dunn's test) and reaction times (Kolmogorov-Smirnov test, KS; Bonferroni-corrected significance level is 0.0167).

Comparison	KS test *P* value	
	Reaction time	Transit time
0.1 vs. 0.5	< 0.0001	0.3158
0.1 vs. 0.9	< 0.0001	0.3396
0.5 vs. 0.9	< 0.0001	0.9340

Table 3: Statistical comparisons of wild-type behaviour in a masking odour task (MCH and OCT). *P* values of pairwise comparisons of accuracies (Kruskal-Wallis ANOVA, KW, followed by Dunn's test) and reaction times (Kolmogorov-Smirnov test, KS; Bonferroni-corrected significance level is 0.0250).

Comparison	KW test *P* value Fraction correct	KS test *P* value Reaction time
0 vs. 1.25	< 0.0001	< 0.0001
0 vs. 1.75	< 0.0001	< 0.0001

Table 4: Statistical comparisons of wild-type behaviour in a mixture discrimination task (MCH and OCT). *P* values of pairwise comparisons of accuracies (Kruskal-Wallis ANOVA, KW, followed by Dunn's test) and reaction times (Kolmogorov-Smirnov test, KS; Bonferroni-corrected significance level is 0.0250).

Comparison	KW test *P* value Fraction correct	KS test *P* value Reaction time
80:20 vs. 70:30	0.2181	< 0.0001
80:20 vs. 55:45	< 0.0001	< 0.0001

Table 5: Statistical comparisons between MCH concentration ratios in wild-type (wt) and *FoxP*$^{5\text{-SZ-}3955}$ mutant flies at 10^{-1} and 10^{-4} absolute odour intensities. *P* values of pairwise comparisons of accuracies (Kruskal-Wallis ANOVA, KW, followed by Dunn's test) and reaction times (Kolmogorov-Smirnov test, KS; Bonferroni-corrected significance level is 0.0083).

Odour intensity	Genotype	Comparison	KW test *P* value Fraction correct	KS test *P* value Reaction time
10^{-1}	wt	0.1 vs. 0.4	> 0.9999	< 0.0001
		0.1 vs 0.7	0.0012	< 0.0001
		0.1 vs 0.9	< 0.0001	< 0.0001
		0.4 vs 0.7	0.0164	0.0017
		0.4 vs 0.9	< 0.0001	< 0.0001
		0.7 vs 0.9	< 0.0001	0.0073
	FoxP$^{5\text{-sz-}3955}$	0.1 vs. 0.4	> 0.9999	0.0135
		0.1 vs 0.7	< 0.0001	< 0.0001
		0.1 vs 0.9	< 0.0001	< 0.0001
		0.4 vs 0.7	< 0.0001	< 0.0001
		0.4 vs 0.9	< 0.0001	< 0.0001
		0.7 vs 0.9	< 0.0001	< 0.0001
10^{-4}	wt	0.1 vs. 0.4	0.5643	< 0.0001
		0.1 vs 0.7	< 0.0001	< 0.0001
		0.1 vs 0.9	< 0.0001	< 0.0001
		0.4 vs 0.7	< 0.0001	< 0.0001
		0.4 vs 0.9	< 0.0001	< 0.0001
		0.7 vs 0.9	< 0.0001	0.0763
	FoxP$^{5\text{-sz-}3955}$	0.1 vs. 0.4	0.2636	0.2285
		0.1 vs 0.7	0.0040	< 0.0001
		0.1 vs 0.9	< 0.0001	< 0.0001
		0.4 vs 0.7	> 0.9999	< 0.0001
		0.4 vs 0.9	< 0.0001	< 0.0001
		0.7 vs 0.9	< 0.0001	< 0.0001

Table 6: Statistical comparisons between wild-type (wt) and *FoxP*$^{5\text{-SZ-}3955}$ mutant flies for MCH concentration ratios at 10^{-1} and 10^{-4} absolute odour intensities. *P* values of pairwise comparisons of accuracies (Kruskal-Wallis ANOVA, KW, followed by Dunn's test) and reaction times (Kolmogorov-Smirnov test, KS 0.0125).

Comparison	Odour intensity	Concentration ratio	KW test *P* value Fraction correct	KS test *P* value Reaction time
wt vs. *FoxP*$^{5\text{-sz-}3955}$	10^{-1}	0.1	> 0.9999	0.0727
		0.4	> 0.9999	0.2844
		0.7	0.0614	< 0.0001
		0.9	> 0.9999	< 0.0001
	10^{-4}	0.1	> 0.9999	0.0014
		0.4	> 0.9999	0.1207
		0.7	0.0463	0.0416
		0.9	0.4780	< 0.0001

Table 7: Statistical comparisons of transit times between wild-type (wt) and *FoxP*$^{5\text{-SZ-}3955}$ mutant flies for MCH concentration rations at 10^{-1} and 10^{-4} absolute odour intensities. *P* values of pairwise comparisons of accuracies (Kruskal-Wallis ANOVA, KW, followed by Dunn's test) and reaction times (Kolmogorov-Smirnov test, KS; Bonferroni-corrected significance level is 0.025).

Comparison	Odour intensity	Concentration ratio	KS test *P* value Transit time
wt vs. *FoxP*$^{5\text{-sz-}3955}$	10^{-1}	0.1	0.3190
		0.9	0.0685
	10^{-4}	0.1	0.8219
		0.9	0.8203

Table 8: Statistical comparisons between MCH concentration ratios across 10^{-1} and 10^{-4} absolute odour intensities for wild-type (wt) and *FoxP*$^{5\text{-SZ-3955}}$ mutant flies. *P* values of pairwise comparisons of accuracies (Kruskal-Wallis ANOVA, KW, followed by Dunn's test) and reaction times (Kolmogorov-Smirnov test, KS; Bonferroni-corrected significance level is 0.0125).

Comparison	Genotype	Comparison	KW test *P* value Fraction correct	KS test *P* value Reaction time
10^{-1} vs. 10^{-4}	wt	0.1	> 0.9999	0.0641
		0.4	> 0.9999	0.1258
		0.7	0.6023	0.1147
		0.9	> 0.9999	0.1128
	FoxP$^{5\text{-sz-3955}}$	0.1	> 0.9999	0.4519
		0.4	> 0.9999	0.1620
		0.7	0.6126	0.1483
		0.9	> 0.9999	0.2508

Table 9: Statistical comparisons between wild-type (wt) and *FoxP*$^{5\text{-SZ-3955}}$ mutant flies at 10^{-1} absolute odour intensity. *P* values of pairwise comparisons of accuracies (Kruskal-Wallis ANOVA, KW, followed by Dunn's test) and reaction times (Kolmogorov-Smirnov test, KS; Bonferroni-corrected significance level is 0.007).

Comparison	Genotype	Comparison	KW test *P* value Fraction correct	KS test *P* value Reaction time
10^{-1} vs. 10^{-4}	wt	0.1	> 0.9999	0.0641
		0.4	> 0.9999	0.1258
		0.7	0.6023	0.1147
		0.9	> 0.9999	0.1128
	FoxP$^{5\text{-sz-3955}}$	0.1	> 0.9999	0.4519
		0.4	> 0.9999	0.1620
		0.7	0.6126	0.1483
		0.9	> 0.9999	0.2508

Table 10: Statistical comparisons between wild-type (wt) and *FoxP* heterozygous, homozygous or transheterozygous alleles. *P* values of pairwise comparisons of accuracies (Kruskal-Wallis ANOVA, KW, followed by Dunn's test) and reaction times (Kolmogorov-Smirnov test, KS; Bonferroni-corrected significance level is 0.0083).

Comparison	Concentration ratio	KW test *P* value Fraction correct	KS test *P* value Reaction time
wt vs. *FoxP*$^{5\text{-sz-3955}}$/+	0.1	0.6788	0.3218
	0.7	> 0.9999	0.0002
wt vs. *FoxP*^{f03746}/+	0.1	> 0.9999	0.0309
	0.7	> 0.9999	0.0050
wt vs. *FoxP*^{GS22100}/+	0.1	> 0.9999	0.2696
	0.7	0.0035	< 0.0001
wt vs. *FoxP*$^{5\text{-sz-3955}}$	0.1	> 0.9999	0.0047
	0.7	> 0.9999	< 0.0001
wt vs. *FoxP*^{f03746}	0.1	> 0.9999	< 0.0001
	0.7	< 0.0001	< 0.0001
wt vs. *FoxP*$^{5\text{-sz-3955}}$/*FoxP*^{GS22100}	0.1	> 0.9999	0.0001
	0.7	< 0.0001	< 0.0001

Table 11: Statistical comparisons between *FoxP > FoxP^{RNAi}*, *OK107 > FoxP^{RNAi}* and respective parental control flies. *P* values of pairwise comparisons of accuracies (Kruskal-Wallis ANOVA, KW, followed by Dunn's test) and reaction times (Kolmogorov-Smirnov test, KS; Bonferroni-corrected significance level is 0.0167).

Comparison	Concentration ratio	KW test *P* value Fraction correct	KS test *P* value Reaction time
FoxP-GAL4 ; *UAS-FoxP^{RNAi}* vs. *FoxP-GAL4*	0.1	> 0.9999	0.0016
	0.9	0.0989	0.1148
FoxP-GAL4 ; *UAS-FoxP^{RNAi}* vs. *UAS-FoxP^{RNAi}*	0.1	> 0.9999	0.1759
	0.9	0.0082	0.0645
FoxP-GAL4 vs. *UAS-FoxP^{RNAi}*	0.1	> 0.9999	0.0975
	0.9	0.9005	0.0074
UAS-FoxP^{RNAi} ; OK107-GAL4 vs. *OK107-Gal4*	0.1	0.8614	0.0460
	0.9	> 0.9999	0.0029
UAS-FoxP^{RNAi} ; OK107-GAL4 vs. *UAS-FoxP^{RNAi}*	0.1	0.3096	0.0663
	0.9	0.1373	0.0006
OK107-GAL4 vs. *UAS-FoxP^{RNAi}*	0.1	> 0.9999	0.0971
	0.9	0.8202	0.3876

Table 12: Statistical comparisons of *NP6024 > FoxP^{RNAi}* and *NP1131 > FoxP^{RNAi}* with parental controls. *P* values of pairwise comparisons of accuracies (Kruskal-Wallis ANOVA, KW, followed by Dunn's test) and reaction times (Kolmogorov-Smirnov test, KS; Bonferroni-corrected significance level is 0.0167).

Comparison	Concentration ratio	KW test *P* value Fraction correct	KS test *P* value Reaction time
NP6024-GAL4 ; *UAS-FoxP^{RNAi}* vs. *NP6024-GAL4*	0.1	0.6882	0.7040
	0.9	> 0.9999	0.0031
NP6024-GAL4 ; *UAS-FoxP^{RNAi}* vs. *UAS-FoxP^{RNAi}*	0.1	0.0398	0.0024
	0.9	0.8753	< 0.0001
NP6024-GAL4 vs. *UAS-FoxP^{RNAi}*	0.1	0.5505	0.0012
	0.9	> 0.9999	0.0008
NP1131-GAL4 ; *UAS-FoxP^{RNAi}* vs. *NP1131-GAL4*	0.1	> 0.9999	0.3514
	0.9	0.0713	0.5450
NP1131-GAL4 ; *UAS-FoxP^{RNAi}* vs. *UAS-FoxP^{RNAi}*	0.1	0.2424	0.2077
	0.9	> 0.9999	0.1366
NP1131-GAL4 vs. *UAS-FoxP^{RNAi}*	0.1	0.1028	0.5853
	0.9	0.0134	0.0049

Table 13: Statistical comparisons between *FoxP > Kir2.1* and parental control flies maintained at 25 °C and 31 °C for 18 h before testing. *P* values of pairwise comparisons of accuracies (Kruskal-Wallis ANOVA, KW, followed by Dunn's test) and reaction times (Kolmogorov-Smirnov test, KS; Bonferroni-corrected significance level is 0.0167).

Temperature	Comparison	Concentration ratio	KW test *P* value Fraction correct	KS test *P* value Reaction time
25 °C	*FoxP-GAL4/UAS-Kir2.1*; *tubP-GAL80^{ts}* vs. *FoxP-GAL4*	0.1	0.6119	0.0167
		0.5	0.4095	0.0958
		0.9	0.6498	< 0.0001
	FoxP-GAL4/UAS-Kir2.1; *tubP-GAL80^{ts}* vs. U*AS-Kir2.1; tubP-GAL80^{ts}*	0.1	> 0.9999	0.2139
		0.5	> 0.9999	0.3666
		0.9	0.3790	0.0005
	FoxP-GAL4 vs. *UAS-Kir2.1; tubP-GAL80^{ts}*	0.1	> 0.9999	0.3142
		0.5	0.3883	0.3873
		0.9	> 0.9999	0.0942
32 °C	*FoxP-GAL4/UAS-Kir2.1*; *tubP-GAL80^{ts}* vs. *FoxP-GAL4*	0.1	0.0124	0.0842
		0.5	<0.0001	0.8951
		0.9	0.0035	0.0002
	FoxP-GAL4/UAS-Kir2.1; *tubP-GAL80^{ts}* vs. U*AS-Kir2.1; tubP-GAL80^{ts}*	0.1	0.0761	0.8281
		0.5	<0.0001	0.9412
		0.9	0.0307	< 0.0001
	FoxP-GAL4 vs. *UAS-Kir2.1; tubP-GAL80^{ts}*	0.1	> 0.9999	0.0518
		0.5	0.7242	0.7900
		0.9	> 0.9999	0.4348

Table 14: Statistical comparisons of *NP6024 > Kir2.1* and *NP1131 > Kir2.1* with parental controls. *P* values of pairwise comparisons of reaction times (Kolmogorov-Smirnov test, KS; Bonferroni-corrected significance level is 0.0167) and accuracies (Kruskal-Wallis ANOVA, KW, followed by Dunn's test).

Comparison	Concentration ratio	KW test *P* value Fraction correct	KS test *P* value Reaction time
NP6024-GAL4 ; *UAS-Kir2.1* ; *tubP-GAL80^{ts}* vs. *NP6024-GAL4*	0.1	> 0.9999	0.2813
	0.9	0.0009	0.0007
NP6024-GAL4 ; *UAS-Kir2.1* ; *tubP-GAL80^{ts}* vs. *UAS-Kir2.1 ; tubP-GAL80^{ts}*	0.1	0.0638	< 0.0001
	0.9	0.0019	< 0.0001
NP6024-GAL4 vs. *UAS-Kir2.1 ; tubP-GAL80^{ts}*	0.1	0.0159	< 0.0001
	0.9	> 0.9999	0.0043
NP1131-GAL4/*UAS-Kir2.1* ; *tubP-GAL80^{ts}* vs. *NP1131-GAL4*	0.1	> 0.9999	0.0666
	0.9	0.234	0.9275
NP1131-GAL4/*UAS-Kir2.1* ; *tubP-GAL80^{ts}* vs. *UAS-Kir2.1 ; tubP-GAL80^{ts}*	0.1	> 0.9999	0.9148
	0.9	> 0.9999	0.8296
NP1131-GAL4 vs. *UAS-Kir2.1 ; tubP-GAL80^{ts}*	0.1	> 0.9999	0.0089
	0.9	0.0175	0.6743

Table 15: Statistical comparisons between wild-type (wt) and *FoxP$^{5\text{-}SZ\text{-}3955}$* homozygous and heterozygous mutant flies performing discrimination between 10^{-4} MCH and air. *P* values of pairwise comparisons of accuracies (Kruskal-Wallis ANOVA, KW, followed by Dunn's test) and reaction times (Kolmogorov-Smirnov test, KS; Bonferroni-corrected significance level is 0.0167).

Comparison	KW test *P* value Fraction correct	KS test *P* value Reaction time
wt vs. *FoxP$^{5\text{-}sz\text{-}3955}$*	> 0.9999	0.0086
wt vs. *FoxP$^{5\text{-}sz\text{-}3955}$/+*	0.4817	0.0171
FoxP$^{5\text{-}sz\text{-}3955}$ vs. *FoxP$^{5\text{-}sz\text{-}3955}$/+*	0.1347	0.0021

Table 16: Raw data and statistical comparisons between *FoxP*$^{5\text{-SZ-3955}}$ heterozygous flies and the deficiency lines for the left arm of 2nd chromosome over *FoxP*$^{5\text{-SZ-3955}}$. Accuracies presented as mean±SEM, together with number of flies tested per genotype; *P* values of pairwise comparisons of accuracies (Kruskal-Wallis ANOVA, KW, followed by Dunn's test). Reaction times presented as mean±SEM, together with number of decisions analysed per genotype; *P* values of pairwise comparisons of reaction times (Kolmogorov-Smirnov test, KS; Bonferroni-corrected significance level is 0.0005618).

Genotype/*FoxP*$^{5\text{-Z-3955}}$	Accuracy			Reaction time		
	Number of flies	Mean±SEM (fraction)	KW *P* values	Number of decisions	Mean±SEM (s)	KS *P* values
CS	670	0.9269 ± 0.0079		2794	2.0520 ± 0.0326	
Df(2L)ED50001	36	0.9628 ± 0.0285	> 0.9999	128	1.8380 ± 0.1837	0.0088
Df(2L)ED19	36	0.9914 ± 0.0060	> 0.9999	179	2.5980 ± 0.1450	< 0.0001
Df(2L)BSC454	40	0.8642 ± 0.0389	> 0.9999	160	2.3720 ± 0.1674	0.0325
Df(2L)BSC106	52	0.8717 ± 0.0363	> 0.9999	179	1.9500 ± 0.1495	0.1017
Df(2L)BSC107	37	0.8329 ± 0.0427	> 0.9999	164	1.7070 ± 0.0945	0.0094
Df(2L)ED105	53	0.9503 ± 0.0181	> 0.9999	229	2.3270 ± 0.1184	0.0143
Df(2L)ED94	78	0.9421 ± 0.0197	> 0.9999	340	2.3320 ± 0.1062	< 0.0001
Df(2L)Exel6005	40	0.8788 ± 0.0373	> 0.9999	165	2.3840 ± 0.2042	0.1721
Df(2L)BSC688	40	0.8695 ± 0.0338	> 0.9999	166	2.1340 ± 0.1248	0.5762
Df(2L)BSC455	39	0.8708 ± 0.0380	> 0.9999	181	1.8420 ± 0.1066	0.3283
Df(2L)Exel7011	53	0.9622 ± 0.0160	> 0.9999	228	2.1660 ± 0.1631	0.7483
Df(2L)ED136	53	0.9622 ± 0.0160	> 0.9999	228	2.1660 ± 0.1631	0.7483
Df(2L)Exel6277	40	0.9563 ± 0.0209	> 0.9999	173	1.9040 ± 0.1331	0.3672
Df(2L)BSC692	38	0.9133 ± 0.0344	> 0.9999	138	2.4050 ± 0.2061	0.6781
Df(2L)BSC180	40	0.8856 ± 0.0347	> 0.9999	206	2.1100 ± 0.1291	0.53
Df(2L)ED4651	36	0.9240 ± 0.0270	> 0.9999	162	2.3230 ± 0.1590	0.0611
Df(2L)drm-P2	39	0.9835 ± 0.0132	> 0.9999	186	1.9580 ± 0.1778	0.0457
Df(2L)BSC292	39	0.8839 ± 0.0350	> 0.9999	149	2.2260 ± 0.1904	0.7963
Df(2L)ED247	74	0.9550 ± 0.0156	> 0.9999	373	2.4440 ± 0.1346	0.1259
Df(2L)ed1	40	0.8673 ± 0.0500	> 0.9999	164	2.8580 ± 0.2526	0.0002
Df(2L)Exel6009	38	0.8279 ± 0.0478	> 0.9999	145	1.8690 ± 0.1090	0.3774
Df(2L)BSC165	38	0.9393 ± 0.0247	> 0.9999	169	2.1580 ± 0.1274	0.2724
Df(2L)M24F-B	40	0.9354 ± 0.0311	> 0.9999	164	2.2630 ± 0.1547	0.0415
Df(2L)ED250	35	0.8997 ± 0.0382	> 0.9999	148	2.5610 ± 0.1320	< 0.0001
Df(2L)ED7853	70	0.9503 ± 0.0196	> 0.9999	339	2.4360 ± 0.1333	0.0955
Df(2L)tkv3	36	0.8532 ± 0.0507	> 0.9999	117	1.8670 ± 0.1171	0.392
Df(2L)BSC172	38	0.9798 ± 0.0123	> 0.9999	150	2.1100 ± 0.1278	0.0413
Df(2L)BSC110	29	0.2874 ± 0.0730	< 0.0001	54	3.4700 ± 0.4866	0.0095
Df(2L)BSC109	38	0.9737 ± 0.0161	> 0.9999	142	1.7090 ± 0.0854	0.0231
Df(2L)Exel6011	37	0.9263 ± 0.0319	> 0.9999	189	2.1220 ± 0.1247	0.3062
Df(2L)Exel6012	73	0.8862 ± 0.0264	> 0.9999	282	2.6300 ± 0.1717	0.0027
Df(2L)BSC169	39	0.8425 ± 0.0519	> 0.9999	124	2.2540 ± 0.1946	0.4521
Df(2L)ED334	55	0.9894 ± 0.0075	> 0.9999	219	2.2240 ± 0.1788	0.055
Df(2L)ED385	30	0.9722 ± 0.0197	> 0.9999	86	2.2730 ± 0.2781	0.0369
Df(2L)BSC6	39	0.9440 ± 0.0291	> 0.9999	140	1.7720 ± 0.1002	0.245
Df(2L)BSC354	38	0.9062 ± 0.0206	> 0.9999	197	1.8140 ± 0.0943	0.0985
Df(2L)BSC188	38	0.9048 ± 0.0403	> 0.9999	149	2.3340 ± 0.1892	0.3007
Df(2L)BSC291	37	0.9162 ± 0.0274	> 0.9999	142	1.9290 ± 0.1127	0.7341
Df(2L)BSC233	38	0.9074 ± 0.0343	> 0.9999	168	2.0420 ± 0.1324	0.429
Df(2L)BSC142	38	0.8064 ± 0.0460	0.1453	186	2.0250 ± 0.1371	0.3491
Df(2L)Exel7034	56	0.9710 ± 0.0140	> 0.9999	217	2.2600 ± 0.1869	0.4525
Df(2L)BSC227	39	0.8038 ± 0.0472	0.3454	178	2.3270 ± 0.1468	0.035
Df(2L)BSC111	37	0.9062 ± 0.0272	> 0.9999	166	1.8930 ± 0.1114	0.4652
Df(2L)ED629	53	0.9591 ± 0.0224	> 0.9999	246	2.0280 ± 0.1086	0.342
Df(2L)BSC204	33	0.9298 ± 0.0348	> 0.9999	127	1.9150 ± 0.1614	0.1357
Df(2L)ED678	54	0.9588 ± 0.0217	> 0.9999	222	1.9770 ± 0.1358	0.0606
Df(2L)ED690	51	0.9825 ± 0.0087	> 0.9999	229	2.0960 ± 0.1262	0.8218
Df(2L)BSC17	40	0.9785 ± 0.0136	> 0.9999	214	1.8080 ± 0.1019	0.0224
Df(2L)BSC240	39	0.9848 ± 0.0088	> 0.9999	194	2.0230 ± 0.1115	0.5826
Df(2L)BSC50	39	0.9654 ± 0.0177	> 0.9999	149	1.6140 ± 0.1293	0.0005
Df(2L)BSC689	37	0.9057 ± 0.0327	> 0.9999	186	2.0690 ± 0.1025	0.6565
Df(2L)BSC143	39	0.8683 ± 0.0402	> 0.9999	148	2.2760 ± 0.2260	0.745
Df(2L)BSC208	38	0.8258 ± 0.0413	0.1826	174	2.2900 ± 0.1842	0.3393
Df(2L)BSC209	61	0.8562 ± 0.0386	> 0.9999	262	2.6930 ± 0.1943	0.0003
Df(2L)ED8142	39	0.8618 ± 0.0426	> 0.9999	169	2.0890 ± 0.1368	0.2863
Df(2L)BSC214	38	0.9092 ± 0.0346	> 0.9999	142	1.8240 ± 0.1348	0.0324
Df(2L)BSC213	36	0.9667 ± 0.0199	> 0.9999	117	2.3770 ± 0.2618	0.7656
Df(2L)BSC145	35	0.9300 ± 0.0347	> 0.9999	127	2.0850 ± 0.1621	0.5301
Df(2L)BSC241	34	0.9272 ± 0.0358	> 0.9999	166	2.1690 ± 0.1602	0.7923
Df(2L)BSC244	53	0.7706 ± 0.0477	0.2861	152	2.7820 ± 0.2314	0.0192
Df(2L)ED761	38	0.9706 ± 0.0144	> 0.9999	182	2.3650 ± 0.1615	0.0467
Df(2L)ED775	36	0.9491 ± 0.0331	> 0.9999	144	2.0830 ± 0.1598	0.8592
Df(2L)BSC277	38	0.9037 ± 0.0293	> 0.9999	156	2.2200 ± 0.1318	0.3996
Df(2L)BSC892	58	0.9721 ± 0.0127	> 0.9999	211	2.4320 ± 0.1843	0.291
Df(2L)BSC159	75	0.9640 ± 0.0199	> 0.9999	277	1.7160 ± 0.0813	0.0047
Df(2L)BSC812	35	0.8171 ± 0.0430	0.5794	130	2.5720 ± 0.1964	0.0132
Df(2L)BSC252	40	0.9053 ± 0.0338	> 0.9999	219	2.2250 ± 0.1299	0.0383
Df(2L)ED793	73	0.9029 ± 0.0263	> 0.9999	284	2.1680 ± 0.1347	0.92
Df(2L)ED3	72	0.9697 ± 0.0110	> 0.9999	301	1.9710 ± 0.1230	0.0044
Df(2L)ED1050	67	0.9647 ± 0.0176	> 0.9999	234	1.4640 ± 0.0860	< 0.0001
Df(2L)r10	38	0.8701 ± 0.0436	> 0.9999	165	2.0920 ± 0.2017	0.3464
Df(2L)BSC690	39	0.9004 ± 0.0289	> 0.9999	150	2.2220 ± 0.1699	0.8856
Df(2L)BSC278	39	0.7792 ± 0.0471	0.0424	121	2.3750 ± 0.2302	0.257
Df(2L)BSC781	38	0.8765 ± 0.0445	> 0.9999	143	1.5810 ± 0.0957	0.0002
Df(2L)ED1102	65	0.9673 ± 0.0186	> 0.9999	279	1.9450 ± 0.1457	0.0032
Df(2L)ED1161	56	0.9747 ± 0.0127	> 0.9999	219	2.0780 ± 0.1288	0.4413
Df(2L)BSC148	37	0.9134 ± 0.0396	> 0.9999	131	1.6640 ± 0.1221	0.0005
Df(2L)Exel7070	38	0.8072 ± 0.0456	0.2719	162	2.2400 ± 0.1612	0.2846
Df(2L)BSC256	34	0.9100 ± 0.0264	> 0.9999	164	1.8680 ± 0.1773	0.0291
Df(2L)Exel8038	37	0.8288 ± 0.0534	> 0.9999	158	2.1040 ± 0.1247	0.5133
Df(2L)BSC149	35	0.8600 ± 0.0426	> 0.9999	137	1.9960 ± 0.2868	0.0002
Df(2L)ED1203	31	0.9226 ± 0.0451	> 0.9999	141	1.7150 ± 0.1052	0.0045
Df(2L)ED1272	30	0.7358 ± 0.0696	0.534	115	2.5960 ± 0.2007	0.0005
Df(2L)ED1315	23	0.9623 ± 0.0178	> 0.9999	93	1.8510 ± 0.1444	0.2713
Df(2L)BSC151	35	0.8726 ± 0.0475	> 0.9999	116	1.6680 ± 0.1113	0.005
Df(2L)lt109	36	0.9537 ± 0.0226	> 0.9999	141	1.9500 ± 0.1777	0.2861
Df(2L)C'	54	0.8564 ± 0.0357	> 0.9999	230	2.7880 ± 0.1333	< 0.0001

Table 17: Raw data and statistical comparisons between *FoxP*$^{5\text{-SZ-3955}}$ heterozygous flies and the deficiency lines for the right arm of 2nd chromosome over *FoxP*$^{5\text{-SZ-3955}}$. Accuracies presented as mean±SEM, together with number of flies tested per genotype; *P* values of pairwise comparisons of accuracies (Kruskal-Wallis ANOVA, KW, followed by Dunn's test). Reaction times presented as mean±SEM, together with number of decisions analysed per genotype; *P* values of pairwise comparisons of reaction times (Kolmogorov-Smirnov test, KS; Bonferroni-corrected significance level is 0.0006493).

Genotype/ *FoxP*$^{5\text{-Z-3955}}$	Accuracy			Reaction time		
	Number of flies	Mean±SEM (fraction)	KW *P* values	Number of decisions	Mean±SEM (s)	KS *P* values
CS	901	0.8957 ± 0.0080		3275	2.1060 ± 0.0305	
Df(2R)M41A10	36	0.9087 ± 0.0282	> 0.9999	158	2.2180 ± 0.1597	0.1191
Df(2R)BSC630	51	0.8828 ± 0.0251	> 0.9999	237	2.6510 ± 0.2021	0.0021
Df(2R)ED1612	35	0.9378 ± 0.0329	> 0.9999	89	2.2520 ± 0.3069	0.1753
Df(2R)ED1673	35	0.9490 ± 0.0301	> 0.9999	139	2.1220 ± 0.1524	0.8921
Df(2R)ED1715	39	0.7489 ± 0.0519	0.0976	134	2.7550 ± 0.2157	< 0.0001
Df(2R)ED1725	29	0.9310 ± 0.0479	> 0.9999	91	1.8810 ± 0.1504	0.1616
Df(2R)BSC267	75	0.6100 ± 0.0413	< 0.0001	247	2.7610 ± 0.1756	0.0015
Df(2R)ED1742	55	0.9745 ± 0.0195	> 0.9999	159	2.1080 ± 0.2275	0.0026
Df(2R)ED1791	29	0.9483 ± 0.0380	> 0.9999	122	1.7550 ± 0.1573	0.0037
Df(2R)BSC280	57	0.6879 ± 0.0426	< 0.0001	251	2.7520 ± 0.1591	< 0.0001
Df(2R)BSC132	70	0.7487 ± 0.0351	0.0001	262	2.6620 ± 0.1793	0.0013
Df(2R)BSC298	38	0.6743 ± 0.0559	0.0007	142	2.5120 ± 0.2099	0.1461
Df(2R)BSC152	37	0.8167 ± 0.0385	0.8451	143	2.5150 ± 0.2118	0.0132
Df(2R)BSC303	39	0.8048 ± 0.0416	0.8965	164	2.7820 ± 0.2702	0.2464
Df(2R)BSC281	37	0.9202 ± 0.0266	> 0.9999	186	2.3490 ± 0.1575	0.3106
Df(2R)BSC595	54	0.9217 ± 0.0230	> 0.9999	167	2.1250 ± 0.1816	0.05
Df(2R)ED2247	32	0.8781 ± 0.0459	> 0.9999	98	2.5270 ± 0.2009	0.0461
Df(2R)BSC199	29	0.8161 ± 0.0602	> 0.9999	93	3.6960 ± 0.4334	< 0.0001
Df(2R)BSC699	33	0.7994 ± 0.0468	> 0.9999	122	2.8380 ± 0.2337	0.0002
Df(2R)BSC425	93	0.7500 ± 0.0314	< 0.0001	312	2.7920 ± 0.1639	< 0.0001
Df(2R)Exel6061	73	0.6933 ± 0.0412	< 0.0001	275	3.0480 ± 0.1619	< 0.0001
Df(2R)BSC305	38	0.7419 ± 0.0572	0.4163	173	2.9870 ± 0.1591	< 0.0001
Df(2R)BSC880	36	0.5987 ± 0.0662	< 0.0001	146	2.9580 ± 0.1564	< 0.0001
Df(2R)BSC485	33	0.7571 ± 0.0624	> 0.9999	106	3.1580 ± 0.3837	0.0353
Df(2R)Exel6062	37	0.7815 ± 0.0494	0.752	120	2.7750 ± 0.2807	0.0018
Df(2R)Exel8057	91	0.8902 ± 0.0235	> 0.9999	378	2.5040 ± 0.1330	0.0969
Df(2R)BSC273	39	0.9013 ± 0.0403	> 0.9999	142	2.1060 ± 0.1766	0.9098
Df(2R)BSC274	39	0.8483 ± 0.0454	> 0.9999	175	2.2080 ± 0.1108	0.2902
Df(2R)BSC307	37	0.8869 ± 0.0397	> 0.9999	116	3.1810 ± 0.3419	0.0927
Df(2R)BSC361	35	0.7915 ± 0.0557	> 0.9999	132	3.0930 ± 0.2656	< 0.0001
Df(2R)BSC383	38	0.8500 ± 0.0405	> 0.9999	149	2.4650 ± 0.2010	0.4469
Df(2R)Exel7130	39	0.8893 ± 0.0391	> 0.9999	180	2.3540 ± 0.1479	0.1799
Df(2R)Exel7131	39	0.9176 ± 0.0266	> 0.9999	161	2.1980 ± 0.1374	0.2248
Df(2R)ED2354	33	0.9333 ± 0.0363	> 0.9999	126	2.2060 ± 0.2114	0.2719
Df(2R)Exel6284	39	0.8799 ± 0.0459	> 0.9999	146	2.0420 ± 0.1389	0.6439
Df(2R)BSC429	39	0.8833 ± 0.0408	> 0.9999	167	2.3930 ± 0.2295	0.6587
Df(2R)BSC651	32	0.7594 ± 0.0589	> 0.9999	88	3.1100 ± 0.4566	0.0701
Df(2R)ED2426	36	0.9282 ± 0.0329	> 0.9999	120	1.9660 ± 0.1319	0.3074
Df(2R)ED2457	17	0.9265 ± 0.0416	> 0.9999	53	1.8960 ± 0.1735	0.8307
Df(2R)ED2487	51	0.9363 ± 0.0271	> 0.9999	176	2.4610 ± 0.1989	0.2429
Df(2R)BSC550	39	0.9621 ± 0.0262	> 0.9999	135	2.6130 ± 0.2022	0.1467
Df(2R)Exel6064	69	0.8570 ± 0.0282	> 0.9999	285	2.4300 ± 0.1284	0.0292
Df(2R)ED2747	52	0.9548 ± 0.0165	> 0.9999	199	2.4530 ± 0.1751	0.1504
Df(2R)BSC331	36	0.8101 ± 0.0530	> 0.9999	122	1.8680 ± 0.1390	0.0405
Df(2R)Exel6066	37	0.7009 ± 0.0640	0.2649	119	2.4960 ± 0.2038	0.181
Df(2R)BSC161	57	0.6926 ± 0.0472	0.0005	188	3.1060 ± 0.2089	< 0.0001
Df(2R)BSC355	38	0.9246 ± 0.0232	> 0.9999	128	2.2560 ± 0.1501	0.0737
Df(2R)Exel7149	40	0.9263 ± 0.0249	> 0.9999	179	2.3240 ± 0.1949	0.7505
Df(2R)BSC347	38	0.8568 ± 0.0428	> 0.9999	172	2.1420 ± 0.1168	0.7679
Df(2R)14H10W-35	17	0.9426 ± 0.0346	> 0.9999	65	2.6950 ± 0.3195	0.0294
Df(2R)ED3610	34	0.9216 ± 0.0361	> 0.9999	165	2.3410 ± 0.2144	0.2415
Df(2R)ED3683	52	0.9024 ± 0.0284	> 0.9999	170	2.5470 ± 0.1826	0.0377
Df(2R)Exel6069	37	0.8211 ± 0.0530	> 0.9999	125	2.6010 ± 0.2531	0.0594
Df(2R)BSC135	40	0.7050 ± 0.0613	0.1539	120	2.1360 ± 0.1454	0.8362
Df(2R)BSC782	75	0.6707 ± 0.0398	< 0.0001	234	3.2180 ± 0.2096	< 0.0001
Df(2R)BSC883	56	0.7223 ± 0.0437	0.0004	200	2.6280 ± 0.1851	0.0659
Df(2R)Exel7162	32	0.8776 ± 0.0376	> 0.9999	110	1.7230 ± 0.1049	0.0501
Df(2R)BSC19	72	0.9245 ± 0.0285	> 0.9999	248	1.7640 ± 0.0996	< 0.0001
Df(2R)BSC701	38	0.7076 ± 0.0600	0.0614	118	2.5860 ± 0.2285	0.2221
Df(2R)BSC702	38	0.7361 ± 0.0516	0.0719	122	2.7680 ± 0.3521	0.1579
Df(2R)BSC885	38	0.9410 ± 0.0224	> 0.9999	158	2.2710 ± 0.1571	0.062
Df(2R)BSC821	36	0.7808 ± 0.0655	> 0.9999	116	1.9020 ± 0.1312	0.2225
Df(2R)BSC664	35	0.7795 ± 0.0467	0.6379	117	3.0320 ± 0.2605	< 0.0001
Df(2R)BSC597	31	0.7999 ± 0.0504	> 0.9999	117	2.3730 ± 0.2089	0.7747
Df(2R)BSC598	38	0.8934 ± 0.0271	> 0.9999	156	2.2460 ± 0.1689	0.2932
Df(2R)BSC787	38	0.8634 ± 0.0304	> 0.9999	144	1.9880 ± 0.1094	0.8344
Df(2R)BSC599	38	0.7566 ± 0.0432	0.0098	137	2.6190 ± 0.2545	0.1362
Df(2R)BSC784	57	0.9071 ± 0.0254	> 0.9999	200	2.1820 ± 0.1587	0.6813
Df(2R)BSC769	39	0.7642 ± 0.0515	0.4145	142	2.7800 ± 0.2305	0.0227
Df(2R)BSC356	53	0.8406 ± 0.0345	> 0.9999	230	2.2640 ± 0.1283	0.2028
Df(2R)BSC780	53	0.8728 ± 0.0327	> 0.9999	225	2.3840 ± 0.1064	< 0.0001
Df(2R)BSC604	35	0.9038 ± 0.0323	> 0.9999	115	2.2310 ± 0.2113	0.9253
Df(2R)BSC608	38	0.8855 ± 0.0413	> 0.9999	138	2.2770 ± 0.1666	0.8275
Df(2R)ED50004	34	0.9441 ± 0.0249	> 0.9999	142	2.5180 ± 0.2822	0.5344

Table 18: Raw data and statistical comparisons between *FoxP*$^{5\text{-SZ-3955}}$ heterozygous flies and the deficiency lines for the left arm of 3rd chromosome over *FoxP*$^{5\text{-SZ-3955}}$. Accuracies presented as mean±SEM, together with number of flies tested per genotype; *P* values of pairwise comparisons of accuracies (Kruskal-Wallis ANOVA, KW, followed by Dunn's test). Reaction times presented as mean±SEM, together with number of decisions analysed per genotype; *P* values of pairwise comparisons of reaction times (Kolmogorov-Smirnov test, KS; Bonferroni-corrected significance level is 0.0007246.

Genotype/FoxP$^{5\text{-Z-3955}}$	Accuracy			Reaction time		
	Number of flies	Mean±SEM (fraction)	KW *P* values	Number of decisions	Mean±SEM (s)	KS *P* values
CS	576	0.8793 ± 0.0104		2174	2.3300 ± 0.0465	
Df(3L)ED50002	52	0.9048 ± 0.0289	> 0.9999	180	2.5170 ± 0.1955	0.8679
Df(3L)ED201	62	0.7665 ± 0.0390	0.3222	214	3.2980 ± 0.1879	< 0.0001
Df(3L)BSC362	38	0.8583 ± 0.0397	> 0.9999	153	2.3820 ± 0.1568	0.3293
Df(3L)BSC289	73	0.7152 ± 0.0370	0.0001	286	2.6870 ± 0.1316	0.0023
Df(3L)BSC800	79	0.9212 ± 0.0222	> 0.9999	342	2.4340 ± 0.1320	0.3244
Df(3L)BSC181	69	0.7564 ± 0.0376	0.0422	259	2.4760 ± 0.1175	0.0221
Df(3L)Aprt-32	92	0.8353 ± 0.0264	> 0.9999	415	2.6330 ± 0.1234	0.0227
Df(3L)ED4287	54	0.8323 ± 0.0418	> 0.9999	178	2.3490 ± 0.2008	0.0112
Df(3L)BSC119	36	0.7847 ± 0.0586	> 0.9999	115	2.9110 ± 0.2968	0.1953
Df(3L)M21	54	0.8334 ± 0.0398	> 0.9999	266	2.7230 ± 0.1474	0.0319
Df(3L)Exel6092	35	0.6873 ± 0.0649	0.1813	115	3.2030 ± 0.3200	0.0176
Df(3L)BSC671	55	0.7632 ± 0.0371	0.0264	214	2.8220 ± 0.1792	< 0.0001
Df(3L)BSC672	37	0.8218 ± 0.0487	> 0.9999	134	3.2390 ± 0.2507	< 0.0001
Df(3L)ED4293	36	0.8926 ± 0.0383	> 0.9999	119	2.4090 ± 0.2109	0.9916
Df(3L)BSC368	38	0.7287 ± 0.0547	0.1165	152	3.3140 ± 0.1794	< 0.0001
Df(3L)ED4341	56	0.9432 ± 0.0213	> 0.9999	266	1.8490 ± 0.1275	< 0.0001
Df(3L)ED210	37	0.9180 ± 0.0325	> 0.9999	137	3.2730 ± 0.2800	0.0002
Df(3L)BSC371	35	0.8541 ± 0.0461	> 0.9999	130	2.2940 ± 0.2279	0.0053
Df(3L)BSC884	58	0.7133 ± 0.0422	0.003	223	3.0930 ± 0.2013	< 0.0001
Df(3L)BSC410	51	0.6417 ± 0.0447	< 0.0001	213	3.5900 ± 0.2046	< 0.0001
Df(3L)BSC411	39	0.7474 ± 0.0526	0.4785	153	2.8930 ± 0.1961	< 0.0001
Df(3L)Exel6109	54	0.7509 ± 0.0400	0.0632	198	4.6740 ± 0.3226	< 0.0001
Df(3L)BSC27	38	0.8526 ± 0.0449	> 0.9999	139	2.0510 ± 0.1638	0.0396
Df(3L)BSC224	75	0.7975 ± 0.0382	> 0.9999	215	2.3110 ± 0.1432	0.9399
Df(3L)BSC117	35	0.8328 ± 0.0369	> 0.9999	139	2.7450 ± 0.2549	0.0576
Df(3L)BSC33	53	0.8081 ± 0.0371	> 0.9999	242	3.1150 ± 0.2111	0.0002
Df(3L)Exel8104	20	0.7947 ± 0.0722	> 0.9999	76	3.0290 ± 0.4049	0.0466
Df(3L)BSC375	71	0.7583 ± 0.0359	0.0575	242	3.4400 ± 0.1882	< 0.0001
Df(3L)BSC388	38	0.7522 ± 0.0543	> 0.9999	125	2.7800 ± 0.2044	0.0002
Df(3L)Exel6112	92	0.7112 ± 0.0341	< 0.0001	332	3.0360 ± 0.1631	< 0.0001
Df(3L)BSC815	38	0.8162 ± 0.0470	> 0.9999	117	3.2130 ± 0.3312	0.0008
Df(3L)BSC389	36	0.8022 ± 0.0500	> 0.9999	107	2.9420 ± 0.2228	< 0.0001
Df(3L)BSC816	38	0.7113 ± 0.0511	0.0208	139	2.8040 ± 0.2430	0.0032
Df(3L)ED4421	32	0.9150 ± 0.0233	> 0.9999	150	2.3990 ± 0.2093	0.2944
Df(3L)AC1	14	0.9048 ± 0.0516	> 0.9999	48	2.9250 ± 0.5267	0.7318
Df(3L)BSC113	68	0.6566 ± 0.0413	< 0.0001	208	2.8290 ± 0.2231	0.129
Df(3L)BSC391	50	0.7080 ± 0.0492	0.0189	195	3.2450 ± 0.2269	< 0.0001
Df(3L)BSC118	72	0.7018 ± 0.0398	0.0002	224	2.9590 ± 0.2176	0.0005
Df(3L)BSC392	33	0.7326 ± 0.0574	0.3519	99	3.7370 ± 0.3742	< 0.0001
Df(3L)BSC673	58	0.8632 ± 0.0315	> 0.9999	310	2.3450 ± 0.1186	0.965
Df(3L)ED4475	35	0.9786 ± 0.0158	> 0.9999	114	1.9460 ± 0.1105	0.0718
Df(3L)BSC730	38	0.7864 ± 0.0366	0.199	192	2.7620 ± 0.1447	0.0003
Df(3L)ED4486	56	0.9129 ± 0.0291	> 0.9999	214	2.1670 ± 0.1727	0.0326
Df(3L)BSC12	37	0.8333 ± 0.0464	> 0.9999	159	1.9470 ± 0.1028	0.1293
Df(3L)ED4502	47	0.9399 ± 0.0276	> 0.9999	174	2.1740 ± 0.1754	0.0367
Df(3L)ED4543	29	0.9622 ± 0.0228	> 0.9999	121	1.8010 ± 0.1264	0.0158
Df(3L)BSC845	39	0.7675 ± 0.0516	> 0.9999	153	2.9390 ± 0.2197	0.0359
Df(3L)BSC774	39	0.7748 ± 0.0522	> 0.9999	124	2.7070 ± 0.2636	0.238
Df(3L)ED4674	59	0.8534 ± 0.0309	> 0.9999	220	3.3770 ± 0.2504	0.0007
Df(3L)ED4685	71	0.8029 ± 0.0348	> 0.9999	303	2.3560 ± 0.1189	0.7245
Df(3L)BSC775	28	0.8452 ± 0.0538	> 0.9999	90	2.4250 ± 0.2763	0.3288
Df(3L)BSC220	37	0.7779 ± 0.0479	> 0.9999	142	2.9270 ± 0.2880	0.5223
Df(3L)BSC20	38	0.9447 ± 0.0294	> 0.9999	138	1.8570 ± 0.1449	0.003
Df(3L)BSC839	39	0.7177 ± 0.0543	0.1102	156	2.4740 ± 0.1660	0.1456
Df(3L)BSC797	40	0.7829 ± 0.0556	> 0.9999	141	3.0900 ± 0.2908	0.0523
Df(3L)BSC449	36	0.9191 ± 0.0288	> 0.9999	107	3.1040 ± 0.3451	0.4347
Df(3L)BSC553	39	0.7796 ± 0.0495	> 0.9999	136	2.5240 ± 0.2295	0.8917
Df(3L)BSC419	72	0.5979 ± 0.0467	< 0.0001	263	2.9470 ± 0.1507	< 0.0001
Df(3L)ED4978	34	0.8333 ± 0.0484	> 0.9999	89	4.0200 ± 0.4836	< 0.0001
Df(3L)BSC223	40	0.7533 ± 0.0473	0.4083	145	3.6730 ± 0.2716	< 0.0001
Df(3L)BSC451	72	0.7679 ± 0.0371	0.2729	224	2.5030 ± 0.1241	0.0064
Df(3L)ED230	36	0.9185 ± 0.0352	> 0.9999	101	2.2150 ± 0.2860	0.0096
Df(3L)ED5017	35	0.9114 ± 0.0343	> 0.9999	152	2.8720 ± 0.2265	0.0037
Df(3L)1-16	36	0.9164 ± 0.0233	> 0.9999	133	2.1670 ± 0.1345	0.7983
Df(3L)6B-29+Df(3R)6B-29	35	0.6629 ± 0.0631	0.0345	108	2.6350 ± 0.2195	0.0118

Table 19: Raw data and statistical comparisons between *FoxP*$^{5\text{-SZ-3955}}$ heterozygous flies and the deficiency lines for the right arm of 3rd chromosome over *FoxP*$^{5\text{-SZ-3955}}$. Accuracies presented as mean±SEM, together with number of flies tested per genotype; *P* values of pairwise comparisons of accuracies (Kruskal-Wallis ANOVA, KW, followed by Dunn's test). Reaction times presented as mean±SEM, together with number of decisions analysed per genotype; *P* values of pairwise comparisons of reaction times (Kolmogorov-Smirnov test, KS; Bonferroni-corrected significance level is 0.0006410).

Genotype/*FoxP*$^{5\text{-Z-3955}}$	Accuracy			Reaction time		
	Number of flies	Mean±SEM (fraction)	KW *P* values	Number of decisions	Mean±SEM (s)	KS *P* values
CS	966	0.8897 ± 0.0080		3524	2.0540 ± 0.0324	
Df(3R)10-65	75	0.8431 ± 0.0282	> 0.9999	329	2.5300 ± 0.1374	< 0.0001
Df(3R)ED5100	83	0.8722 ± 0.0264	> 0.9999	273	2.2510 ± 0.1832	0.1562
Df(3R)ED5147	31	0.9215 ± 0.0286	> 0.9999	118	2.2760 ± 0.2735	0.813
Df(3R)ED5156	36	0.9713 ± 0.0140	> 0.9999	147	1.8650 ± 0.1206	0.621
Df(3R)BSC549	32	0.9479 ± 0.0272	> 0.9999	149	2.2860 ± 0.2213	0.8764
Df(3R)ED5177	58	0.8655 ± 0.0369	> 0.9999	240	2.3670 ± 0.1452	0.0009
Df(3R)BSC464	37	0.8158 ± 0.0545	> 0.9999	128	2.2880 ± 0.1535	0.0026
Df(3R)BSC47	48	0.8845 ± 0.0343	> 0.9999	176	2.7460 ± 0.2926	0.0899
Df(3R)Tpl10	39	0.8239 ± 0.0515	> 0.9999	120	1.9760 ± 0.1886	0.7861
Df(3R)BSC681	38	0.7626 ± 0.0504	0.4373	155	2.5010 ± 0.2511	0.006
Df(3R)BSC738	37	0.8319 ± 0.0484	> 0.9999	148	2.6310 ± 0.2196	0.0006
Df(3R)BSC467	39	0.8115 ± 0.0536	> 0.9999	166	2.1400 ± 0.1397	0.2664
Df(3R)Antp17	34	0.7195 ± 0.0554	0.006	143	2.8400 ± 0.2402	< 0.0001
Df(3R)BSC633	39	0.9551 ± 0.0275	> 0.9999	141	2.3720 ± 0.2262	0.0132
Df(3R)ED5339	58	0.9319 ± 0.0274	> 0.9999	206	3.1480 ± 0.2747	0.0001
Df(3R)BSC507	89	0.7640 ± 0.0349	0.0061	323	4.9150 ± 0.2324	< 0.0001
Df(3R)BSC476	39	0.9109 ± 0.0385	> 0.9999	173	2.4590 ± 0.2128	0.0339
Df(3R)Exel6264	36	0.9255 ± 0.0284	> 0.9999	124	1.9960 ± 0.1774	0.9545
Df(3R)Exel6154	51	0.8616 ± 0.0445	> 0.9999	215	2.5530 ± 0.2386	0.1227
Df(3R)Exel6155	38	0.8015 ± 0.0447	> 0.9999	158	2.3580 ± 0.1736	0.0334
Df(3R)BSC621	39	0.7718 ± 0.0521	> 0.9999	147	2.4550 ± 0.1648	< 0.0001
Df(3R)ED5474	38	0.7668 ± 0.0512	0.3368	127	2.6010 ± 0.2099	< 0.0001
Df(3R)BSC568	33	0.7328 ± 0.0659	> 0.9999	123	1.8050 ± 0.1290	0.0498
Df(3R)BSC469	43	0.6787 ± 0.0610	0.0406	116	2.8290 ± 0.3053	0.1273
Df(3R)BSC486	71	0.8435 ± 0.0310	> 0.9999	290	2.3370 ± 0.1451	0.5039
Df(3R)ED5644	51	0.8036 ± 0.0429	> 0.9999	183	2.5490 ± 0.2403	0.057
Df(3R)ED10555	33	0.9222 ± 0.0306	> 0.9999	115	1.7110 ± 0.2774	< 0.0001
Df(3R)BSC750	39	0.8117 ± 0.0474	> 0.9999	132	2.6200 ± 0.2639	0.427
Df(3R)BSC741	33	0.7241 ± 0.0538	0.033	108	2.9800 ± 0.2945	0.0005
Df(3R)BSC515	87	0.8282 ± 0.0341	> 0.9999	301	2.2430 ± 0.1307	0.177
Df(3R)BSC728	37	0.9063 ± 0.0320	> 0.9999	167	2.1540 ± 0.1230	0.0142
Df(3R)Exel7328	38	0.8741 ± 0.0400	> 0.9999	142	1.8520 ± 0.1432	0.3067
Df(3R)BSC887	55	0.6642 ± 0.0483	< 0.0001	207	2.7390 ± 0.2045	< 0.0001
Df(3R)P115	38	0.8585 ± 0.0455	> 0.9999	157	2.1900 ± 0.1752	0.5636
Df(3R)ED10639	23	0.7681 ± 0.0796	> 0.9999	53	3.1910 ± 0.5609	0.006
Df(3R)ED10642	37	0.8000 ± 0.0541	> 0.9999	113	2.3750 ± 0.2214	0.0297
Df(3R)Exel6270	67	0.8092 ± 0.0367	> 0.9999	192	2.3690 ± 0.2246	0.1482
Df(3R)Ubx109	37	0.8829 ± 0.0483	> 0.9999	140	2.3240 ± 0.1969	0.5378
Df(3R)BSC748	37	0.8607 ± 0.0394	> 0.9999	171	1.9560 ± 0.1058	0.5945
Df(3R)ED5780	36	0.8787 ± 0.0496	> 0.9999	110	2.5890 ± 0.2838	0.2587
Df(3R)ED2	38	0.8650 ± 0.0439	> 0.9999	156	1.9530 ± 0.1630	0.2756
Df(3R)ED6025	49	0.9439 ± 0.0255	> 0.9999	149	1.6790 ± 0.1117	0.0871
Df(3R)BSC517	36	0.9386 ± 0.0316	> 0.9999	104	2.3030 ± 0.2449	0.3105
Df(3R)BSC141	57	0.8393 ± 0.0391	> 0.9999	240	3.1580 ± 0.2080	< 0.0001
Df(3R)Exel6272	39	0.9238 ± 0.0368	> 0.9999	168	1.9290 ± 0.2010	0.0364
Df(3R)BSC677	98	0.8724 ± 0.0217	> 0.9999	425	2.4550 ± 0.1122	0.0004
Df(3R)ED6096	68	0.9103 ± 0.0259	> 0.9999	225	2.3540 ± 0.1965	0.0271
Df(3R)slo3	31	0.8712 ± 0.0482	> 0.9999	100	3.1110 ± 0.3479	0.0022
Df(3R)BSC619	37	0.8634 ± 0.0441	> 0.9999	126	2.4740 ± 0.2361	0.0231
Df(3R)BSC137	37	0.8231 ± 0.0495	> 0.9999	156	1.6580 ± 0.1009	0.1198
Df(3R)BSC489	40	0.8351 ± 0.0466	> 0.9999	163	2.0560 ± 0.1292	0.675
Df(3R)Exel6196	72	0.6245 ± 0.0421	< 0.0001	296	3.1360 ± 0.1513	< 0.0001
Df(3R)Exel6197	93	0.9015 ± 0.0221	> 0.9999	358	2.1430 ± 0.0894	0.0003
Df(3R)ED6187	49	0.9010 ± 0.0359	> 0.9999	168	2.2280 ± 0.2030	0.8183
Df(3R)ED6220	36	0.8780 ± 0.0419	> 0.9999	125	2.8080 ± 0.2372	< 0.0001
Df(3R)Exel6201	74	0.8551 ± 0.0322	> 0.9999	282	2.0510 ± 0.1242	0.0115
Df(3R)FDD-0317950	38	0.9206 ± 0.0326	> 0.9999	162	2.2440 ± 0.1519	0.1767
Df(3R)Exel6202	35	0.8439 ± 0.0510	> 0.9999	144	2.2550 ± 0.1527	< 0.0001
Df(3R)Exel6203	36	0.9028 ± 0.0395	> 0.9999	112	2.0960 ± 0.2063	0.1598
Df(3R)BSC321	39	0.8506 ± 0.0473	> 0.9999	166	1.9510 ± 0.1921	0.1588
Df(3R)BSC140	53	0.9223 ± 0.0273	> 0.9999	220	2.0010 ± 0.1121	0.7319
Df(3R)ED6232	16	0.8362 ± 0.0534	> 0.9999	72	1.6300 ± 0.1251	0.0165
Df(3R)ED6255	34	0.9289 ± 0.0286	> 0.9999	131	2.3930 ± 0.2648	0.1912
Df(3R)BSC497	37	0.8429 ± 0.0391	> 0.9999	169	2.2070 ± 0.1472	0.0122
Df(3R)BSC501	31	0.9664 ± 0.0187	> 0.9999	122	2.1000 ± 0.1728	0.8115
Df(3R)BSC547	28	0.9491 ± 0.0263	> 0.9999	156	2.1160 ± 0.1316	0.0101
Df(3R)L127	18	0.9610 ± 0.0184	> 0.9999	101	2.4560 ± 0.2130	0.1005
Df(3R)BSC620	59	0.8408 ± 0.0305	0.8205	277	2.5540 ± 0.1047	< 0.0001
Df(3R)X3F	60	0.9044 ± 0.0315	> 0.9999	232	2.7310 ± 0.1684	< 0.0001
Df(3R)BSC502	38	0.8487 ± 0.0516	> 0.9999	133	2.4160 ± 0.1409	< 0.0001
Df(3R)BSC503	38	0.8271 ± 0.0435	> 0.9999	188	2.1490 ± 0.1237	0.001
Df(3R)BSC504	47	0.8583 ± 0.0391	> 0.9999	204	2.1240 ± 0.1670	0.5196
Df(3R)Exel7378	38	0.9105 ± 0.0343	> 0.9999	160	2.6460 ± 0.2061	< 0.0001
Df(3R)ED6346	52	0.7600 ± 0.0458	0.2598	187	2.5810 ± 0.1998	0.0007
Df(3R)BSC749	37	0.8263 ± 0.0419	> 0.9999	161	2.4120 ± 0.1704	< 0.0001
Df(3R)BSC793	73	0.8281 ± 0.0307	> 0.9999	270	2.4060 ± 0.1246	< 0.0001
Df(3R)ED50003	34	0.9759 ± 0.0138	> 0.9999	121	1.6170 ± 0.1802	0.0009

Table 20: Statistical comparisons between wild-type (wt) and *FoxP*$^{5\text{-SZ-3955}}$ homozygous and heterozygous mutant flies performing discrimination between 10^{-4} MCH and air. *P* values of pairwise comparisons of accuracies (Kruskal-Wallis ANOVA, KW, followed by Dunn's test) and reaction times (Kolmogorov-Smirnov test, KS; Bonferroni-corrected significance level is 0.0167).

Comparison	KW test *P* value Fraction correct	KS test *P* value Reaction time
wt vs. *FoxP*$^{5\text{-sz-3955}}$/+	0.4854	0.0171
wt vs. Df(3R)ED5428/+	> 0.9999	0.0691
Df(3R)ED5428 *vs. FoxP*$^{5\text{-sz-3955}}$/+	0.6055	0.9967

Table 21: Deficiencies that exhibit increased reactions times and the number of genes affected in each.

Deficiency	Number of genes
Df(2L)ED19	64
Df(2L)ED94	111
Df(2L)ed1	96
Df(2L)ED250	65
Df(2L)BSC209	93
Df(2L)ED1272	152
Df(2R)ED1715	152
Df(2R)BSC199	82
Df(2R)BSC699	9
Df(2R)BSC305	32
Df(2R)BSC361	118
Df(2R)BSC664	45
Df(2R)BSC780	30
Df(3L)ED201	83
Df(3L)BSC672	10
Df(3L)BSC368	91
Df(3L)ED210	134
Df(3L)BSC411	151
Df(3L)Exel6109	45
Df(3L)BSC33	32
Df(3L)BSC375	48
Df(3L)BSC388	106
Df(3L)BSC389	57
Df(3L)BSC392	83
Df(3L)BSC730	24
Df(3L)ED4674	96
Df(3L)ED4978	83
Df(3L)BSC223	37
Df(3R)10-65	18
Df(3R)BSC738	38
Df(3R)ED5339	226
Df(3R)BSC621	63
Df(3R)ED5474	67
Df(3R)BSC141	71
Df(3R)BSC677	37
Df(3R)Exel6197	36
Df(3R)ED6220	180
Df(3R)Exel6202	57
Df(3R)BSC620	82
Df(3R)X3F	81
Df(3R)BSC502	51
Df(3R)Exel7378	63
Df(3R)BSC749	32
Df(3R)BSC793	24

Table 22: Statistical comparisons between wild-type flies' performance in naive and trained MCH discrimination at 10^{-1} absolute odour intensity. *P* values of pairwise comparisons of the fraction of choices towards the lower MCH concentration (Kruskal-Wallis ANOVA, KW, followed by Dunn's test) and reaction times (Kolmogorov-Smirnov test, KS; Bonferroni-corrected significance level is 0.0062).

Comparison	Concentratio ratio	KW test *P* value Fraction lower [MCH]	KS test *P* value Reaction time
Trained vs. Naive	0.1	0.0011	0.3458
	0.2	0.0042	0.1542
	0.4	< 0.0001	0.0431
	0.5	< 0.0001	0.0203
	0.7	< 0.0001	< 0.0001
	0.8	< 0.0001	< 0.0001
	0.9	0.0030	< 0.0001
	0.95	0.0423	< 0.0001

Table 23: Statistical comparisons between MCH concentration ratios in wild-type (wt) and *FoxP*$^{5\text{-SZ-3955}}$ mutant flies performing naive MCH discrimination at $10^{-1.5}$ absolute odour intensity. *P* values of pairwise comparisons of the fraction of choices towards the lower MCH concentration (Kruskal-Wallis ANOVA, KW, followed by Dunn's test) and reaction times (Kolmogorov-Smirnov test, KS; Bonferroni-corrected significance level is 0.0056).

Genotype	Comparison	KW test *P* value Fraction lower [MCH]	KS test *P* value Reaction time
wt	0.05 vs. 0.1	> 0.9999	0.7246
	0.05 vs. 0.2	> 0.9999	0.0004
	0.05 vs. 0.3	> 0.9999	0.2516
	0.05 vs. 0.4	0.0129	0.0003
	0.05 vs. 0.5	0.0264	0.0005
	0.05 vs. 0.6	< 0.0001	< 0.0001
	0.05 vs. 0.7	0.0038	0.0005
	0.05 vs. 0.8	< 0.0001	< 0.0001
	0.05 vs. 0.9	< 0.0001	< 0.0001
FoxP$^{5\text{-sz-3955}}$	0.05 vs. 0.1	> 0.9999	0.9203
	0.05 vs. 0.2	0.9024	0.0391
	0.05 vs. 0.3	> 0.9999	0.0023
	0.05 vs. 0.4	< 0.0001	< 0.0001
	0.05 vs. 0.5	< 0.0001	< 0.0001
	0.05 vs. 0.6	< 0.0001	< 0.0001
	0.05 vs. 0.7	< 0.0001	< 0.0001
	0.05 vs. 0.8	< 0.0001	< 0.0001
	0.05 vs. 0.9	< 0.0001	< 0.0001

Table 24: Statistical comparisons between wild-type (wt) and *FoxP*$^{5\text{-SZ-3955}}$ mutant flies performing naive MCH discrimination at $10^{-1.5}$ absolute odour intensity. *P* values of pairwise comparisons of the fraction of choices towards the lower MCH concentration (Kruskal-Wallis ANOVA, KW, followed by Dunn's test) and reaction times (Kolmogorov-Smirnov test, KS; Bonferroni-corrected significance level is 0.0050).

Comparison	Concentratio ratio	KW test *P* value Fraction lower [MCH]	KS test *P* value Reaction time
wt vs. *FoxP*$^{5\text{-sz-3955}}$	0.05	< 0.0001	0.2189
	0.1	< 0.0001	0.1527
	0.2	0.0018	0.0314
	0.3	0.0014	0.0032
	0.4	0.0142	0.5600
	0.5	0.5475	< 0.0001
	0.6	0.0148	< 0.0001
	0.7	> 0.9999	0.0017
	0.8	> 0.9999	< 0.0001
	0.9	> 0.9999	< 0.0001

Table 25: Statistical comparisons between *OK107 > shi^{ts}* and parental control flies tested for naive MCH discrimination at 25 °C and 30 °C. *P* values of pairwise comparisons of the fraction of choices towards the lower MCH concentration (Kruskal-Wallis ANOVA, KW, followed by Dunn's test) and reaction times (Kolmogorov-Smirnov test, KS; Bonferroni-corrected significance level is 0.0125).

Temperature	Comparison	Concentration ratio	KW test *P* value Fraction lower [MCH]	KS test *P* value Reaction time
25 °C	*UAS-shibire^{ts}; OK107-GAL4* vs. *OK107-GAL4*	0.1	> 0.9999	0.7448
		0.3	0.7496	0.0807
		0.5	> 0.9999	0.4140
		0.7	> 0.9999	0.1350
	UAS-shibire^{ts}; OK107-GAL4 vs. *UAS-shibire^{ts}*	0.1	> 0.9999	0.0029
		0.3	0.8754	0.4073
		0.5	> 0.9999	0.0951
		0.7	0.3333	0.5039
	OK107-GAL4 vs. *UAS-shibire^{ts}*	0.1	0.8312	0.0004
		0.3	> 0.9999	0.6166
		0.5	> 0.9999	0.3452
		0.7	> 0.9999	0.0173
32 °C	*UAS-shibire^{ts}; OK107-GAL4* vs. *OK107-GAL4*	0.1	< 0.0001	< 0.0001
		0.3	0.0598	< 0.0001
		0.5	> 0.9999	0.0030
		0.7	0.4388	0.0020
	UAS-shibire^{ts}; OK107-GAL4 vs. *UAS-shibire^{ts}*	0.1	< 0.0001	< 0.0001
		0.3	0.5176	0.0002
		0.5	0.6537	0.0034
		0.7	> 0.9999	0.2322
	OK107-GAL4 vs. *UAS-shibire^{ts}*	0.1	> 0.9999	0.1250
		0.3	> 0.9999	0.4351
		0.5	> 0.9999	0.3397
		0.7	> 0.9999	0.0003

Table 26: Statistical comparisons across concentration ratios for *OK107 > shi^{ts}* tested for naive MCH discrimination at 25 °C and 30 °C. *P* values of pairwise comparisons of the fraction of choices towards the lower MCH concentration (Kruskal-Wallis ANOVA, KW, followed by Dunn's test) and reaction times (Kolmogorov-Smirnov test, KS; Bonferroni-corrected significance level is 0.0167).

Temperature	Comparison	KW test *P* value Fraction lower [MCH]	KS test *P* value Reaction time
25 °C	0.1 vs. 0.3	0.1717	0.0003
	0.1 vs. 0.5	< 0.0001	< 0.0001
	0.1 vs. 0.7	< 0.0001	< 0.0001
32 °C	0.1 vs. 0.3	> 0.9999	> 0.9999
	0.1 vs. 0.5	> 0.9999	0.1168
	0.1 vs. 0.7	> 0.9999	0.2184

Table 27: Statistical comparisons between *247-MB > GAL80, OK107 > shi^{ts}* and parental control flies tested for naive MCH discrimination at 30 °C. *P* values of pairwise comparisons of the fraction of choices towards the lower MCH concentration (Kruskal-Wallis ANOVA, KW, followed by Dunn's test) and reaction times (Kolmogorov-Smirnov test, KS; Bonferroni-corrected significance level is 0.0125).

Comparison	Concentration ratio	KW test *P* value Fraction lower [MCH]	KS test *P* value Reaction time
247-LexA, LexAop-GAL80; *UAS-shibire^{ts}; OK107-GAL4* vs. *247-LexA, LexAop-GAL80*; *OK107-GAL4*	0.1	> 0.9999	< 0.0001
	0.3	> 0.9999	0.0051
	0.5	0.2680	< 0.0001
	0.7	> 0.9999	< 0.0001
247-LexA, LexAop-GAL80; *UAS-shibire^{ts}; OK107-GAL4* vs. *UAS-shibire^{ts}*	0.1	> 0.9999	< 0.0001
	0.3	0.0808	0.2064
	0.5	> 0.9999	0.0001
	0.7	> 0.9999	0.0002
247-LexA, LexAop-GAL80; *OK107-GAL4* vs. *UAS-shibire^{ts}*	0.1	> 0.9999	0.0520
	0.3	0.0029	0.4351
	0.5	> 0.9999	0.6227
	0.7	> 0.9999	0.0020

Table 28: Statistical comparisons of *OK107 > shi^{ts}* and *247-MB > GAL80, OK107 > shi^{ts}* with parental control flies, tested for naive MCH detection against air at 30 °C. *P* values of pairwise comparisons of the fraction of choices towards air (Kruskal-Wallis ANOVA, KW, followed by Dunn's test) and reaction times (Kolmogorov-Smirnov test, KS; Bonferroni-corrected significance level is 0.0125).

Comparison	KW test *P* value Fraction air
UAS-shibire^{ts}; OK107-GAL4 vs. *OK107-GAL4*	> 0.9999
UAS-shibire^{ts}; OK107-GAL4 vs. *UAS-shibire^{ts}*	> 0.9999
OK107-GAL4 vs. *UAS-shibire^{ts}*	0.7181
247-LexA, LexAop-GAL80; *UAS-shibire^{ts}; OK107-GAL4* vs. *247-LexA, LexAop-GAL80*; *OK107-GAL4*	> 0.9999
247-LexA, LexAop-GAL80; *UAS-shibire^{ts}; OK107-GAL4* vs. *UAS-shibire^{ts}*	0.656
247-LexA, LexAop-GAL80; *OK107-GAL4* vs. *UAS-shibire^{ts}*	> 0.9999

Table 29: Statistical comparisons between *OK107 > FoxP^{RNAi}* and parental control flies tested for naive MCH discrimination. *P* values of pairwise comparisons of the fraction of choices towards the lower MCH concentration (Kruskal-Wallis ANOVA, KW, followed by Dunn's test) and reaction times (Kolmogorov-Smirnov test, KS; Bonferroni-corrected significance level is 0.0125).

Comparison	Concentration ratio	KW test *P* value Fraction lower [MCH]	KS test *P* value Reaction time
UAS-FoxP^{RNAi}; OK107-GAL4 vs. *OK107-GAL4*	0.1	> 0.9999	0.0289
	0.3	> 0.9999	0.0003
	0.5	> 0.9999	0.0125
	0.7	> 0.9999	< 0.0001
UAS-FoxP^{RNAi}; OK107-GAL4 vs. *UAS-FoxP^{RNAi}*	0.1	> 0.9999	0.0197
	0.3	0.6969	0.0403
	0.5	> 0.9999	0.0237
	0.7	0.1042	< 0.0001
OK107-GAL4 vs. *UAS-FoxP^{RNAi}*	0.1	> 0.9999	0.9801
	0.3	> 0.9999	0.1088
	0.5	> 0.9999	0.1504
	0.7	> 0.9999	0.7125